

Timing meter for mechanical ignition distributors

© copyright Frodo Irrxsom 2003-2023

Synopsis: A set of instruments and sensor schemes is presented for the accurate measurement of ignition timing and the vacuum / centrifugal timing advance of mechanical ignition distributors in both bench testing and on-road use.



CONTENTS

1. MOTIVATION	4
1.1. SAFETY RECOMMENDATIONS AND DISCLAIMER	5
1.2. GLOSSARY, UNITS AND ABBREVIATIONS	6
2. MECHANICAL DISTRIBUTOR THEORY	7
2.1. STATIC IGNITION ADVANCE	7
2.2. CENTRIFUGAL IGNITION ADVANCE	7
2.3. VACUUM IGNITION ADVANCE	8
2.4. IS VACUUM ADVANCE NECESSARY?	9
2.4.1. Engine at idle	9
2.4.2. Acceleration	9
2.4.3. Cruising (part throttle)	9
2.4.4. Engine braking (deceleration)	10
3. MAPPING CRITERIA FOR THE MID	11
3.1. COMPRESSION RATIO	11
3.2. CAMSHAFT PROFILE	11
3.3. INDUCTION / EXHAUST SYSTEM	11
3.4. FUEL CHARACTERISTICS	11
3.5. DRIVING CHARACTERISTICS / CONDITIONS	11
4. COMPONENTS OF THE MID	12
4.1. POINTS PLATE	12
4.2. DISTRIBUTOR ROTOR SHAFT	12
4.3. CENTRIFUGAL ADVANCE MECHANISM	13
4.4. VACUUM ADVANCE UNIT	14
4.5. ROTOR ARM	15
5. IGNITION CIRCUIT ELECTRICAL THEORY	16
5.1. ACCURATE DETERMINATION OF THE POINTS STATE	18
6. MEASUREMENT OF IGNITION TIMING IN THE MID	21
6.1. PERIODIC MID EVENTS AND ENGINE SPEED	21

6.2. DWELL ANGLE	21
6.3. IGNITION TIMING ANGLE	22
7. AN ELECTRONIC TIMING SENSOR FOR THE MID	23
7.1. CASE STUDY: TIMING THE LUCAS DM2	23
7.2. MAGNET MOUNTING	25
7.3. SENSOR MOUNTING	26
8. ELECTRONIC MEASUREMENT OF THE TIMING INTERVAL	28
8.1. TACHOMETER OUTPUT	30
8.2. TIMING CIRCUITS	31
8.3. TIMING METER TEST CIRCUIT	33
8.4. TACHOMETER BAR GRAPH	34
8.5. VACUUM ADVANCE SENSOR	35
8.6. VACUUM ADVANCE BAR-GRAPH	37
8.7. DISTRIBUTOR CABLING	38
8.7.1. Points buffer and strobe buffer noise filtering	40
8.7.2. Points plate grounding	40
8.7.3. Positive earth installation	40
8.8. TIMING METER ASSEMBLY	41
8.9. CALIBRATING THE TIMING METER	41
8.9.1. Setting the display <i>SCALE</i> adjustment	41
8.9.2. Setting the display <i>OFFSET</i> adjustment	41
8.10. TESTING AND TROUBLESHOOTING	42
8.11. A WORKSHOP MID ANALYSER	44
9. DATA LOGGER MID-MAPPING	47
9.1. ASSEMBLING THE DATA LOGGER	48
9.2. CONFIGURING THE DATA LOGGER PROGRAM	49
9.3. TESTING THE DATA LOGGER	52
9.4. ACCURATE CALIBRATION OF THE VACUUM ADVANCE SENSOR	54
9.5. VERIFYING THE VACUUM SENSOR CALIBRATION USING LOGGED DATA	55
9.6. TECHNICAL: DATA LOGGER OPERATING SCHEME	56
10. USING THE TIMING METER AND DATA LOGGER	58
10.1. FIRST CHECK - THE DWELL METER	58
10.2. USING THE TIMING METER	59
10.2.1. Engine starting	60
10.2.2. Static ignition timing check	60
10.2.3. Centrifugal advance curve	60
10.2.4. Vacuum advance optimisation	61

10.3. USING THE DATA LOGGER	62
10.3.1. Dwell curve analysis	63
10.3.2. Acceleration through gears	64
10.3.3. Highway cruising	65
10.3.4. Using overdrive	65
10.4. LOG FILE ERROR INDICATORS	66
10.4.1. Points event error (PTSERR)	67
10.4.2. Strobe event error (STRERR)	67
10.4.3. Specific error combinations	68
10.5. BREAKERLESS POINTS REPLACEMENTS	68
11. DATA LOGGER PROGRAM SCRIPT	70
12. MODIFYING / RECALIBRATING THE VACUUM ADVANCE UNIT	74
12.1. DISASSEMBLY	74
12.2. RECONDITIONING	74
12.3. RECALIBRATION	75
12.3.1. Increasing the operating vacuum level	75
12.3.2. Decreasing the operating vacuum level	75
12.3.3. Increasing / decreasing the max vac advance	75
12.3.4. Increasing / decreasing the zero vac advance position	75
12.4. ESTIMATING THE VACUUM SPRING CALIBRATION	75
13. MAGNETIC SENSOR SCHEME SELECTION GUIDE	77
13.1. THERMAL COMPENSATION CORRECTION	78
13.1.1. Sensor / magnet thermal characterisation	79
13.1.2. Thermistor compensation	81
13.1.3. Reference sensor thermal compensation	83
13.1.4. Engine temperature thermal compensation	86
13.1.5. Data logger program temperature correction function	86
13.1.6. Data logger temperature correction calibration	87
14. MODIFICATIONS FOR 6, 8 OR 12 CYLINDER MIDS	88
15. LUCAS DM2 / 25D VACUUM SENSOR CARRIER	89
16. LUCAS DM2 CENTRIFUGAL ADVANCE RESTRICTOR PLATE	91
17. REFERENCES	93

1. Motivation

This document comprises a former tutorial on electronic instrument design expanded into a detailed primer on automotive ignition control achieved using mechanical methods in ignition distributors of the pre-semiconductor era. Most distributors of this period used a combination of engine speed and inlet manifold vacuum sense mechanisms to advance (and in some cases, retard) ignition timing in proportion to anticipated (not measured) air/fuel density and mixture ratio (stoichiometry) within the engine cylinders. Ignition distributors of this type such as the Lucas, Delco and Bosch models constituted an elegant and simple “analog computer”, although primitive by comparison with modern sensor-mapped electronic ignition systems. They were used in millions of vehicles of the post-war era but today survive largely in vintage and “classic” vehicles whose owners choose to retain these devices in some form.

In the period of their standard fitment and service support by vehicle manufacturers, these simple devices were expected to last the lifetime of the vehicle to which they were fitted, with periodic replacement of arc-eroded components such as breaker points, rotors and terminal caps. Each model of distributor was further specialised to suit specific induction, camshaft profile / valve timing, engine speed, fuel quality, compression ratio, and later, emissions control factors. Production of this large array of specific distributor subtypes was labour intensive and necessitated the management of large tables of distributor characteristics indexed by serial number. In the years following the discontinuance of each model and later demise of the manufacturer, much of the data on specific distributor versions was lost, although some models remained well documented through their support by enthusiasts. Today there is a small industry in restoring and maintaining these devices, some of which are approaching their centenary, as well as reproductions with varying degrees of modernisation and adherence to the original design.

One of the major issues facing use of an original, period mechanical ignition distributor (MID) is the lack of any means of measuring its expected functions quantitatively *in situ*. These devices were expected to be factory-set for the vehicles they were destined for use in, and not require recalibration apart from static ignition timing at fitment. It was never considered that such devices may need to be recalibrated or reconfigured for use in another vehicle. The subsequent retirement of the generation of automotive electricians familiar with this outmoded technology has left its users with a small group of expert technicians salted around the world who can still rebuild and recalibrate these units. Given that a modern electronic ignition system is field programmable and supplies full diagnostic data (subject to manufacturer’s permissions) as well as a more exacting model of engine efficiency management, the continued use of the MID is arguably erroneous. There are many reasons to retain them in period vehicles however, such as:

- **Simplicity.** Replacement with sensor-driven electronic engine management units is often highly intrusive on other engine components and requires expert technical skills and knowledge to retrofit and achieve any real improvement over the original system.
- **Authenticity.** When considering the replacement of original components in a period vehicle with later and/or better alternatives, where do you stop? Given the other technological shortcomings of a historic or classic vehicle, it might make more sense to replace the entire drivetrain if the goal is a more modern standard of efficiency or performance – as is frequently the case in motorsport. Such modifications may also impact upon the perceived value of a vehicle to collectors or its eligibility for heritage status, concours participation etc.
- **Maintainability.** Many motoring enthusiasts expect to be able to maintain their vehicles themselves, and draw satisfaction from doing so. They may want their vehicle to conform to the specifications listed in its manufacturer’s Workshop Manual so that they have a single technical reference to consult, a known set of part-numbers to seek replacements with, and the certainty that the manufacturer-specified component will perform the intended function correctly. Knowledge gained from experience of the wear characteristics and failure modes

of standard components may be replaced with unknown compatibility factors or sudden failure without warning with the use of alternative components.

- **Reliability.** Issues of quality and ongoing support for aftermarket or OEM automotive parts may also be a factor. Retrofit ignition systems in particular suffer from issues of proprietary information retention, fault diagnosis and continuity of component supply over time. Although electro-mechanical automotive systems have a reputation for unreliability, this is mostly the result of poor maintenance and an unreasonable expectation that these components should operate indefinitely when, in fact, these units were made to be reconditioned periodically by (expert) hand. In particular, the MID typically gives ample warning of imminent failure by poor running, and a simple adjustment by the roadside may be sufficient to continue on. In contrast, the failure of a primary semiconductor component in an electronic ignition typically results in immediate engine failure, with total replacement of the ignition control module as the only option. Even with a spare module in hand, replacement may not be possible outside a workshop. Such sudden failure modes leave the motorist with no easy means of diagnosis of the fault in the absence of a modern user-interactive engine-management system or diagnostic instruments, with a tow to the nearest garage as the only recovery option.
- 1. **Cost.** The simple design of the mechanical distributor, necessitated by the lack of advanced technology available today, resulted in a unit that is relatively inexpensive to repair or rebuild. A carefully restored and regularly serviced unit may operate indefinitely, provided that its consumable components remain available. The cost and availability of these parts depends on demand, so a large group of enthusiasts dedicated to preserving a particular model of distributor will maintain demand and support expert restorers.

Having chosen to use a period MID, there are several factors to consider in achieving a fit-for-function reliable ignition system. The first is restoration: a used unit must be examined for cost-effective recovery potential and worn parts replaced; secondly the suitability of the specific unit to the intended vehicle must be established if the part is not original; and finally the unit must be re-calibrated against either original or revised specifications. Conventionally, these tasks are achieved by an expert automotive electrician with the appropriate workshop and calibration equipment, with subsequent (but optional) one-time verification of the ignition system performance on a roller-bed dynamometer to measure power produced at the wheels against induction and exhaust composition, as is achieved dynamically in a modern engine management system. An experienced technician may even include engine wear and any modifications in their re-calibration of the distributor, as the factory-specified values may no longer apply. Such expertise is becoming rare and difficult to obtain, but with some research and effort this simple device can be analysed and adjusted to achieve its best possible performance.

1.1. Safety recommendations and disclaimer

The engine of a motor vehicle contains dangerous moving parts when operating and its ignition system produces potentially lethal voltages. No physical contact should be made with any part of the vehicle's engine when running and the vehicle should be secured in position externally during stationary engine running without an occupant at the controls.

The construction, testing and use of bench-test equipment involving motorised drives and automotive ignition coils furnish similar moving-part and electrocution risks as for the vehicle engine. Safety considerations regarding the use of such equipment is left wholly to the constructor.

No warranty of fitness for purpose is made for the devices, circuits and schemes described in this document. The author is not liable for any damage or accident caused by the construction or use of any devices derived from information presented in this document.

1.2. Glossary, units and abbreviations

For brevity and readability, the following units and abbreviations will be used in this text. The timing intervals will assume a 4-cylinder 4-stroke engine such as the BMC A or B series motors. Modifications to the given instruments for 6 / 8 / 12 cylinder distributors are listed in section 14.

CD / DD: Crankshaft degrees / Distributor degrees. It is assumed in this text that the distributor (and camshaft) rotates at half crankshaft speed so that $1DD = 2CD$.

Cent: Centrifugal timing advance or component part.

DD/KRPM: Distributor degrees per 1000 crankshaft RPM. Unit of linear dwell duration shift due to points signal delay or ignition primary circuit thermal effects.

Dwell angle: Distributor shaft rotation-angle over which the points are closed. In a breakerless ignition system, the equivalent coil-primary charging time expressed in DD.

DVM: Digital voltmeter, either as a bench instrument or monolithic component module.

DLM: Data logging module comprising a microcontroller and data storage medium.

GND: Chassis ground or earth potential in negative earth vehicles. Zero potential otherwise.

IGN: Vehicle ignition circuit power supply from ignition switch. Assumed to equal V(+12) unless used in reference to positive earth vehicles.

MID: Mechanical ignition distributor. Specifically, rotor-type distributors including centrifugal and vacuum ignition timing advance mechanisms.

TDC: Top dead-centre. Crankshaft position where a piston (#1 by default) is at the topmost position of its travel. Conventionally taken as the 0-degree position of crankshaft rotation. Prefixed by A (after) or B (before) to indicate direction of an angular offset from TDC.

Points: Distributor contact-breaker points. Normally closed to charge the ignition coil; opened by the distributor rotor cam to discharge ignition coil through the rotor to each engine cylinder spark-plug.

RPM: Crankshaft rotations per minute. Each 30RPM equals 1 ignition per second in a 4-cylinder 4-stroke engine.

Timing curve: Relationship between ignition timing and engine speed, conventionally described by a graph or table in crankshaft degrees vs. crankshaft RPM. Typically includes only centrifugal advance when used to characterise the MID.

V(+12): Nominal vehicle 12V supply. May range between 10V to 15V depending on charge state.

Vac: Vacuum timing advance or component part.

2. Mechanical distributor theory

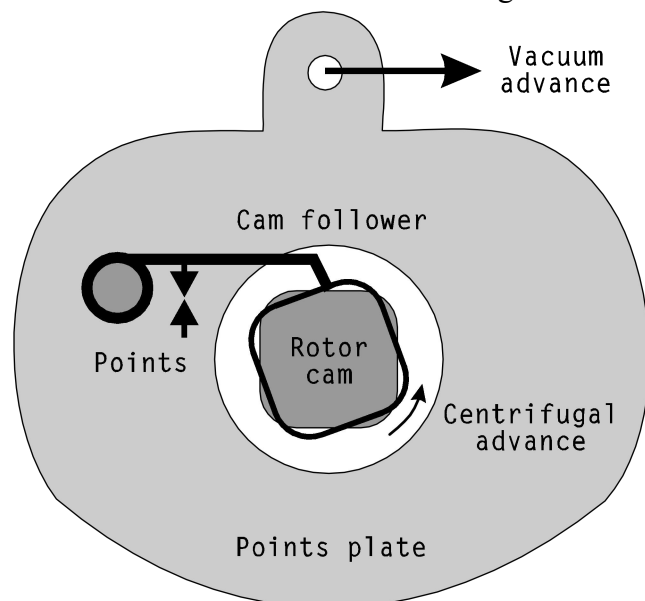
The function of the MID is to supply discharge current from the ignition coil to the spark plug of the appropriate engine cylinder approaching maximum compression, and then recharge the ignition coil for the next ignition. The “distribution” of ignition discharge to each engine cylinder in the correct sequence is achieved by using a gear on the camshaft to drive a rotor within the distributor cap, where it directs each discharge to the nearest terminal as it rotates. The discharge current is then conducted to the appropriate engine cylinder spark plug by a high-tension lead, and the correct sequence of cylinder ignitions is set by their connection order to the distributor cap terminals around the rotor’s circular path. Fixed immediately under the rotor, a cam with n lobes (n being the number of engine cylinders serviced by the distributor) rotates in sync with the rotor to open a “points” contact breaker which discharges the ignition coil through the rotor. The exact instant that this discharge is applied to the cylinder is controlled by several factors to optimise the ignition and combustion of the air/fuel mixture in the cylinder. The factors controlling the ignition timing are:

2.1. Static ignition advance

The rotor within the distributor arrives at each discharge terminal in the distributor cap, and the distributor points open to discharge the coil, at an angle between the rotor and the distributor body set by the fixing of the distributor to the engine. At fitment with the engine stationary (static), the rotor remains fixed while the distributor body is free to rotate around it until clamped down. The static advance angle sets the fixed mounting angle between the rotor and distributor body required to open the points at a specified crankshaft angle before the top of the cylinder’s compression stroke (TDC). In the absence of other ignition timing factors (such as at slow engine idle speeds) this static advance angle is exactly the crankshaft angle, conventionally stated in degrees before top-dead-centre (BTDC) of the piston compression stroke, at which the ignition discharge is transmitted to the spark plug. It will be repeated identically for each serviced engine cylinder (#1 to # n) by the n -fold symmetry of the rotor cam. Practically, the static advance is set correctly by observing the distributor’s ignition of #1 cylinder using a flashtube “timing gun” which is induction triggered by the discharge current through the #1-cylinder ignition lead. This flashtube is typically directed at the engine crankshaft pulley, where a notch on the pulley will be illuminated stroboscopically beside an angular scale marked on the timing-chain cover under the pulley. At slow engine idle, the distributor body is incrementally rotated until the desired static advance angle is observed at the crankshaft pulley, whereupon the distributor body is clamped down to the engine block. Some distributors (such as the various Lucas models) include a vernier adjustment built into the distributor body permitting fine adjustment of the static advance without disturbing the distributor mounting clamp, effectively by rotating the distributor’s whole internal timing assembly with respect to its body within a small angular range.

2.2. Centrifugal ignition advance

The distributor rotor/cam assembly is able to rotate within a small angular range with respect to its drive shaft from the camshaft gear. This movement is controlled by a pair of pivoted weights carried on a plate fixed to the distributor drive shaft spindle such that the weights are flung outwards by centrifugal force as the spindle rotates. The weights are



spring-loaded to remain pivoted inwards against a detent at slow engine speeds, but progressively move radially outwards against increasing spring tension as engine speed increases. However, their motion with respect to the fixed plate they pivot against is relatively small and provides an accurate, proportional mechanical measurement of the engine's crankshaft rotation speed which is transmitted to the rotor/cam assembly by a further pivot motion. This results in the cam rotating fractionally *towards* the points as the engine speed increases, so that the ignition discharge will occur earlier in the cylinder compression stroke. This is desirable to permit the air/fuel mixture more time to fully combust within the reduced compression-stroke time available at higher engine speeds. The use of such a mechanical arrangement to measure and transmit the speed of a rotating shaft has its origin in the Watt steam engine governor, where it fulfilled a similar function in timing control.

2.3. Vacuum ignition advance

The ignition points contact breaker is fixed on a plate which can also rotate within a small angular range with respect to the body of the distributor. A vacuum chamber connected to either the inlet manifold or carburettor contains a diaphragm linked to this plate which pulls it *towards* the rotor/cam assembly's oncoming rotation and thus open the points earlier in each cylinder compression stroke. The vacuum diaphragm is spring-loaded to begin pulling at a specific level of applied vacuum, and then proportionally more with increasing vacuum (decreasing pressure) up to a detent-fixed maximum length. This length corresponds to the angular rotation range of the points plate, so the ignition timing is advanced by the presence of high vacuum (or absence of pressure) corresponding to a partially or fully closed throttle and lower cylinder compression pressures. Vacuum advance units are thus specified by three parameters: vacuum level required to initiate movement; vacuum level required for maximum movement and the corresponding angular ignition timing advance produced between these vacuum levels. Some later models of distributor have a second diaphragm arranged in opposition to the first, to pull the points plate in the opposite direction and effect a retardation of the ignition timing in specific manifold-vacuum conditions where reduced combustion emissions are desired.

Vacuum and centrifugal advance together may be considered dynamical timing controls, as opposed to static ignition timing. In modern electronic ignition systems, the absolute position of the crankshaft in the engine is ascertained typically by means of a magnetic sensor positioned to sense a unique point on the crankshaft (or flywheel / timing pulley etc) as it passes the fixed sensor. This signal is used to provide a time reference point from which the electronic ignition unit calculates the optimal ignition times for each cylinder in sequence, based on engine speed, temperature, fuel stoichiometry, throttle position and other factors. This method of ignition timing is referred to as "crank triggering" and eliminates the need to perform static distributor timing. In most cases the rotary distributor itself has been eliminated in favour of a single solid-state electronic module that connects directly to each spark plug and that may also include an internal ignition coil. The set of ignition timing values produced by an electronic ignition system as a function of each engine-state sensor is usually referred to as its "map", often literally an n -dimensional array of stored timing lookup values corresponding to each possible discrete combination of the n engine sensors' states. In the simpler case of the MID, a two-dimensional array indexed by engine speed and inlet manifold pressure would be sufficient to map all possible timing states of the distributor; however the fact that manifold pressure is essentially atmospheric (so that the vacuum advance unit is not active) under acceleration allows the disregard of this factor in the determination of ignition timing as a function of (accelerating) engine speed. Accordingly, the ignition timing "map" reduces to a one-dimensional "timing curve" of ignition timing versus engine speed alone. Whether this assumption is valid in all vehicles and driving conditions requires case-by-case analysis.

2.4. Is vacuum advance necessary?

Vacuum advance is one of the few engine system components whose complete failure may go unnoticed by the motorist, even for the life of the vehicle. Like early emissions control devices in later vehicles, the vacuum advance unit may fail completely within the first decade of a vehicle's use without any indication or possible diagnosis save removal and inspection of the unit. Perhaps for this reason many classic vehicle enthusiasts assume it is also some early form of emissions control device that can be ignored or discarded. In fact the use of vacuum advance in the MID predates any emissions controls by decades; the real motivation for its use was fuel characteristics in the early-to-mid 20th century. The combination of slow-burning fuels and low compression ratios necessitated early ignition in the compression stroke to achieve optimum combustion under load, with even more ignition advance being desirable for the lower cylinder pressures present at cruising speeds. To achieve the required degree of ignition control, vacuum units were either connected to the inlet manifold directly to sense the ambient manifold vacuum level, or to an orifice directly beside the throttle flap in the body of the carburettor to sense the mixture flow-rate over a specific small throttle angle range. In the latter case the vacuum unit is operated by a small pocket of low pressure produced by the *venturi effect* immediately behind the throttle flap. In general, early MIDs intended for low-performance engines used inlet-manifold driven vacuum units, while the later carburettor-driven units supplied better timing control where manifold vacuum levels were not a reliable indicator of engine state, such as in high-performance engines with multiple carburettors or strong induction harmonics from long or overlapped camshaft durations. This arrangement afforded an early analog of the air density and throttle position sensors used in modern ignition control systems. Note: some carburettors provided a vacuum port located well behind the throttle flap for use with manifold-vacuum sensing units. These should be considered manifold-driven units in the following discussion.

A consideration of the engine states that vacuum ignition timing advance is intended to apply to must be made in order to ascertain if its omission is now either acceptable or warranted. In terms of readily discernable driving conditions, these are:

2.4.1. Engine at idle

A partial vacuum exists in the inlet manifold with the throttle closed and the engine at idle, which will instantly vanish when the throttle is opened. Accordingly, the application of any vacuum-advance at idle is equivalent to extra static advance in the absence of vacuum advance – requiring the disconnection of the vacuum unit to set static ignition timing correctly. A manifold-driven vacuum unit may produce some advance at idle but a carburettor-driven unit should not. Note that some manufacturers specified little or no static advance for vehicles fitted with manifold-driven vacuum advance as the latter was sufficient to provide the required timing at idle. Some such vehicles may have had an “ignition timing at idle” specification for setting the distributor angle with the vacuum unit still attached to the inlet manifold.

2.4.2. Acceleration

Under hard acceleration the inlet manifold is essentially at air pressure and the vacuum advance unit is inactive, possibly apart from momentary transients during gearshifts. This remains the case under moderate acceleration for a manifold-driven vacuum unit, but carburettor-driven vacuum advance will increase above a certain engine speed if the requisite throttle-angle is maintained. Added to centrifugal advance, this may lead to the bizarre phenomenon of engine “pinking” under (over-gear) load at a specific amount of throttle, but not either more or less.

2.4.3. Cruising (part throttle)

At constant engine speeds maintained by a part-open throttle, varying levels of vacuum will develop in the inlet manifold. In this situation the engine cylinders under compression will be incompletely filled with air/fuel mixture and an earlier ignition can be safely performed to combust the cylinder

contents completely and extract maximum gas expansion force in each power stroke. This uses fuel more efficiently by reducing the amount of throttle required to maintain a given engine speed, effecting a negative-feedback optimisation. In manifold-driven configuration, the vacuum advance unit's characteristics must be accurately matched to the engine's manifold vacuum range at the desired cruising speeds to achieve the desired degree of efficiency. In the carburettor-driven case, the manufacturer of the carburettor has determined a specific small range of throttle angles and gas flow rates to suit the specified cruising speed range of the intended engine installation, and has set the venturi orifice position and diameter accordingly.

2.4.4. Engine braking (deceleration)

Also depending on engine speed, the degree of vacuum in the inlet manifold is greatest under closed-throttle conditions and thus for manifold-driven units the degree of vacuum advance is greatest in this state. This permits early ignition of the low-pressure air/fuel mixture in a compressing engine cylinder to both ensure complete combustion and (in some cases) even develop pressure *against* the rising piston to assist braking. The low pressure air/fuel mixture has a slower flame propagation rate, necessitating an earlier ignition to fully combust the cylinder contents. Piston "knocking" or "pinking" does not occur despite the early ignition due to the partial charge of mixture to the cylinder before compression begins. No vacuum advance is produced by carburettor-driven vacuum units when the throttle is closed.

These criteria immediately make apparent one case in which the vacuum unit is redundant: track motorsport. If a vehicle is used only to perform repetitive hard acceleration and braking under racing conditions, the vacuum unit can and should be dispensed with. It is also likely in such cases that high-performance camshaft profiles will preclude the use of vacuum advance due to their irregular manifold pressure harmonics and absence of appreciable manifold vacuum at intermediate engine speeds. For a well-tuned road car however, an appropriate degree of vacuum advance will produce fuel efficiency at highway cruising speeds otherwise unachievable without a more modern sensor-mapped electronic ignition distributor.

3. Mapping criteria for the MID

Given the basic timing control functions of the MID, it may well be argued that rebuilding a used unit with new components to achieve the equivalent of original factory specifications for its timing control characteristics is sufficient. This assumption is only valid if all original engine specifications, tuning state *and fuel grade* are also respected. Small changes in these criteria can result in significant differences between optimal ignition timing programmes – Lucas alone listed over 300 distributor advance profiles by 1955. The range of factors that must be considered in the selection of a MID ignition timing “map” include:

3.1. Compression ratio

It is almost a given that any engine reconditioning performed on an original engine produced before 1980 will include decking either the cylinder block or head to increase compression ratio and take better advantage of modern fuels. This will reduce the maximum dynamic ignition timing advance permissible due to the risk of piston “knock” or detonation as well as changing the optimum profile for ignition timing with engine speed.

3.2. Camshaft profile

Using a different camshaft profile from that originally specified will change the valve timings at each cylinder, leading to different manifold vacuum levels and cylinder filling ratios across most engine states. In particular, inlet manifold vacuum may become erratic or resonant in certain intermediate engine states and a valid control range for vacuum advance timing at highway cruising speeds may need to be determined experimentally.

3.3. Induction / exhaust system

Changing the induction system of the engine for either increased performance (e.g. larger or more carburettors) or better air/fuel mixture (e.g. indirect fuel injection) will often reduce inlet manifold vacuum under part-throttle conditions compared with the original system. Likewise, the use of header / extractor exhaust manifolds will improve cylinder purging in the exhaust stroke and thus reduce the partial pressure of air/fuel mixture in the subsequent induction stroke (reduced “back-pressure”) unless a longer inlet valve duration is also applied by a revised camshaft profile. These factors alone will vary the ideal distributor timing map from that embodied in an original unit.

3.4. Fuel characteristics

The original vacuum and centrifugal ignition timing advance profiles produced by MIDs of the post-war period (particularly in the UK) were chosen to achieve combustion of poor quality, low-octane leaded fuels in relatively low-compression engines. For example, the Lucas distributors fitted to BMC sedans in the mid-1950’s produced up to 40CD of centrifugal advance alone at 5000RPM. Fitting such a distributor to a high-compression engine using modern unleaded fuel would result in piston damage. As such fuels are no longer used (although modern high-octane unleaded fuels also have slow combustion characteristics) it is erroneous to assume the manufacturer’s specification of distributor timing is still applicable today.

3.5. Driving characteristics / conditions

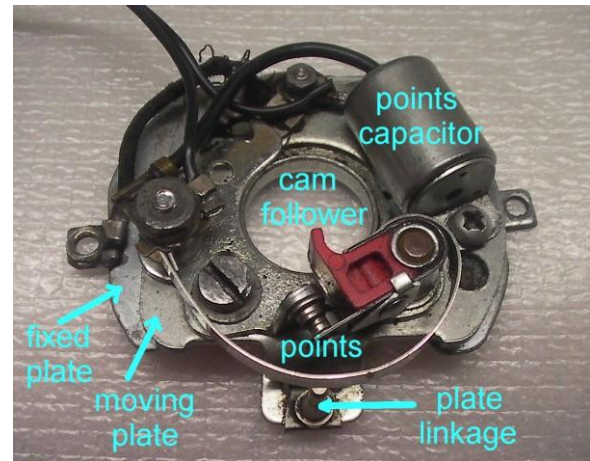
As stated above, an engine built for track motorsport will not require vacuum control in its ignition timing programme, but will require a different centrifugal timing curve from the vehicle’s original specification for any or all of the reasons listed above. In road use, factors such as (prevalent) altitude, temperature and humidity, vehicle mass (load) and fuel economy will bias the optimal ignition timing map as a function of both engine speed and manifold vacuum.

4. Components of the MID

We now examine the key components of the MID and their function in ignition timing, using the simple Lucas DM2 distributor as an example.

4.1. Points plate

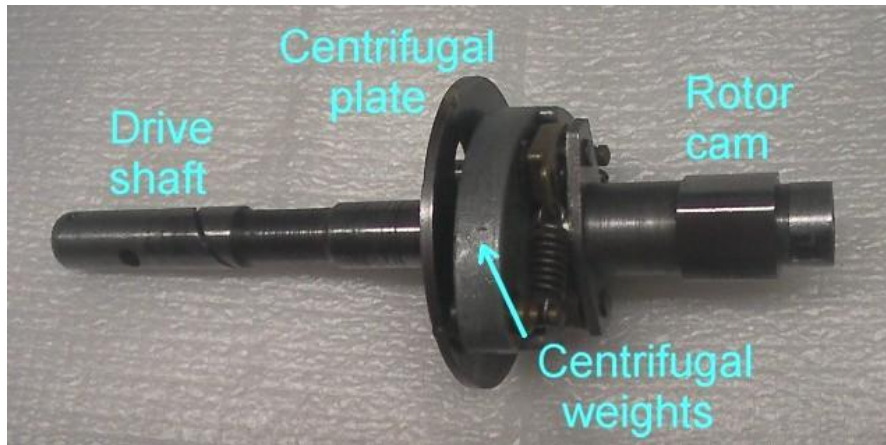
This assembly consists of two flat steel plates with a concentric hole in each through which the rotor cam protrudes. The upper plate is bushed to rotate over the lower plate, the latter being fixed to the distributor body. The contact breaker points are fixed to the upper moving (points) plate, so rotation of this plate will change the angle between the points cam follower and the rotor cam for every position of the latter, but specifically the angle at which the points are opened by the cam. If the points plate is rotated *towards* the oncoming rotation sense of the rotor cam, the points will open earlier in the rotor's travel and the spark discharge will be *advanced* in time; conversely a rotation of the plate away from the cam rotation will produce a delay or *retardation* of the spark discharge. At the bottom of the points plate image a peg extending below the plate is visible. This is the attachment point for the vacuum advance unit and is the only point of control of the rotary motion of the points plate. At inlet manifold vacuum levels below the minimum required to operate the vacuum unit, the points-plate is held at an angle corresponding to the static ignition timing set by the orientation of the distributor assembly on the engine block. At higher levels of manifold vacuum the points plate is progressively pulled by the vacuum unit towards earlier ignition discharge timings, up to a limit fixed by the vacuum unit. The points plate also carries a capacitor for arc suppression across the points at opening and adjustments to set the static height at which the cam follower makes first contact with the cam as it rotates, often defined in terms of the "points gap" clearance observed when the cam-follower rests on the peak of a cam lobe. The angular range, expressed in distributor degrees, over which the points are closed between the cam lobes is known as the *dwell angle* but is typically measured electrically at the points. It is constant (apart from contact noise) at all engine speeds up to a limit at which the large, curved spring in the image is no longer able to close the points effectively between passages of the cam lobes. This condition, known either as *points bounce* or *points float*, will immediately cause ignition timing errors and potential engine damage so the points breaker is designed to be very light (minimising its reciprocal momentum) and free of any harmonic spring resonances in its expected working range of engine speeds. If a breakerless ignition system is used in the MID, dwell angle loses its geometrical relevance and is observed as the coil-primary circuit charging time instead. Retrofit contact sets or breakerless ignition kits from aftermarket part manufacturers will also exhibit different "zero advance" orientations of the distributor with respect to the rotor cam.



At the bottom of the points plate image a peg extending below the plate is visible. This is the attachment point for the vacuum advance unit and is the only point of control of the rotary motion of the points plate. At inlet manifold vacuum levels below the minimum required to operate the vacuum unit, the points-plate is held at an angle corresponding to the static ignition timing set by the orientation of the distributor assembly on the engine block. At higher levels of manifold vacuum the points plate is progressively pulled by the vacuum unit towards earlier ignition discharge timings, up to a limit fixed by the vacuum unit. The points plate also carries a capacitor for arc suppression across the points at opening and adjustments to set the static height at which the cam follower makes first contact with the cam as it rotates, often defined in terms of the "points gap" clearance observed when the cam-follower rests on the peak of a cam lobe. The angular range, expressed in distributor degrees, over which the points are closed between the cam lobes is known as the *dwell angle* but is typically measured electrically at the points. It is constant (apart from contact noise) at all engine speeds up to a limit at which the large, curved spring in the image is no longer able to close the points effectively between passages of the cam lobes. This condition, known either as *points bounce* or *points float*, will immediately cause ignition timing errors and potential engine damage so the points breaker is designed to be very light (minimising its reciprocal momentum) and free of any harmonic spring resonances in its expected working range of engine speeds. If a breakerless ignition system is used in the MID, dwell angle loses its geometrical relevance and is observed as the coil-primary circuit charging time instead. Retrofit contact sets or breakerless ignition kits from aftermarket part manufacturers will also exhibit different "zero advance" orientations of the distributor with respect to the rotor cam.

4.2. Distributor rotor shaft

The central rotating drive shaft that transmits both crankshaft position and speed to the MID is driven by a gear on the camshaft, typically through a spur shaft that engages a flange coupling at the distributor's base. This shaft is housed in a simple bronze-bush bearing lubricated by engine oil which is drawn along the shaft by a helical groove. At the top of the drive shaft is a rotary cam with a lobe corresponding to each of the engine cylinders the distributor services. This cam is not fixed to the drive shaft, but can rotate only over a small angular range with respect to it. The rotor arm discharge contact of the distributor is fixed to the top of the cam and rotates with it to pass each discharge terminal in the distributor cap at the correct point of each ignition cycle.



4.3. Centrifugal advance mechanism

At the centre of the drive shaft a fixed plate carries centrifugal weights (also called *rolling weights*) which constitute the centrifugal timing advance mechanism of the distributor. These engage the rotor cam through pegs and dictate its twist-angle to the drive shaft. Springs hold the weights against each other at low drive-shaft rotation speeds, but centrifugal force moves them apart against increasing spring tension as speed increases. This motion is transmitted to the rotor cam as an increase of its twist angle to the drive shaft and results in an earlier cam lobe contact with the points' cam-follower and opening of the points in each ignition cycle.



Zero centrifugal advance

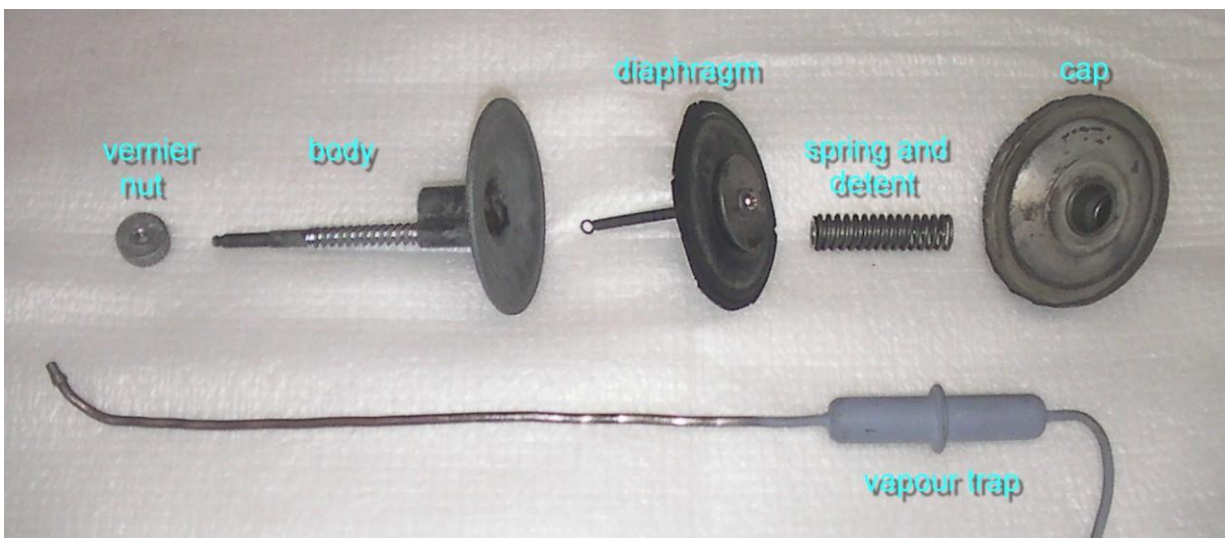


Maximum centrifugal advance

The images above show the centrifugal weights at fully closed (no cent advance) and fully open (max cent advance) positions, for the same orientation of the drive shaft. The pivot centres for each weight are located at the pins to which the springs are attached, at left and right of the carrier plate in each image. The weights' maximum outward displacements are limited by pegs protruding through holes in the carrier plate under each weight. Note the small change in orientation of the rotor cam evident from its peg flange visible atop the lower weight in the image; this small rotation corresponds to the full centrifugal advance produced by this distributor. The two weights are identical in this Lucas DM2 distributor, as are their springs and pivot-action geometry on the rotor-cam pegs, providing a nearly linear increase in rotor angle with increasing engine speed and hence a "flat" *timing curve* or centrifugal timing advance / engine speed relationship. Other models of distributor employ "rolling" weights, unequal springs and/or complex engagement geometries with the rotor cam to achieve nonlinear timing curves. For example, one weight may have a light spring which is fully extended at an intermediate engine speed above which the other weight engages a stronger spring for higher speeds. These timing curves were obtained from a combination of theory and testing by vehicle manufacturers for each set of engine characteristics they produced, and the distributor design was then specialised to reproduce the desired timing curve in the production unit.

4.4. Vacuum advance unit

The image below shows a dismantled Lucas vacuum advance unit from a late-model DM2 distributor. A rubberised-cotton diaphragm is sandwiched between two halves of a vacuum chamber. The left side is always open to atmospheric pressure whilst the right side is always under inlet manifold pressure. The spring extending from the diaphragm attaches to the points plate to drag it forward under applied vacuum, and the large vacuum counter-spring pushes both the diaphragm and points plate back when vacuum drops. Note that the vacuum spring has a central detent peg which limits how much the spring can be compressed by applied vacuum (maximum vac advance). When the two halves of the vacuum chamber are clamped together, the vacuum spring is partially compressed so that a certain degree of vacuum is required to overcome its resistance before the diaphragm begins to move (minimum vac advance). The remaining length of the compressed spring equates to the amount of vacuum ignition timing advance the unit produces between min and max applied vacuum and may be calculated directly by the distance of travel of the diaphragm coupling spring (which is used for its flexibility only and is never stretched), expressed as twice (in crankshaft degrees) the angle through which it rotates the points-plate.



Also shown in this image is the ingenious (patented) way the Lucas engineers permitted the fine adjustment of static ignition timing without moving the body of the distributor. The vernier nut (at left in the image) is held between two surfaces of the body casting so that turning it pushes the screw within it back or forth rather than the nut moving. This screw, extending from the body of the vacuum unit shown beside it, accordingly pushes or pulls the entire vacuum unit back or forth through its recess in the distributor body casting – and so rotates the points-plate attached to the vacuum unit along with it. The vacuum unit retains the same range of motion over the points plate, so the min/max vacuum points and vac timing advance range are unchanged, but the points plate is moved to a new rest position angle (at zero vac and cent advance) with respect to the rotor shaft. There is even a scale machined on the vac-unit body showing crankshaft degrees of timing advance added / subtracted as it moves out of / into the distributor body.

At the bottom of the image is an often-neglected or discarded but crucial part of the vacuum advance control: the vapour trap. This prevents fuel vapour that condenses in the vacuum feed pipe from draining into the vacuum chamber of the vacuum advance unit. In its absence, fuel will build up in the vacuum chamber, causing the rubber diaphragm to harden over time and eventually perforate – at which point the unit ceases operating and a small permanent air leak into the inlet manifold results. The vapour trap must be mounted *vertically* at a point above its connection to the inlet manifold or carburettor union, so that condensed fuel can drain back to the manifold. It does *not* impose any significant delay to the reaction time of the vacuum advance unit whatsoever.

4.5. Rotor arm

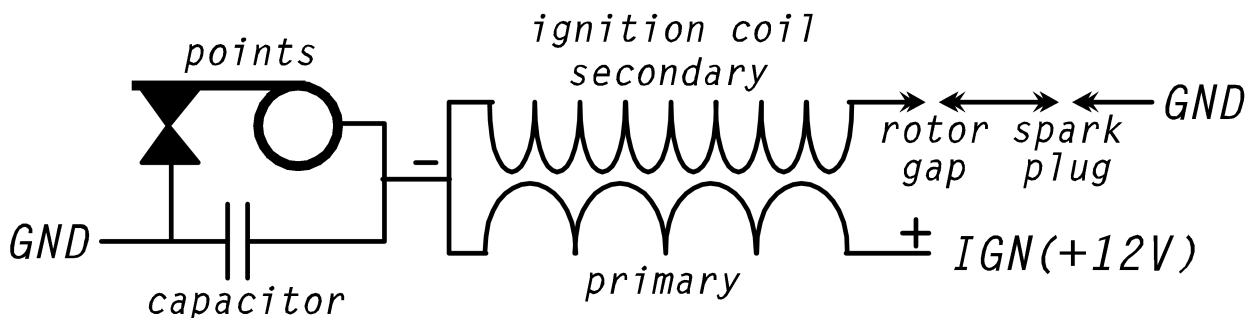
The rotor that sits atop the cam on the driveshaft is electrically insulated from the parts below it, so it can conduct the electrical discharge from the coil from a carbon contact brush on its spin axis, along its length and across a small air gap to each terminal post in the distributor cap as it rotates. The arc-discharge end of the arm must be wide enough to find the appropriate terminal for all amounts of timing advance produced by the distributor, as it is twisted forward in its motion by cent advance and also sees an earlier discharge from vac advance. This permits a ready assessment of the overall timing advance



range of a distributor by inspecting the arc-scorch track on the edge of the rotor arm after first polishing it before a sustained period of road use. The angle subtended at the rotor centre by the length of the scorch track is equal to half the total timing advance in crankshaft degrees. In the pictured case, a track of length 7mm at a rotor-arm radius of 21.5mm subtends an angle of 18.7 degrees at the rotor centre, giving a total dynamic advance (sum of vac and cent) of 37.4 crankshaft degrees, which tallies well with the known max vac advance of 16CD and max cent advance of 22CD (total 38CD) for this particular unit.

5. Ignition circuit electrical theory

The deceptively simple ignition circuit shown below constitutes the basis of the MID ignition system. The points and their capacitor are housed inside the distributor and their common GND connection is made through the distributor body to the engine block. The ignition “coil” actually consists of a primary coil wound around a secondary coil and sharing a common connection at the points terminal end. At ignition, the high-voltage discharge from the secondary coil crosses air-gaps from the rotor to distributor cap terminal post and then across the spark plug gap to GND potential at the engine block. The electrical circuit is completed to the vehicle battery via the engine earth strap to the chassis and the coil primary connection to the IGN supply. These last two often-neglected connections are critical to the performance of the ignition system and must be included in the analysis of the ignition event sequence when using points voltage levels as a reference.

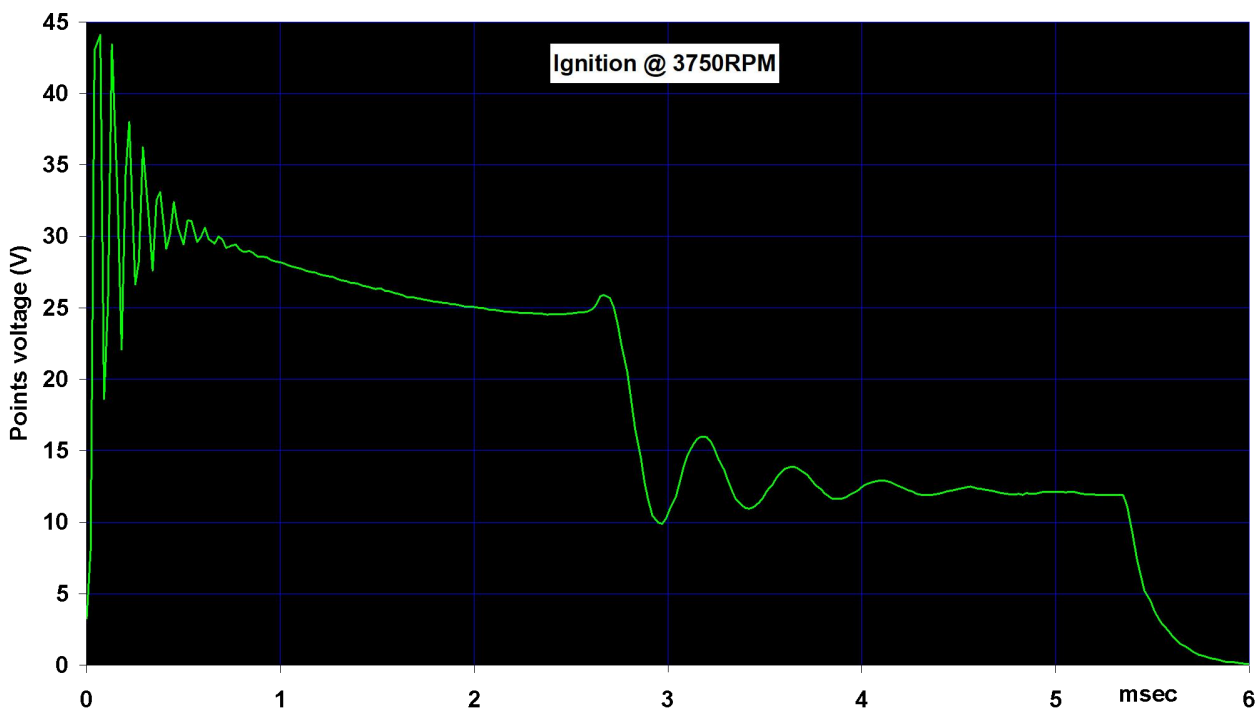


Two electrical circuits comprise the ignition system: the ignition coil primary (charging) circuit and its secondary (discharging) circuit. The secondary circuit conducts the high-voltage discharge from the coil to the spark plugs via the rotor arm and distributor cap and is isolated electrically from any other components to prevent arcing or charge leakage. Direct analysis of coil discharge characteristics may only be performed with specialist equipment and is beyond the scope of this document. However, the correct function of an ignition coil in good condition may be established by the analysis of current flow in its primary circuit via measurement of voltage across its terminals, or equivalently across the points contacts that control its charge state. The sequence of electrical events that constitute an ignition charge/discharge cycle must be understood to gain any information from these observed voltage values.

The two coaxially-wound wire coils forming the ignition coil unit are designed to develop and maintain a static magnetic field while the primary coil carries a constant current. The two coils are wound with opposite handedness so that the magnetic field established by charge current in the primary will induce current flow in the opposite direction (away from the points) in the secondary coil at discharge. As the secondary coil has many times more windings than the primary, a far larger potential difference will form across its extent with any *change* in magnetic flux through its windings. While the points remain closed, current only flows through the primary windings and ground potential exists at the secondary output terminal. Immediately upon points opening, the points capacitor appears to the coil primary as an alternative virtual short to ground, thus protecting the points from forming a high-voltage discharge arc. The points capacitor then reaches 12V charge saturation and current flow through the primary circuit ceases, causing the magnetic field in the coil to collapse. Induced current flow in the coil secondary will now drive up the capacitor charge further to produce a potential “spike” in excess of 100V instantaneously at their common connection point, the open points terminal. Crucially, the points capacitor *detunes* resonant discharge of the secondary coil back through the primary while magnetic induction occurs - too little or too much points capacitance would allow the secondary to discharge conductively before breakdown potential is achieved. Instead, reverse current through the coil primary creates an opposing magnetic field to that of the secondary coil, thus limiting the amount of current the secondary can discharge back through the primary (the primary is said to “choke” this reverse current). This results in a rapidly increasing *virtual* potential at the points relative to the secondary

coil's discharge terminal, and a voltage of 20-40KV develops across the secondary coil until the series (dielectric, *not* thermionic) breakdown potential of air at the distributor-rotor to terminal-post gap and the gas mixture in the engine cylinder at the spark-plug gap are both exceeded and ignition spark discharge occurs.

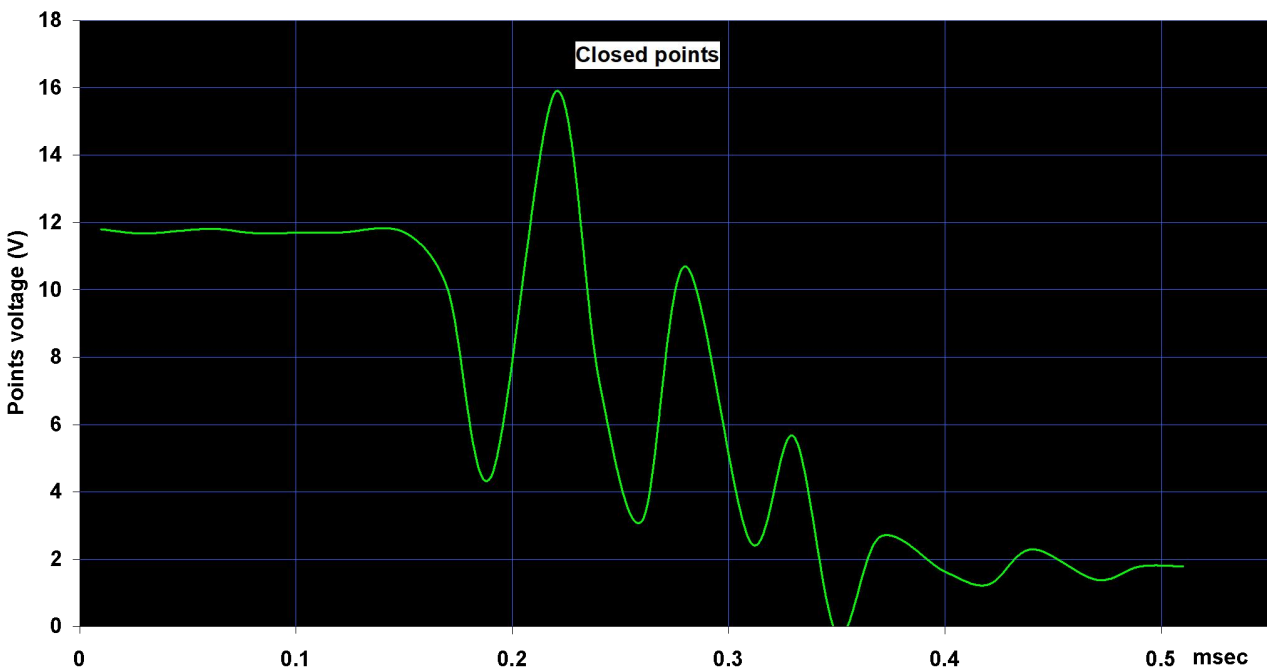
As the stored magnetic flux in the coils dissipates, the voltage at the distributor rotor spark gap eventually falls below the air-breakdown potential and the spark discharge ceases. Remaining magnetic flux then induces current to flow through the two coils back to the supply terminal. The points capacitor also discharges back through the coil primary, which having only a 12V potential at its opposite terminal now appears as a virtual earth to the points capacitor. Small "ring-down" currents may continue to resonate between the coil primary and secondary windings while the points remain open. At the instant of points contact, the uncharged coil primary circuit appears as a short-circuit to the vehicle's power supply and the coil commences recharging through the closed points contacts with an initial inrush current in excess of 10A before the magnetic field in the coil is re-established, falling to a steady 6A after 1ms. The points capacitor discharge current from only 12V at points closure is negligible by comparison. Although the points are intended to transmit such current surges, a small electrical resistance arises across them maintaining a positive potential voltage on the coil side of the points during the current surge. If this potential remains above a set detection threshold due to points-contact damage or insufficient grounding, it is seen by our instruments as an extension of the open-points duration and reported as a reduction of the measured dwell duration.



The oscilloscope capture shown above illustrates the described phenomena within a single ignition cycle for a ballasted Bosch "Red" GT40R ignition coil and 0.22 μ F points capacitor. Capacitive input coupling limits the amplitude of high frequency features in the plot. The green curve represents the observed points voltage from the moment of points opening, as the coil primary circuit current "rings up" due to induced secondary coil current passing back through it to the supply terminal. The ringing effect is caused by resonant energy transfer between stored magnetic field and induced current in the coils and is limited in magnitude by the points capacitor. Periods of field generation and re-induction will alternate until equilibrium is reached and the discharge current stabilises. The secondary coil is fully discharged after 2.5msec, after which the points voltage "rings down" to 12V just before the points close. Note that the actual current flow in the coil primary circuit is negligible after the ignition discharge is complete while the points remain

open. The coil primary inrush current then maintains the *closed* points voltage above zero for a further 1.2msec.

Rather than being defined by zero points voltage, the conventional *dwell angle* represents the distributor rotation angle over which the points are physically closed. Referring to the plot above, the steep voltage increase produced by the ignition coil primary circuit at points opening furnishes an exact reference endpoint for the dwell interval. However, the slower decay of points voltage after points closure due to inrush current makes the exact instant of physical points closure more difficult to discern. In extreme cases of insufficient points circuit grounding or high points-contact resistance, the closed-points voltage even may be seen to “ring down” towards zero as the coil charges, as is seen in the following oscilloscope plot. This time delay to the points voltage reaching zero after points closure will be *constant* for each ignition cycle, whereas the duration of each ignition cycle will *decrease* with increasing engine speed, so that the apparent dwell duration as measured by points voltage will be seen to decrease linearly with increasing engine RPM. Accordingly, a measurement of “dynamic” dwell duration (as opposed to geometrical dwell angle) as a function of engine speed affords information about the state of the coil primary charge circuit as well as the points-contact gap setting. This will be examined in more detail in section 10.3.1.



For the purpose of measuring ignition timing and dwell duration, the actual points voltage between the opening and closing events described above is largely immaterial. The high-voltage transient discharge “spike” at points opening does not contribute to the ignition timing or dwell angle measurements, with its peak value occurring up to 1ms after the points open. In fact, voltage-integrating capacitive dwell meters must specifically exclude this spike (typically using a choke and Zener diode) to obtain a correct reading. Ringing of the coil primary circuit may have sufficient amplitude to reduce the apparent points voltage to zero instantaneously. To preclude these phenomena from biasing our timing measurements, we must select specific representative points voltages as reference levels for our timing intervals and then design our measurement circuits to register them only, based on this understanding of the electromechanical ignition system.

5.1. Accurate determination of the points state

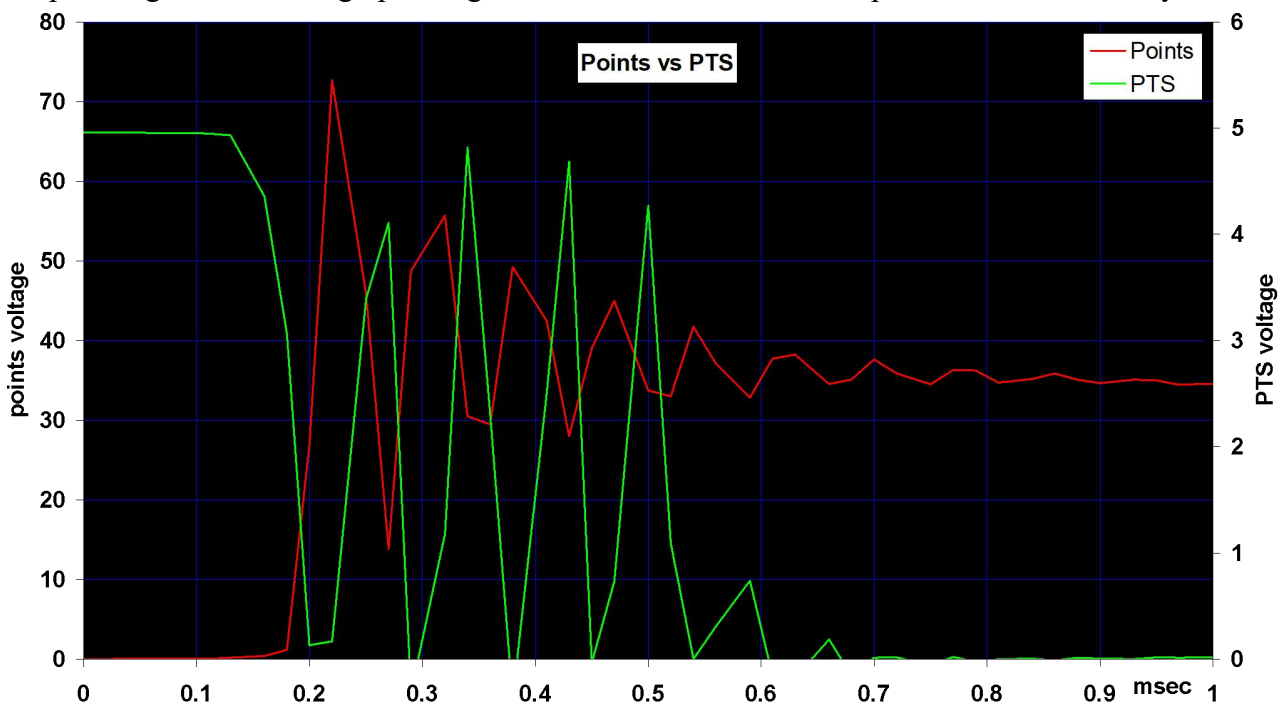
The preceding section describes the phenomena that complicate determination of the state of the ignition primary circuit as measured by points voltage. Any scheme to identify specific points in the ignition sequence accurately must be unambiguous, precise and robust with respect to ignition system electrical noise. For example, measuring coil primary circuit current could be achieved non-

invasively by detecting the magnetic field produced by the wire connecting the points to the coil. Notionally, this field will be present when the points are closed and $\sim 6A$ is conducted through the coil primary. In practice however, this field is relatively small in magnitude and any magnetic flux detection scheme sensitive enough to measure it will be prone to extraneous noise from the remainder of the ignition system. Resolution of the termination points of the magnetic flux signal is also reduced by ringing currents between the two coil circuits. With regard to achieving a measurement of the *effective* dwell (points closed) duration during which the ignition coil is held under charge, we can investigate simple electrical circuits that interpret the points voltage to obtain this value using basic analog signal processing.

As the connection point between the points capacitor and ignition coil secondary winding joins with the points, to prevent reduction of discharge current from the ignition coil any extra permanent connection made at this junction must not abstract significant current from nor add effective capacitance to the circuit. In particular, these criteria must be observed for peak discharge voltage which exceeds 100V over several microseconds. The image at right shows the *normal* points gap discharge arc at 5000RPM present despite the action of the points capacitor when a high-performance ignition coil (Bosch “Red” GT40R) is used. As well as being a source of electrical noise within the primary ignition circuit, this arc is a considerable source of RF noise for any nearby electronics and the 6A+ currents being switched by the points will produce significant local point potentials above battery ground in the points plate and distributor body. To obtain reliable voltage levels from such an environment requires a high-impedance detector with effective noise filtering and screening.

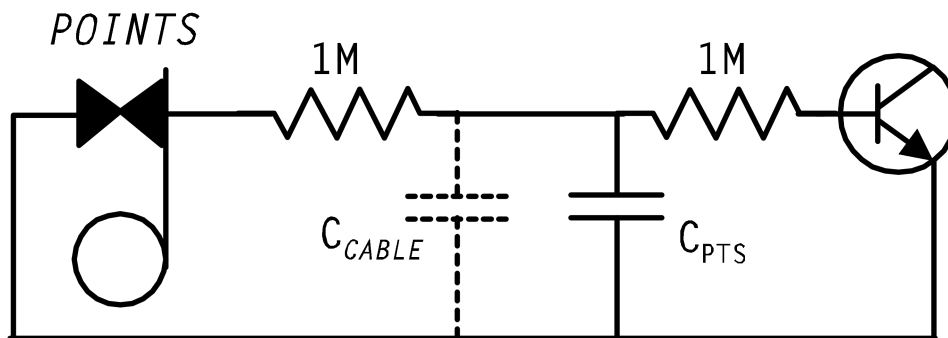


As the goal of dwell duration measurement dictates a simple on/off output signal representing the coil primary charge current state (as opposed to the notional points state), a transistor switching a constant supply voltage must form the output stage of an idealised “points state sensor”. This transistor must be biased to switch on at a precise voltage level on the rising edge of the points voltage at opening and then switch off at a similar voltage level when the points close. Apart from the pathological case of high points-ground resistance shown in the previous section, it may be



expected that switching at fixed levels of a few volts above ground potential should be sufficient to discern the notional points state simply by connecting the transistor to the points via a large-value resistor. This scheme would furnish a representative value of the points voltage with no additional points capacitance and less abstracted coil primary circuit current than is lost normally to leakage from the points capacitor. Unfortunately, transient ringing voltages produced by the coil will range from more than 100V to less than 0V at the points terminal over microseconds, to which the transistor will exhibit full-range switching in response as the oscilloscope plot above shows. The PTS curve represents output from a PN100 biased to switch fully on at 3V in response to an active ignition primary circuit (points voltage curve, capacitively attenuated) connected to its base via a 2M resistor. The points voltage “ring-down” to 12V at the end of the secondary coil discharge may elicit similar behaviour from the transistor at the initial voltage drop.

Strategies to counter the high-frequency transient voltages present in the points signal such as the use of a FET, choke or capacitive filtering all introduce time delays to the desired output signal. This would not be a problem with a symmetrical source signal, where such delays could be arranged to cancel out and produce a (meaningless) phase shift instead. The high-impedance input criterion of our points state detection circuit precludes the use of a choke and Zener diode to furnish such a symmetrical signal as in conventional dwell meters. With a view to other practicalities such as the physical location of a points “buffer” transistor circuit outside the distributor itself, circuit simplicity, minimal component count and the observation that the coil discharge voltage transient phenomena occur over relatively short timescales relative to the ignition timing and dwell durations, the strategy employed in our timing circuits to counter this problem consists of splitting the input



impedance over two series resistors, one of which is connected directly to the points and is located in the distributor, and the other on the transistor input. This arrangement permits the addition of a small filter capacitance at the junction of the two resistors where it will not add to the points capacitance and will have minimal effect on the transistor’s response curve. Where the transistor is located outside the distributor, this filter capacitance will be imposed wholly or in part by cable capacitance between the two resistors; otherwise it must be included as a fixed capacitor. Crucially, any time delay to detection of the points opening introduced by the filter capacitance will be constant for all engine speeds and so may be offset completely in the definition of our ignition timing reference strobe sensor location. In contrast, the measured dwell duration will be affected by the asymmetrical transition voltages at points opening and closing in proportion to their relative magnitudes. The drop from 12V at points closing will add a greater delay than that from the large rise in voltage at points opening, resulting in a net constant delay time subtracted from each dwell interval. As these angularly-defined intervals decrease linearly with increasing engine speed, subtracting a constant delay time from each interval will result in linearly decreasing reported dwell duration with increasing engine speed instead of a constant dwell time, expressed in DD. Such default behaviour of the dwell “curve” must be characterised so that any departure from it can be used as an indicator of ignition primary circuit condition. It may be excluded from our instruments via a systematic correction where this is readily achieved.

6. Measurement of ignition timing in the MID

As a simple mechanical computer designed to perform a specific task without supervision, the MID offers no ready means of analysing its functions accurately *in situ* without temporary attachment of a set of diagnostic equipment on a roller-bed dynamometer. In contrast, a modern electronic engine management system can collect and store engine state data continuously for subsequent analysis. Some of the functionality of the latter can be replicated in the MID to allow fault analysis and / or tuning optimisation of the ignition system. In this section we examine the tasks required to measure timing characteristics accurately in the MID and design simple electronic circuits to collect, display and store the resulting data in real time.

6.1. Periodic MID events and engine speed

The shaft that drives the MID turns at half-crankshaft speed and reproduces uniquely the position of the pistons in their respective cylinders at each point in its rotation. This permits a one-to-one mapping of rotor angle in the distributor to ignition lead terminal for each serviced cylinder. Thus in the case of the 4-cylinder 4-stroke engine the distributor full rotation of 360DD is divided into four quadrants of 90DD, each representing 180CD or a single stroke of the associated piston. The physical orientation of the distributor on the engine is chosen to discharge the ignition coil to each cylinder as it approaches the end of its compression stroke. Importantly, this process must remain stable and accurately synchronised with the crankshaft over the full range of engine speeds produced. There are two time intervals managed by the distributor that achieve this result:

6.2. Dwell angle

The conventional definition of breaker-points “dwell angle” is the angular distributor rotor rotation interval (in DD) over which the points are physically closed, with the intention of providing a relevant figure in device units for the period over which the ignition coil primary circuit receives charge. The points-open duration is thus 90DD minus the dwell angle.

The distributor is required to recharge the ignition coil fully between discharges, despite the short time available to do so at high engine speeds. When the rotor cam opens the points, the ignition coil is immediately discharged while the points remain held open by the rotor cam for a fixed angular fraction of its rotation. After the cam has rotated through the required angle, the points close and the coil commences recharging. The points must remain closed long enough to fully recharge the coil at the highest attainable engine speed. Accordingly, the points open and closed durations are selected to achieve both full coil discharge and recharge in the available time at full engine speed. These durations are set by the symmetric geometry of the rotor cam to be constant at all engine speeds and identical for each engine cylinder. As the cam rotates, the fixed angles of opening and closing correspond to a time interval that decreases linearly with increasing rotation speed of the cam. This means that at low engine speeds, the coil primary circuit is held open to discharge and closed to recharge for much longer than is necessary. A modern ignition system (or a good breakerless electronic points replacement for a MID) uses a fixed coil-recharge time instead to reduce wasted energy and heating of both the coil primary circuit and its own power transistors.

Dwell angle is typically obtained from a time-averaged measurement of the voltage across the points of a running engine at idle speed ONLY, scaled into DD against a reference calibration. Meters to measure the dwell angle dynamically in a points-based MID use a convenient electrical fact to obtain this value non-intrusively: as the duration of each discharge cycle decreases with rising engine speed, there are more such cycles per second such that the *average* time that the points are open for is also constant, again set by the fixed angular geometry of the rotating points cam. Accordingly, the dwell angle measurement should be independent of the engine speed. This permits a simple time-averaged DC voltage measurement to obtain the dwell angle within a few DD, and can be performed with a high-impedance digital voltmeter (DVM) at the coil terminals: simply divide the voltage seen *between* the coil primary terminals at engine idle by the voltage with points

closed and multiply by 90DD to obtain the conventional dwell angle. At low RPM, the DVM may oscillate with a beat-frequency between its sample period and the ignition cycle period necessitating a time-averaged reading. However, such dwell duration measurements will be biased downward by the ignition discharge voltage “spike” present at the points upon opening, and the requirement that the dwell measurement is made at engine idle minimises the number of these spikes contributing to the time-integrated points voltage. In contrast, the analog dwell meter circuit presented in section 8.2 may be used together with any voltmeter to measure dwell angle accurately across the engine speed range for any MID without modification.

6.3. Ignition timing angle

As we have seen, the rotor angle at which the MID discharges the coil with respect to the piston position in the appropriate cylinder is in parts both pre-set (static) and variable (dynamic). As the MID timing scheme omits an absolute reference for crankshaft position, there is no way to ascertain the absolute timing with respect to piston position as exists in crank-triggered electronic ignitions. To this end we have to introduce a mechanism to obtain an absolute timing reference into the MID. This can be done by fitting a crankshaft (or timing-belt pulley, or flywheel) position sensor and measuring the time interval between an ignition discharge and its reference signal. As this information actually *is* present already in the MID in the form of its absolute input-shaft angle, a sensor placed inside the MID can provide the necessary information whilst being minimally intrusive on the engine. The presence of a timing signal corresponding to (for example) TDC of the compression stroke would then permit a simple timing circuit to measure the time interval between ignition and TDC, and this would include the static and dynamic contributions to ignition timing. By convention, ignition timing angles are quoted numerically in crankshaft degrees *before* TDC (BTDC) yielding an increasing value with increasing timing advance. As the point of ignition is readily detected by monitoring the points state, it is convenient to place our timing signal *later* in the ignition cycle to produce a time interval directly proportional to the desired value. Better still, as an angular-rotation defined quantity, this time interval decreases with increasing engine speed but increases in frequency analogously to the dwell angle measurement, allowing a similarly simple time-averaged voltage measurement by the timing circuit to obtain a value for the timing angle. Engineering a rotor shaft angle sensor into the MID is the only difficult task in obtaining an absolute timing angle measurement.

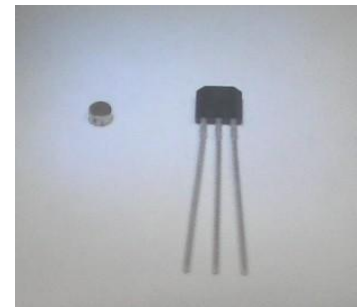
A timing scheme based upon measurement of the rotor shaft angle relative to the MID itself introduces one calibration issue – most period MIDs were designed to permit their mounting on the engine block at any angle with respect to the distributor drive jackshaft, by means of a simple pinch clamp on the neck of the distributor. This arrangement permits the correct static advance setting to be achieved *irrespective of the actual points gap present* by rotating the distributor body until the desired static advance figure is observed on a timing reference instrument at engine idle, typically at the crankshaft pulley. As our proposed timing sensor must be fixed to the body of the distributor, timing values will be reported with respect to the specific orientation of the distributor on the engine. Accordingly, in the following discussion of timing sensor location in the distributor in absolute crankshaft degrees (CD), it is assumed that the latter is correctly oriented on the engine for the nominal points gap setting. Note that once a sensor location in the distributor has been fixed and determined relative to the crankshaft, changes in static ignition timing due to points gap variation, points plate rest position shifts or cent mechanism rest-state offset error will be reported correctly by the timing meter unless the distributor mounting angle is altered. It is highly recommended that some form of datum marking between the distributor and engine block is made for future reference after the intended static timing is established for a correct points gap setting.

7. An electronic timing sensor for the MID

An examination of the above section on MID components presents a convenient location for a shaft-angle sensor to obtain absolute crankshaft position by proxy: the edge of the centrifugal-advance mechanism carrier plate (cent plate). This plate offers the largest radius-of-rotation of any component in the distributor and thus the greatest angular resolution at its circumference. We can adopt the technology used to sense periodic rotary motions by modern electronic ignition systems: either an optical notch sensor or magnetic sensor. As the cent plate is exposed to engine oil vapour from the distributor drive shaft, the magnetic sensor is a more prudent option. This can be fixed to the inside of the distributor body at the edge of the cent plate to sense either a notch (with a coupling magnet behind the sensor) or a magnet attached to the cent plate. The sensor can be placed anywhere around the edge of the cent plate and the notch or magnet positioned at the edge of the plate at some convenient reference point, for example corresponding to TDC on #1 cylinder. This position on the cent plate can be established by manually rotating the crankshaft to the 0CD position on the #1 compression stroke and marking both the cent plate and distributor body at the desired location of the sensor. As the sensor will lie below the fixed plate carrying the points it will be well shielded from transient magnetic fields and electrical arc noise from the rotor above.

7.1. Case study: timing the Lucas DM2

The choice of sensor geometry and layout represents a good basic exercise in electromechanical design. Given the limited space available within the distributor body at the edge of the cent plate, a small Hall-effect magnetic flux sensor such as the UGN3503UA by Allegro MicroSystems is a good candidate for a magnetic flux sensor in this application. Designed in 1978, this inexpensive IC remains the most widely available compact Hall-effect magnetic sensor, providing a linear output voltage gain with increasing intercepted magnetic flux.



The width of its active sense region is 0.5mm, potentially providing an angular resolution of the output-pulse rising edge of 1DD with a similarly-sized notch at the cent plate radius of 28mm. Assuming a maximum engine speed of 6000RPM, the highest frequency seen by this sensor would be $6000 / (60 * 2)$ or 50Hz, which is relatively slow. More of an issue is the engine idle speed: taking 600RPM as a convenient value, a 5Hz signal is too slow to integrate effectively in a circuit that should also provide a dynamic output of timing transients in real time. Upon further consideration of the quantity we seek to measure accurately – dynamic timing *advance* – we can make a design decision to sacrifice absolute timing of a particular engine cylinder stroke in favour of making an averaged measurement over all equivalent timing intervals in all the engine cylinders. This is reasonable as the timing intervals are supposed to be identical anyway, set by the symmetry of the rotor cam, and any transient dynamic timing phenomena we may seek to observe would occur in more than one complete distributor rotation. Physically, this change would be achieved by using four notches spaced 90 degrees apart around the cent plate instead of one, yielding a 20Hz timing signal at 600RPM and 200Hz at 6000RPM - still slow, but better in the mid-to-high speed region where an accurate analysis of dynamic timing is more important.

The next design issue we face in the use of the magnetic sensor is its signal size and duration as a function of engine speed. It is very difficult to calculate actual magnetic flux density across the device geometrically and would require a prior characterisation of the source magnetic field. Practically, it is much easier to build a test rig and observe the output of the device for a range of flux density change gradients. Doing this using the manufacturer-recommended 5VDC supply voltage and geometry of a small neodymium coupling magnet mounted immediately behind the sensor, with a notch in a rotating mild steel plate directly in front of it produces a millivolt-scale pulse signal at notch frequencies in the range 20-200Hz. Amplification of such a small signal in an electrically noisy environment such as inside an automotive ignition system is not conducive to reliable measurement. Increasing the magnet size, notch size or number of sensors around the plate

will not appreciably increase the signal-to-noise ratio either. More recent designs of Hall-effect sensor ICs offer higher magnetic flux sensitivity and better thermal characteristics but may be difficult to source (see section 13). The only remaining option is to replace notches on the cent plate with magnets and omit the magnet behind the sensor, potentially to replace it with a mild-steel pin to couple magnetic flux if the distributor casing is non-ferrous. This reversal of the magnet geometry produces a more concentrated magnetic flux gradient at the sensor. In particular, the sensor will only register flux cutting through its small active diameter so the magnet need not be any larger physically if it produces sufficient flux density at the sensor. A further test using 2mm-diameter, 1mm-thick neodymium magnets rotating in front of the sensor produced 1-volt pulses using the UGN3505UA, a far better signal-to-noise ratio requiring minimal amplification for accurate pulse registration. In comparison, the similarly-sized Texas Instruments DRV5056A1 magnetic sensor produces a 4-volt pulse (4.6 volt amplitude above a 0.6V quiescent level) in the same test configuration and includes thermal compensation for the drop in magnetic flux due to magnet heating at engine running temperatures. Examining the available sensor options detailed in section 13 before committing to a MID installation is highly recommended.

The pulse width produced by the sensor is given by the arc-length of the magnet's transit across its 0.5mm-wide active region. Again, as we are considering fixed angular rotation intervals, we can express the sensor pulse width in terms of geometrical angles which are constant for all engine speeds. At the cent plate radius of 28mm, 1DD corresponds to a width of 0.49mm. Thus a 2mm-magnet crossing the sensor subtends an angle at the rotation axis of $(0.5 + 2 + 0.5) / 0.49 = 6DD$ (full-width) or a crankshaft duration of 12CD. In practice, the full pulse width from the sensor is not used. We only require a fixed voltage level on the rising edge of the pulse as our timing reference point and this will remain angularly fixed with respect to the distributor drive shaft (and hence crankshaft) for all engine speeds. The sensor response time must be much faster than the maximum distributor sector speed such that the pulses do not decrease in amplitude with rising engine RPM.

The most intricate task in engineering this sensor into the MID is fitting the small magnets to the cent plate. Depending on the specific make and model of distributor, this plate may have a shape that complicates the selection of a set of locations to place the magnets. In some cases it may be more prudent to consider a different location altogether, such as the underside of the cent plate, with a protrusion to carry the sensor. If a max cent advance restrictor plate is being used in the DM2, the magnets may be fitted to it instead of the cent plate (see section 16). Alternatively a metal or plastic ring may be fixed to the cent plate to carry the magnets. In our case, the cent plate is 2mm thick, barely enough to fit the 2mm-diameter magnets into its edge. Our specification of neodymium magnets for this task is based on their high relative strength and common availability in small sizes, although typically they lose 10% of their magnetic flux density at engine temperatures and better alternatives such as alnico or Sm-Co rare-earth magnets may be used with more sensitive current-generation magnetic flux sensors (see section 13).

If the intention is to make a road-worthy permanent MID installation, it is important to ascertain the condition of the unit first. If the rotor cam can be felt to move laterally when pushed across the distributor, the drive shaft bush is too worn for accurate ignition timing to be performed by the unit. If a better unit is not obtainable, the unit must be re-bushed by an expert machinist. If so, have the unit returned disassembled to permit access to the cent plate, or better still have the machinist perform the task of attaching the magnets. Otherwise, the DM2 requires the removal of a parallel pin securing its drive flange to its drive shaft for removal of the latter. This must be performed carefully, with both the distributor body and drive flange supported securely to prevent the drive shaft being bent. First, punch mark both the drive flange and the exposed end of the drive shaft to retain their relative orientation at refit. The tapered end of the parallel pin will be visible on one side of the drive flange and must be driven out with a punch and mallet from this side. As this pin is likely to have been in place for more than half a century, it may take time, lubrication and patience to free it. Remove the drive flange and flange washer under it then withdraw the drive shaft from the distributor body. Do not lose the plastic float spacer under the cent plate on the drive shaft. After

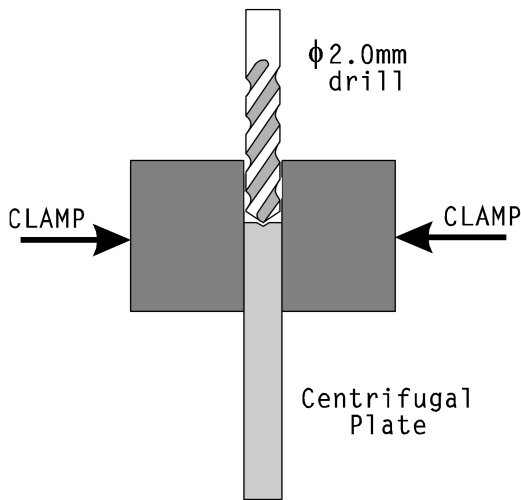
removing and cleaning the distributor drive shaft assembly, dismantle the cent mechanism and note any points of excessive side float on the pivots for the rolling weights and rotor cam. The easiest path to reconditioning this mechanism is to replace components where possible. Alternatively, pivot holes can be bushed and the brass cam linkages brazed over and re-drilled. The rolling-weight springs must at least keep the weights closed at rest – however these may be swapped out later if different cent-advance curves are being tested. In particular, if the rotor cam is heavily tracked across its cam lobes it may be too worn to use with a new set of points (but perfectly adequate for use with a breakerless ignition kit). The rotor-cam is one component that is frequently remanufactured for popular MID versions.

Our previous discussion of the possible layout of sensor and magnets around the cent plate suggested placing one magnet beside the desired sensor position at the observed location of #1-cylinder TDC and the rest at 90-degree intervals around the plate. This assumes the distributor body is oriented on the engine for correct static ignition timing, which is set by the rest position of the vac advance and points plate. If the distributor has a vernier static timing adjustment, this should be set to zero (centre of vac-unit body scale) prior to the static timing procedure. The points plate may then be removed from the distributor *in situ* to mark a position on the cent plate. The choice of #1TDC for the sensor signal is arbitrary; however for reasons explained later it is ideal to include at least 5DD more duration, or 10CD after TDC (specifically, at least the largest static timing angle ever likely to be needed plus the maximum vernier-adjustment retardation angle, both in DD), to provide a positive meter-scale timing offset. Even more may be needed if it is desired to time distributors using a vacuum retardation unit. The exact value of this offset from TDC does not matter, as it will be scaled out in the calibration of the timing meter. It can be set by turning the crankshaft by the required angle in CD past TDC and marking the cent plate against the sensor position, or leaving the crankshaft at #1TDC and marking the cent plate the required angle in DD *clockwise* from the sensor position, noting that 10DD = 4.9mm at the edge of the cent plate.

Using a retired DM2 to make a bench-test prototype, the UGN3505UA sensor was located beside the lower air vent with its leads oriented upwards along the inside of the distributor body towards the electrical terminal plate and the magnets adjacent to the pivot pegs and halfway between them on the cent plate, producing a sensor angle of about 27CD ATDC. Fix these parts as follows:

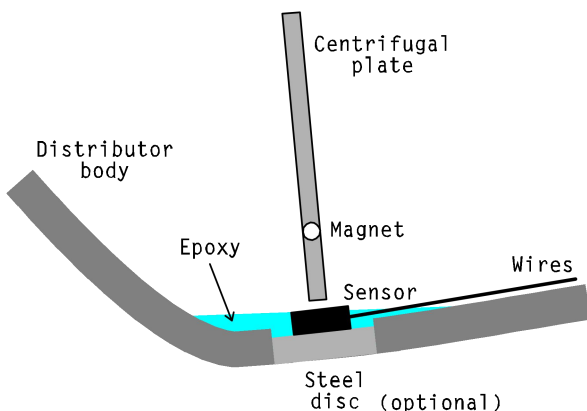
7.2. Magnet mounting

First fit the magnets to the cent plate before fitting the sensor. Once having decided the circumferential location of the first magnet by the above method, mark and centre punch a drilling point at the vertical centre of the edge of the plate. Clamp small pieces of flat steel on either side of the plate around the drilling point to help prevent drill bit wander. Use a drill press if available and sharp 2mm-diameter drill bit to drill a hole no more than 1.5mm deep after ensuring the plate edge is completely square to the drill, both radially and vertically. Repeat this process at precise 90-degree intervals around the edge of the cent plate. Next, locate the south pole of each magnet by passing it across the front (chamfered, printed) side of the sensor while monitoring the sensor output. A single rising voltage pulse for a passage of the magnet indicates its south pole. Mark the side of the magnet facing the sensor with a permanent marker then attach the *marked* side to a flat screwdriver blade. With the drive shaft supported in a vice, place a small drop of superglue in the drilled hole at the edge of the cent plate and position the magnet on top. Warning – the magnet is likely to flip over as it approaches the hole unless it is already attached to a steel surface. **Gently** tap the magnet into the hole and slide the screwdriver away. Check that the marked side of the magnet is facing outward or use the sensor to ensure its correct pole orientation. If the magnet is not yet flush with the edge of the disc, place a piece of wood or plastic over it before further gentle tapping to avoid shattering it. Do not tap-fit unplated rare-earth Sm-Co magnets as they will shatter.



7.3. Sensor mounting

With the cent plate fitted, check for sufficient space between the extreme edge of the cent plate and the distributor body to fit the chosen sensor in-between with at least 0.5mm of clearance. If not, a flat recess may be created at the desired location in the distributor body side wall using a miniature grinding tool to permit a sensor-plate clearance of 0.5mm there. In other distributors, if the sensor must be mounted on a platform to reach the magnet-rotation arc it is ideal to use a 3mm-diameter mild-steel pin or screw directly under the sensor to act as a magnetic flux coupler. In non-ferrous bodied distributors a similar mild-steel disc may be located under the sensor to improve the output signal, but ascertain any potential for improvement in a mock-up assembly first. Solder leads to the sensor and insulate their exposed length with heat-shrink tubing. With the drive shaft and its plastic float ring in place in the distributor body, place the back (flat, unchamfered side with no printing) of the sensor against the distributor body and position it such that the centre of the sensor package aligns vertically with the centre of the cent plate edge. The height must align within 0.5mm and the sensor-magnet separation less than 1mm from each other for a good signal using the UGN3503UA. Clip it in place temporarily using some tweezers held shut with a rubber band. Connect the sensor to a 5VDC supply and check its output as the cent plate is rotated past the sensor. It should read about 2.5V with no magnet nearby and at least 3.5V with a magnet directly above the sensor for each magnet on the plate. Nudge the sensor up or down the body of the distributor to maximise the observed voltage for all magnets on the cent plate. When an optimal position is achieved, place a drop of superglue under the sensor and hold it in place until the glue sets. Check that the sensor output remains optimal. If the sensor is misaligned, it can be freed by soaking the glue repeatedly in acetone until it detaches. When satisfied with the sensor position, disconnect the sensor and remove the drive shaft from the distributor body before placing the latter in a vice sideways such that the

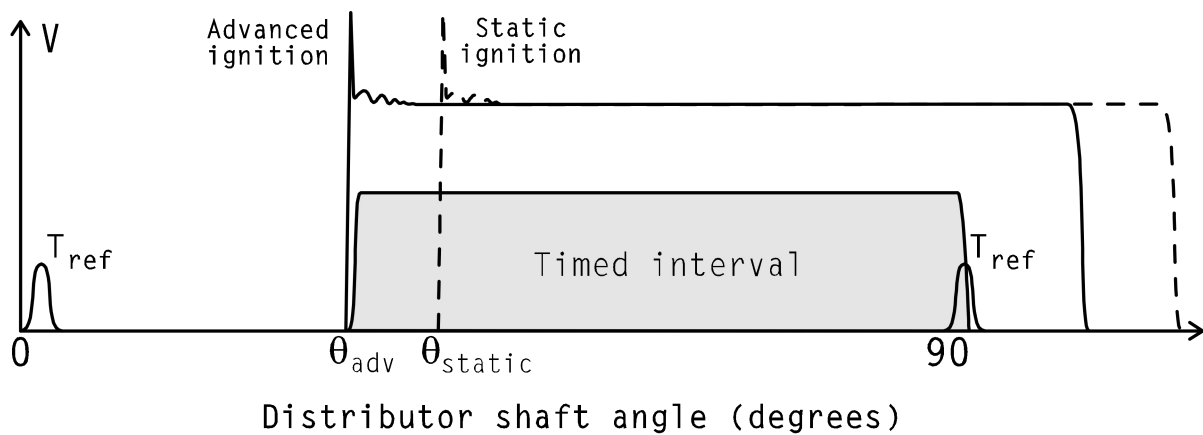


sensor is horizontal and facing directly upwards. Drip just enough epoxy glue around the sensor's edges to form a puddle around the sensor and its leads, flush with its surface. Once the glue has set the drive shaft and its float spacer can be refitted and the sensor output re-checked before the flange washer is replaced and the drive flange fixed to the drive shaft, noting the correct orientation of these before refitting the parallel pin from the same side it was driven out of, tapered end first.

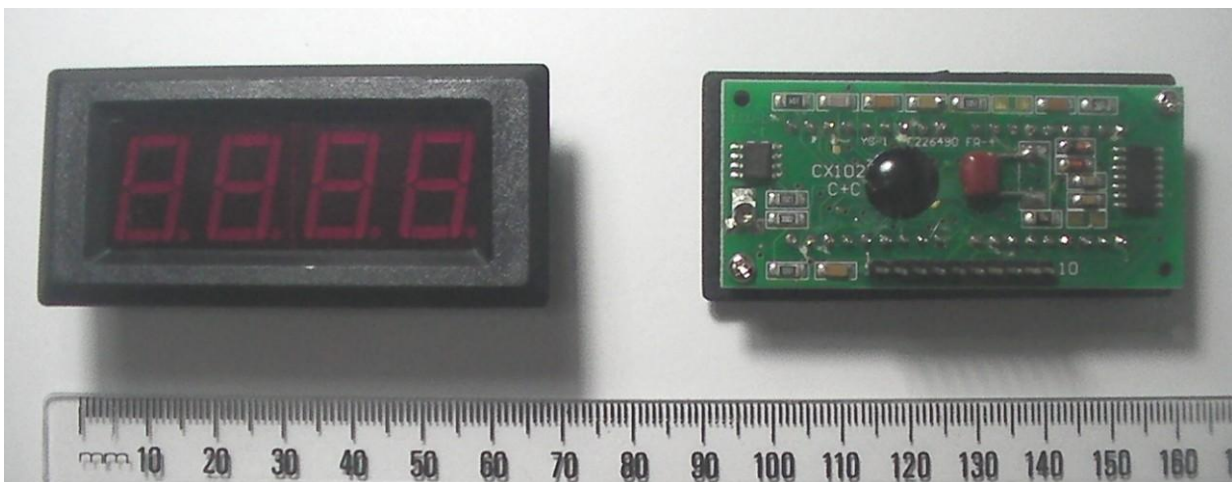
For distributors in which it is impractical to fit a sensor at the periphery of the cent plate, consider using the DRV5056-A1 (or -Z1). This sensor has ~15x the magnetic flux sensitivity of the UGN3503UA and may be placed further from the magnet rotation arc to produce a similar signal if space constraints in the distributor dictate a sensor position under the cent plate or elsewhere around the distributor body. This is particularly desirable where a small cent plate diameter necessitates location of the magnets at the edge of the plate to gain angular resolution of the strobe pulses, but no practicable sensor position exists inside the distributor. In this case, the sensor can be attached to the *outside* of the distributor casting at the cent plate plane in aluminium-bodied distributors or over a hole at the same plane in steel-bodied distributors. A greater degree of waterproofing is required for external sensor installations.

8. Electronic measurement of the timing interval

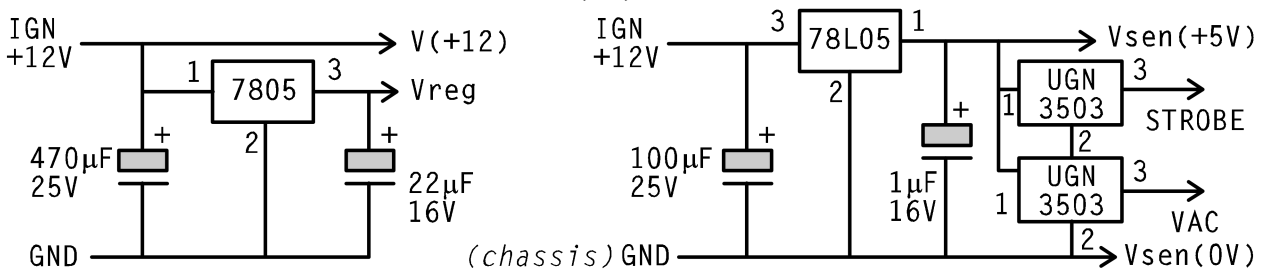
Having built an absolute timing reference into the MID, we can design an instrument to measure the time interval between the ignition points opening (coil discharge) and our timing reference point signal and then scale this interval in crankshaft degrees. The timing diagram below uses our timing reference pulse to provide a quadrant-end reference for each timing interval, all four of which will be equivalent. The points will open at a shaft-angle θ and close again at an angle equal to $\theta + d$, with $(90DD - d)$ being the constant points-dwell angle. The angle θ will *decrease* from its static upper limit as the distributor timing advance increases, so we must time the angular rotation interval from θ to our reference pulse T_{ref} and ignore the falling-edge signal of the closing points. The rising edge of the points-opening waveform also includes coil discharge and contact-breaker noise which must be excluded by the points-state detection scheme to prevent bias of the timing measurement.



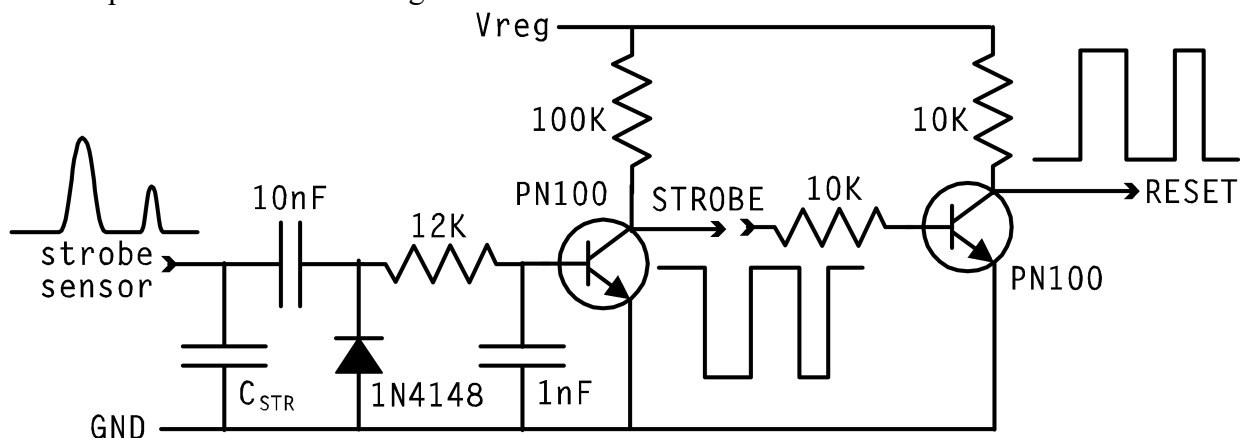
To register the relative state of the two signals that bound the timed interval we will require a set-reset (RS) latch that will provide a constant voltage output over the desired timing interval and zero elsewhere. Giving some thought to *how* this rectangular wave will be time-integrated, recall the simple use of the DVM to measure dwell angle. In its DC mode, the DVM uses a capacitive circuit to sample the input voltage and continuously integrate it, typically over 0.3sec intervals. Although this response time is slower than an analog voltmeter, it is fast enough to observe any transient timing phenomena produced by the mechanical timing controls of the MID as well as being more readable as a dashboard instrument. It also has the advantage of having high input impedance, avoiding the need for an op-amp if using an analog meter. One issue remains however; a DVM uses an internal absolute voltage reference while our automotive power source can vary in voltage between 11.5V-14.5V (15.6V if a dynamo is used) so a voltage regulator must be used to produce a constant voltage from the latch for the DVM to integrate. For this project we will employ a commonly available 3.5-digit LED DVM module that displays voltages in the range 0 to +/- 199.9mV, providing a ready scale of $1mV = 1degree$ to display angles up to 180.0CD. The DVM



module must also have separate negative input and power supply ground terminals so that it can measure voltage differences independent of its supply voltage. The module used for this project requires a regulated 5VDC 500mA supply so an LM7805 5-volt DC, 1A regulator is used to both power the DVM module and produce the latch reference voltage. It should be attached to a flat aluminium-plate heat sink of area at least 10cm² in the timing meter. In contrast, the sensors can be powered by the smaller (TO-92) sized 78L05 5VDC, 100mA voltage regulator. A single 470µF filter capacitor may be used if both voltage regulators share a common input line connected to the *IGN* supply outside the distributor, and may be located at their common connection point (see section 8.7). An extra 1µF capacitor must be located adjacent to the sensors if the 78L05 is located outside the distributor. **DO NOT earth $V_{sen}(0V)$ in the distributor.**



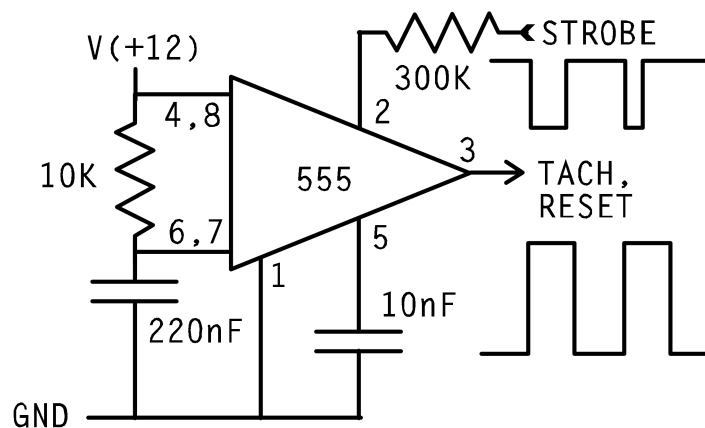
The quiescent output V_{NULL} of the UGN3503 with no magnet present is approximately half its supply voltage, or 2.5V. The 1-volt pulses produced at low magnet translation speeds will decrease in width with increasing speed as the output represents the time-fraction of magnetic flux linkage through the active region of the sensor. The magnetic field strength of the neodymium magnets will also decrease by ~10% at engine running temperature, reducing the pulse amplitude. Removing the sensor's DC offset using a coupling capacitor without amplification will also decrease the signal at higher pulse frequencies. The sensor output is also likely to carry significant HT discharge noise from the points circuit. Together these factors result in a signal too small to directly toggle the latch state reliably and some signal processing is required. This can be achieved readily with a simple buffer amplifier/filter circuit using two transistors as shown below.



The 10nF capacitor and diode reject the DC component of the signal and any high-frequency noise is excluded by the combination of cable capacitance C_{STR} and the 12K / 1nF low-pass filter on the input transistor base. A fixed capacitor of ~200pF may be required for C_{STR} if the buffer transistor is located outside the timing meter (see section 8.7). The second transistor inverts the output of the first and provides a low-impedance output. The circuit achieves an extremely high slew-rate response for all pulse sizes and a consistent trigger point on the pulse waveform. Although the rectangular pulses produced by this circuit will still decrease in duration (in proportion to the sensor pulses) as the rotor shaft speed increases, only the rising edge of the RESET output is required to trigger the latch in our timing meter. Alternatively, a DRV5056 magnetic flux sensor could be used to drive the latch directly without amplification through a 3:1 voltage divider and low-pass filter. With a view to other potential uses of the sensor signal for reference purposes, we will also consider an alternative amplification method.

8.1. Tachometer output

If we use a Schmitt-trigger / timer such as the NE555 as our amplifier instead, we can produce *fixed-duration* rectangular pulses from the sensor pulses, independent of their size and duration. Unlike the *fixed-angle* signals we have considered until now, fixed-duration rectangular pulses produced from our sensor will not change waveform with increasing rotor shaft speed. Accordingly, each pulse contains a fixed amount of energy so that a time integral of their energy is proportional to the *number* of pulses integrated, or their frequency. Such a time integral is exactly that performed by the capacitive sample circuit of our DVM, so that the voltage displayed is proportional to the pulse frequency, which in turn is set by the engine speed. Thus we may have an accurate engine-speed tachometer output from our magnetic sensor by replacing the inverter transistor in the above circuit with an IC, and as the timing meter latch only registers rising-edge input signals, the tachometer output can drive the timing meter RESET latch input directly as well.



Conveniently, the NE555 is designed to operate with a falling-edge signal. It will trigger when the voltage at its input falls below $1/3$ of its supply voltage $V(+12)$. Our previous strobe amplification circuit readily achieves this with a 12V supply voltage. With no signal from the sensor, the transistor is switched off and $V(+12)$ will be applied to the trigger input. A pulse from the sensor at least 0.3V above V_{NULL} will then provide sufficient base current to lower the trigger voltage below 4V. As the input transistor and NE555 trigger circuit share the same reference voltage $V(+12)$ the trigger point on the STROBE pulse remains constant.

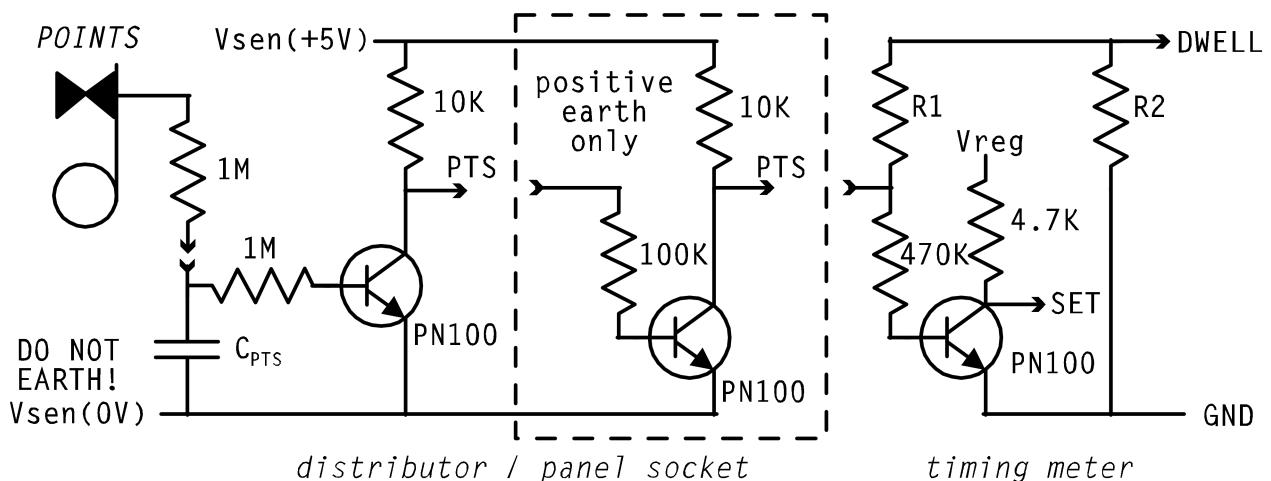
The resistor and capacitor tied to pins 6 and 7 of the NE555 set the time base of its output pulse by their product, or RC constant. Triggering causes the discharge pin (7) to open, allowing the 220nF capacitor to charge through the 10K resistor, as well as setting the device output high. When the capacitor charge reaches $2/3$ of the supply voltage at the threshold pin (6) the capacitor is discharged and the device output set low. This arrangement yields the high-output state duration as approx. $1.1 \times R \times C$ (capacitors have large error tolerances - always check). Dimensionally, Ohms \times Farads = seconds, so $K\Omega \times \mu F = msec$. We set our tachometer-pulse duration by choosing an upper integrated-voltage limit corresponding to a maximum engine speed. The choice of max tachovoltage depends on the input range of devices using this signal. The tacho-pulse amplitude will be close to the supply voltage $V(+12)$, so the fraction of this voltage we choose as our maximum integrated tacho-voltage is the same fraction of the quadrant period at maximum engine speed, which we take as the tacho-pulse duration. For example: at 6000RPM our sensor produces 200 pulses per second, limiting our tacho-pulse duration to a maximum of 5msec. The suggested RC constant of $(10K \times 0.22\mu F) = 2.2msec$ yields a corresponding integrated tacho-voltage of $(12 * 2.2 / 5) = 5.3V$ at 6000RPM, and 0.53V at 600RPM.

There is also a lower-bound limit to the tacho-voltage we must check: the trigger will not reset until the input voltage rises above $1/3$ of the supply voltage, so trigger pulses longer than 2.2msec below this voltage level will produce output pulses of similar duration from the timer instead of the RC -fixed pulses. We calculated previously the sensor pulse full width as 10CD, so assuming the two-thirds width of the inverted amplified pulse is at the trigger reset level, we can estimate 4CD for the

trigger hold angle, or $(4 / 180) = 2.2\%$ of a stroke. This fraction will equal our tachopulse duration when the distributor quadrant period equals $(2.2\text{msec} / 2.2\%) = 100\text{msec}$, or 10 pulses/sec, or 300RPM – safely below our engine speed range of interest. Finally, as the timer IC's V(+12) supply voltage is unregulated, the integral of the *TACH* pulse train must be scaled against the same supply voltage by any scaling circuit to remain accurate.

8.2. Timing circuits

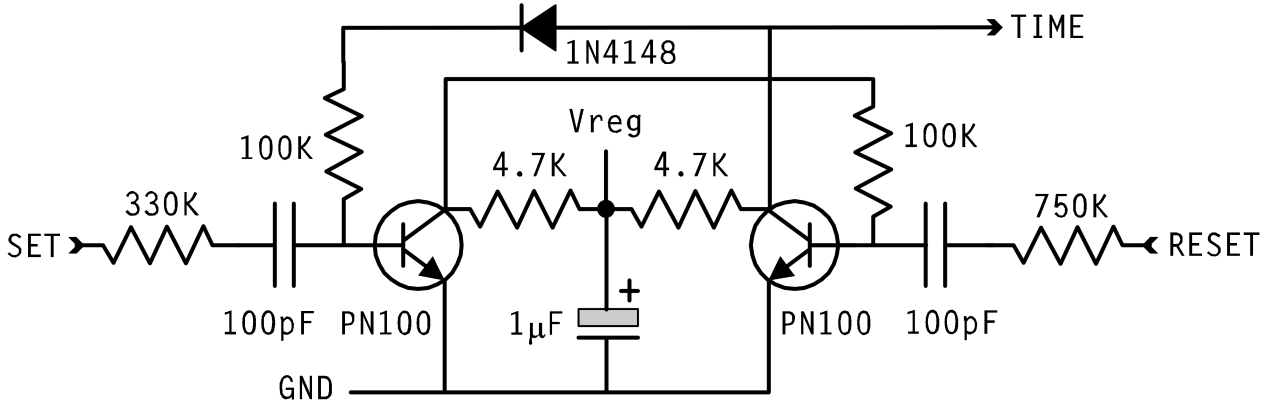
It is important to maintain high input impedance in any circuit continuously connected to the points, as any current leakage from the coil primary will delay collapse of the magnetic field stored by the coil and thus weaken the high-voltage ignition discharge from the secondary coil. To minimise interference to the coil discharge circuit, the points line connection is made through a 1M resistor located in the distributor. The small current abstracted from the coil primary circuit by our points connection necessitates minimal signal transmission path before amplification to avoid the effects of ignition noise and stray capacitance. To achieve this, we must locate a buffer transistor either in the distributor or nearby and include adequate line filtering capacitance C_{PTS} (see section 8.7.1). This transistor will simply switch the 5V regulated sensor supply voltage V_{sen} , thus isolating the timing circuits from the points voltage and whatever type of ignition system is producing the signal. We select bias resistors to switch the transistor fully on at 3V and fully off at 2V, corresponding to the designated points voltages for points state identification. The inverted PTS signal thus produced corresponds to the conventional dwell timing interval and we may connect the *PTS* line directly to our DVM via a voltage divider so that the integration circuit of the DVM produces a time-averaged voltage reading representing the points-closed duration in DD. The *PTS* line filtering capacitance C_{PTS} then sets the default (negative) linear gradient of the dynamic dwell curve. Accordingly, the reported dwell figure yields a more accurate characterisation of the ignition coil switching circuit than a direct measurement of the points voltage. This scheme is also necessary for an accurate dwell measurement circuit operating across all engine speeds, as traditional points-voltage based dwell meters typically are calibrated to read correctly at engine idle speeds only. This circuit may also be used with any unmodified MID to measure dwell angle using a voltmeter connected to the *PTS* output. An additional inverter transistor is required to use our timing circuits in a positive-earth vehicle (see 8.7.3).



The resistors R1 and R2 in the above circuit are chosen to produce a constant full-scale voltage V_{FS} across the DVM inputs corresponding to a displayed dwell value of 90.0DD with points closed, corresponding to an off-state buffer transistor voltage V_{cls} at the *PTS* output. The resistors R3 and R4 shown in the DVM circuit below offset the negative input of the DVM against the buffer transistor on-state voltage V_{opn} at the *PTS* output with points open less the cable *PTS* line voltage drop. The $10\mu\text{A}$ current drawn from *PTS* by the SET input inverter is included by subtracting 10mV in the voltage divider equation. Measured values for V_{opn} and V_{cls} obtained at the end of the timing meter accessory cable with a high-impedance voltmeter must be used.

$$\frac{R_2}{R_1 + R_2 + 10K} = \frac{V_{FS}}{V_{cls} - V_{opn} - 10mV}$$

A typical cold-ignition-sourced value for V_{opn} of $\sim 100mV$ is offset with $R_3=20\Omega$ and $R_4=47K$. For our DVM module, a display of 90.0 corresponds to a V_{FS} of 90mV, so choosing $R_1=15K$ and $R_2=470\Omega$ then provides the required 90mV reference voltage within 1% for $V_{cls}=5.0V$. A multi-turn trimpot may be used for R_2 if no fixed-value resistors offer a good match for R_1 .

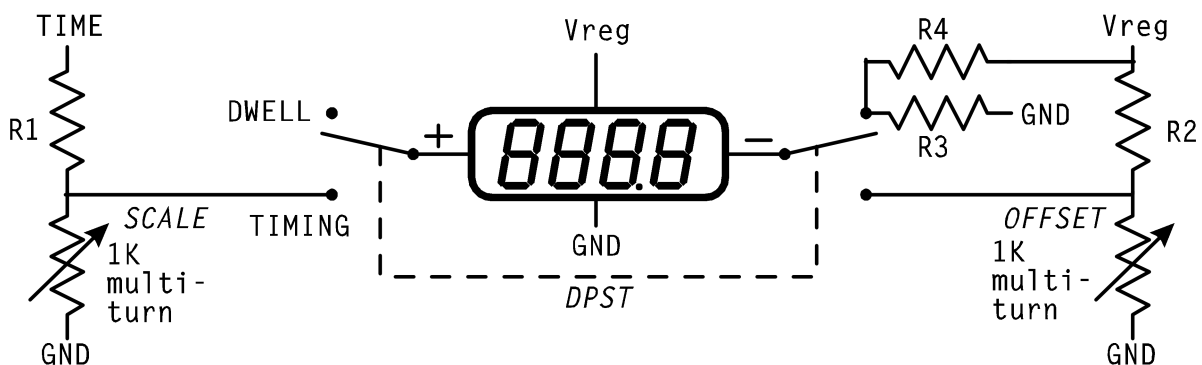


To initiate an ignition timing integration, the SET input to our latch must be set by the points opening. To exclude the noise-laden points voltage again, we can use the falling edge of the PTS signal to trigger the SET input via another inverter transistor rather than sourcing the points voltage. Triggering the SET input of the latch produces a constant V_{reg} voltage level on the $TIME$ output until the RESET input is triggered by the strobe pulse, at which point $TIME$ goes to zero volts. The time-integrated average value of this rectangular waveform corresponds to the desired ignition timing duration and is performed by our DVM as for the dwell measurement. By adding a double pole, single throw (DPST) switch, the same DVM module can measure the ignition timing angle by swapping the (+) input to $TIME$ through a scaling voltage divider, with the (-) input connected to an offset voltage divider, as shown below. This permits the display to be scaled to crankshaft degrees and correctly offset to the previously measured static timing figure at engine idle. The timing output is scaled by noting that continuously open points will produce a static maximum voltage near V_{reg} on the $TIME$ output corresponding to a nominal crankshaft duration of 180CD, for which our DVM requires $V_{FS} = 180mV$. A variable resistor is used for the smaller of the two resistors in this voltage divider to produce the exact resistance required to match the fixed resistor. To place the variable resistor near the middle of its range, we use a 1K multi-turn trimpot but treat it as a 0.5K resistor in our calculations. This gives the value of R_1 as

$$\frac{0.5K}{R_1 + 0.5K} = \frac{V_{FS}}{V_{reg}}$$

which for our DVM and V_{reg} of 5V yields a value of 13.39K for R_1 . Using a 13K resistor for R_1 then allows us to adjust the scale variable resistor for exact scaling at calibration (sec. 8.9.1).

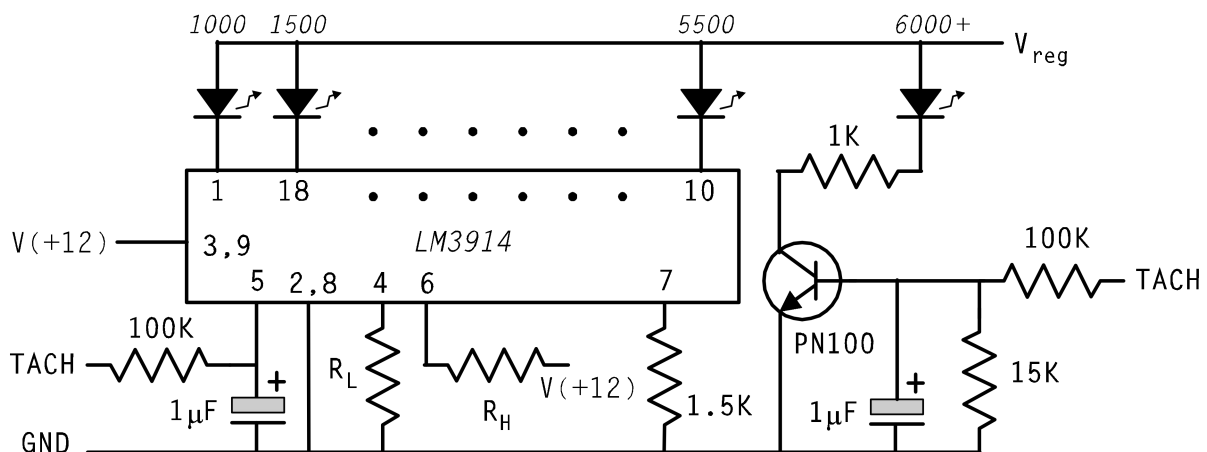
If the timing (-) input to the DVM were simply grounded, the meter would always time (in CD) relative to the position of our sensor's angular location in the distributor. As we arranged for this



The output of the timer is a rectangular waveform between zero and $\sim 11V$, and is applied to an NPN transistor that inverts the NE555 output to reproduce the PTS input of the timing meter. Alternatively, the *points* output simulates the points voltage for the points buffer transistor circuit and also permits monitoring of the timer frequency and duration using a DVM. The time-averaged voltage at this output equals the *HIGH* fraction of the waveform. Note that when both pots are set to zero the oscillator will halt and the voltage at *points* is the static waveform maximum. To simulate a pulse from the sensor, we use a capacitor tied to the same transistor to generate a small pulse to apply to a 2.5V voltage divider representing the (UGN3503) sensor quiescent output level V_{NULL} , together reproducing the strobe sensor signal. The 15K resistor is chosen to render the output pulse small intentionally, ensuring a realistic test of the timing meter's input amplification at the equivalent of high engine RPM. Note that this signal will not drive a high-impedance load so a short cable must be used between the tester and timing meter. The 30K resistor in the PTS output is selected to reproduce the voltage drop from V_{reg} across 10K in the PTS circuit, which in this case becomes the drop from +12V across 15K + 30K. The output frequency ($1/T$) of the timer IC is a proxy for the engine speed in ignitions per second ($= RPM / 30$) and the pulse *HIGH* duration is a proxy for the total timed interval of the timing meter. The rising edge of the timer's waveform will simulate the points opening and the falling edge will simulate both the points closing and sensor strobing. The dwell meter circuit will just report the pulse *LOW* duration in DD. It is useful to monitor the output frequency of the timer visually using an LED at low speeds or frequency meter at higher speeds. The brightness of this LED also indicates the *HIGH* duration of the timed interval. Increasing duration beyond the nominal value for overlap of the RESET pulse and next points-opening SET pulse will be observable on the timing meter display as a loss of timing signal.

8.4. Tachometer bar graph

If the timing meter is to be used on the road, a ready visual reference of engine speed beside the timing readout is useful to note specific timing values against. Precise values of engine RPM are not necessary, and another digital readout could be confusing, so an LED bar graph can be used to display increasing engine speed incrementally. This is easily achieved using a linear bar-graph driver IC such as the LM3914, which lights up to ten LEDs in sequence with rising input voltage between a lower limit (V_L) and upper limit (V_H) set by external voltage divider resistors. This feature of the device is particularly relevant as our time-integrated *TACH* signal must be scaled against the unregulated $V(+12)$ supply voltage, rather than the device's built-in voltage regulator. The independence of the scaling circuit in the device even permits reversal of the LED display sequence, simply by reversing the two limit voltages. This feature is helpful to mitigate PCB layout issues such as upside-down placement of the IC to locate a header-strip for the LED array at the outer edge of the board.



The *TACH* output from our trigger / timer circuit is integrated by a capacitor and applied to the input pin (5) of the IC. This constant voltage is compared to voltages along a chain of identical resistors by comparators, and where the input voltage is higher an op-amp is enabled to drive the

LED attached to its output. All the LEDs are current-limited identically according to the value of a reference-resistor on pin 7.

A consideration of how this simple display is best utilised over the engine-speed range is up to the designer. As the timing meter will only read static timing values near engine idle speed, a lower limit of 1000RPM to light the first LED is appropriate and speeds below this are indicated by an absence of any display. It is then natural to consider an engine-speed increment that allows the 10 LEDs to cover the full range of engine speeds desired – but as a reference for the timing meter, only the range up to full timing advance is relevant and at higher engine speeds the timing display should remain constant. With this constraint in mind, the observation that most period MIDs reached maximum advance before 6000RPM suggests an increment size of 500RPM for each LED in the display, with the final LED lighting at 5500RPM. Engine speeds above this limit may be indicated by a further LED, attached to a transistor whose input is biased to turn the transistor on when the integrated *TACH* voltage exceeds a level equivalent to 6000RPM. In the timing meter prototype, 5mm-diameter green LEDs were used for the 1000's RPM indicators and 3mm-diameter green LEDs for the 500's RPM in between, with the 6000+RPM indicator being a high-brightness red LED which will become progressively brighter as engine speed further increases. If a frequency meter is not available, the voltages V_L and V_H may be estimated by first measuring the static high output level of the tacho circuit (by grounding the NE555 input pin (2)) and multiplying this voltage by both the tacho-pulse frequency at the relevant engine speed and tacho-pulse duration. For example, with a static high *TACH* voltage of 11.5V and pulse-rate of 200Hz (6000RPM) with 2.2msec pulses, the voltage $V_H = (11.5 * 200 * 0.0022) = 5.06V$.

To calculate the required values of R_L and R_H , first measure the total resistance of the voltage divider chain inside the IC between pins 4 and 6. This may vary between 8K and 17K, according to manufacturer-stated production tolerances. Assuming the nominal device value of 12K, or ten 1.2K resistors in series, we may obtain voltage-divider equations for the calibration points:

$$\frac{R_L + 1.2K}{R_L + R_H + 12K} = \frac{V_L}{V(+12)} \quad \text{and} \quad \frac{R_L + 12K}{R_L + R_H + 12K} = \frac{V_H}{V(+12)}$$

where V_L and V_H are the integrated *TACH* voltages at pin 5 corresponding to 1000RPM and 5500RPM respectively. Dividing the equations by each other gives

$$\frac{R_L + 1.2K}{R_L + 12K} = \frac{V_L}{V_H} \quad \text{or} \quad R_L = \frac{12V_L - 1.2V_H}{V_H - V_L} = \frac{12K \times 1000 - 1.2K \times 5500}{5500 - 1000} = 1.2K$$

since the *TACH* voltages are just scaled engine speeds. R_L may be back-substituted into either voltage divider equation to obtain R_H . For the values of tachometer-pulse duration and static tacho-output above, we obtain a value for R_H of 21K.

8.5. Vacuum advance sensor

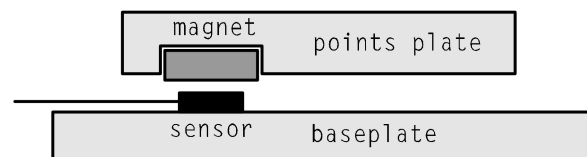
A means of reporting the degree of vacuum advance independent of the total dynamic advance measurement made by the timing meter is desirable to ascertain both its correct operation and real-time contribution to the displayed total timing advance. Although the amount of vacuum advance present at a particular engine speed may be calculated approximately if the centrifugal advance curve is well characterised (simply by subtracting the cent advance from the measured total dynamic advance), the large timing hysteresis inherent in the cent advance mechanism precludes accurate characterisation of the vac advance unit and this calculation may mask timing error introduced by the vac advance mechanism (see section 10.2).

No provision of any kind was made in MID designs to observe the action of the vacuum advance unit during use and as a pneumatically sealed unit it may not be disassembled readily or altered internally. Typically its sole externally-moving contact with the rest of the distributor is its connection to the points plate which rotates the latter around the rotor cam by the angle required to

apply the desired degree of timing advance in response to low inlet manifold pressure levels. This movement is physically small – the maximum rotation at the points plate circumference may be less than 10mm. Typically there is also little space around the vacuum unit attachment site in the distributor for additional electromechanical components without major modification of the distributor body. If we instead turn our attention to measurement of the points plate movement, we may be able to locate a suitable method and location inside the distributor to affix a small motion sensor.

The primary requirement for such a sensor in the MID is that it must not impact on the operation of the timing mechanisms in any way, or interfere with the high-tension coil discharge circuit. Our placement of the shaft-rotation magnetic sensor under the points-plate carrier achieved this admirably. We can utilise our experience with the same magnetic-flux sensor to monitor the position of the points plate relative to some other fixed point in the distributor by the same means. If we place a small magnet on the outer edge of the points plate, it will move back and forth together with the plate in response to the action of the vacuum advance unit. A magnetic flux sensor can be fixed to the points baseplate near the magnet to register its position as a change in intercepted flux. Unlike the rotating-shaft position encoder, this sensor will only produce a different static DC voltage for each position of the nearby magnet. The small physical size, exact reproducibility and complete non-interference in the motions of the mechanical timing components make the magnetic sensor a good candidate for a vacuum advance sensor, although the adoption of static field measurement introduces issues of sensor linearity as well as mechanical and thermal stability. It is **strongly** recommended that section 13 is read before choosing a sensor/magnet pairing if high accuracy will be required, e.g. for data logging. The UGN3503UA may be used to achieve a measurement of vacuum advance within 1DD at engine running temperature for the timing meter.

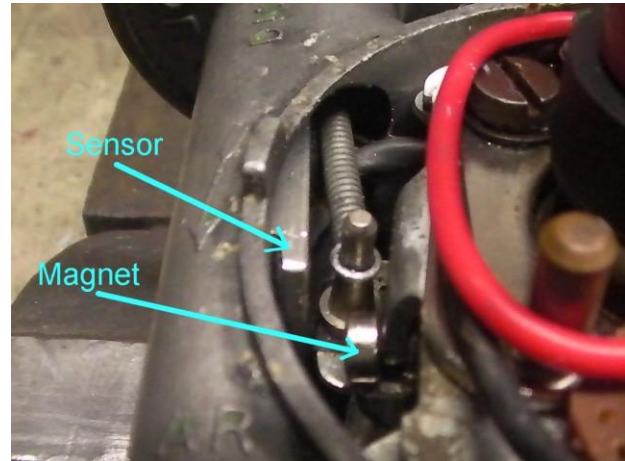
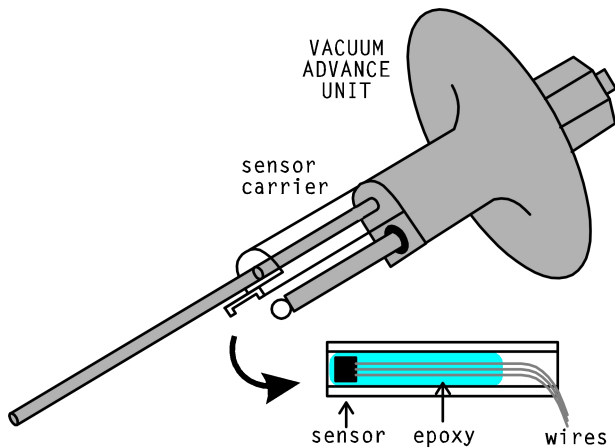
Key considerations in locating the sensor are thermal stability and any thermal compensation scheme employed. These factors rely on maintaining the sensor and magnet at the same temperature as the magnet heats up to engine running temperature.



Ideally, the magnet should be located in a shallow recess milled on the underside of the points plate at its outer edge with the sensor fixed under its arc of motion on the points baseplate. These should be fixed with thermal transfer compound on their contact surfaces. Placement of this sensor/magnet combination in any one particular MID unit will be necessarily highly version specific, and in this example we will again use the Lucas DM2 as a representative model. This distributor has the added complication that the entire vacuum advance unit is able to move with respect to the distributor body to adjust static ignition timing, under the action of a vernier adjustment nut. This motion changes the rest position of the timing plate with respect to the distributor body, but *not* with respect to the vacuum unit itself. In this case it is desirable to attach the sensor to the vacuum unit rather than the distributor body, despite the loss of thermal contact and extra engineering involved.

To make the sensor carrier, a piece of aluminium is shaped to fit inside the vacuum-advance unit recess of the distributor body, over the vacuum-unit adjustor spindle rod (see section 15). On the side of this carrier that faces the vacuum-unit diaphragm attachment spring, a channel is cut to locate the sensor just clear of the spring and its attachment to the points plate, at a point 2mm past the points plate attachment pin. The sensor carrier is cut back under the sensor to allow the vac-unit its previous range of adjustment motion under the action of the vernier nut. A 6mm-diameter, 3mm-thick neodymium magnet may now be placed on the steel bracket of the vac-unit attachment pin under the points plate, south pole outwards, so that it nestles into the pocket formed by the base of the attachment pin and its right-angled bracket. No adhesive or machined recess is necessary, as the magnet is impervious to shock or vibration under its own attractive force alone. The placement of the sensor, slightly above and away from the magnet along its path of movement with the points plate, results in a slowly increasing sensor output voltage with increasing proximity of the magnet's south-pole face. The final position of the sensor on its carrier should be found through trial-and-

error until an increasing voltage is observed over all points in the points plate's rotation range from rest up to the limit set by the vacuum unit, after which the sensor can be fixed within its groove on the carrier by pouring epoxy over the whole sensor and its leads. Prior to reassembly, check for end play of the vernier-adjustor nut in its recess. If the vac-unit may be moved against it to any extent, a crinkle washer should be fitted beside the nut at final assembly. To re-assemble the unit, the sensor carrier must be placed in the vac-unit recess first and the vac-unit spindle rod passed through it, the end-float spring and finally the vernier-adjustor nut / washer. Apply a small amount of glue to the spindle rod to fix the position of the sensor carrier up against the vac-unit body if necessary. Wires



from the sensor should be suspended under the points plate assembly, clear of the centrifugal weights' rotation arcs, to an attachment point at the distributor's outer terminal block. The vac sensor should be powered by the same regulated 5VDC supply used for the timing strobe sensor.

Consideration should also be given to the magnetic field produced by the points in positioning the sensor. In the above image, the thick red wire is the connection to the coil primary from the points, and is only 12mm from the sensor. This wire, and the large curved points-contact spring (not visible) immediately below it carry significant currents and will produce considerable radial magnetic fields when the points are closed. Although no discernable effect is seen in this UGN3503 implementation (<10mV sensor output variation between points open / closed) the chosen sensor's response to ambient magnetic fields from the points plate under current load should be checked when selecting a sensor location.

The scheme given above is sufficient to map points plate rotation producing a magnet translation range of about 7mm. The single magnet produces a virtual north-pole at the vac-linkage pin in addition to its open south-pole surface. Where a more thermally stable but weaker SmCo or AlNiCo magnet type is used, larger translation ranges may be accommodated by using two magnets located at opposite ends of the range of motion. Placing the magnet corresponding to minimum vac advance north-pole toward the sensor and the max vac advance magnet south-pole towards the sensor will produce a monotonically increasing sensor voltage with increasing vac advance. However, if thermal compensation is employed with bipolar-ratiometric sensors such as the UGN3503, the magnet(s) must be configured to produce voltages above $V_{SS}/2$ only (see section 13).

8.6. Vacuum advance bar-graph

We can use the same circuit shown previously for the tachometer bar-graph display to produce a real-time monitor of the vacuum advance unit operation, using red LEDs to differentiate the two displays and omitting the over-range indicator. Note that many period vac advance units were made to suit various intake-manifold configurations and the actual advance range produced in any given vehicle may only be a fraction of the vac unit's stated total range. As we have up to 10 LEDs available for our display, we may choose to scale the output of the vacuum advance sensor as 0-100% of full vacuum advance in 10% increments, or 1DD per LED where the full vacuum timing advance *actually produced* is 10DD or less. The two calibrations are identical where the max vac

advance is equal to 10DD. However, depending on the specific installation of sensor and magnet in the distributor, the output from the sensor may not be completely linear with points-plate rotation angle, or timing advance. In such cases the bar graph display is approximate only and the vac unit sensor output must be made linear for any quantitative use as a timing reference (see 9.4). We substitute the rest-position output voltage of the vac unit sensor for V_L and the max vac-advance position sensor-voltage for V_H , measured with the sensor and magnet heated to the equivalent of normal engine operating temperature for the distributor, to calculate values for the voltage divider resistors. However, we must tie R_H to V_{reg} instead of $V(+12)$ and make the same substitution in our calculations as the sensor supply voltage is regulated. The equations for R_L and R_H presented for the tachometer bar-graph now become

$$\frac{R_L}{R_L + R_H + 12K} = \frac{V_L}{V_{reg}} \quad \text{and} \quad \frac{R_L + 12K}{R_L + R_H + 12K} = \frac{V_H}{V_{reg}}$$

assuming the use of all ten LEDs. Again, dividing these equations by each other yields

$$\frac{R_L}{R_L + 12K} = \frac{V_L}{V_H} \quad \text{or} \quad R_L = \frac{12K \times V_L}{V_H - V_L}$$

which we can back-substitute to obtain R_H as before. For example: a sensor voltage of 2.9V at the rest position of the points plate and a sensor voltage of 4.2V at max vac advance yields $R_L = 27K$ and $R_H = 7.5K$. Finally, the sensor output should be tied to the bar-graph IC input pin (5) through a 10K resistor.

Combined vacuum advance/retard units may be accommodated by assigning full retard to V_L and full advance to V_H . The retard and advance display segments may use different LED colours to indicate the correct rest position of the vac unit.

8.7. Distributor cabling

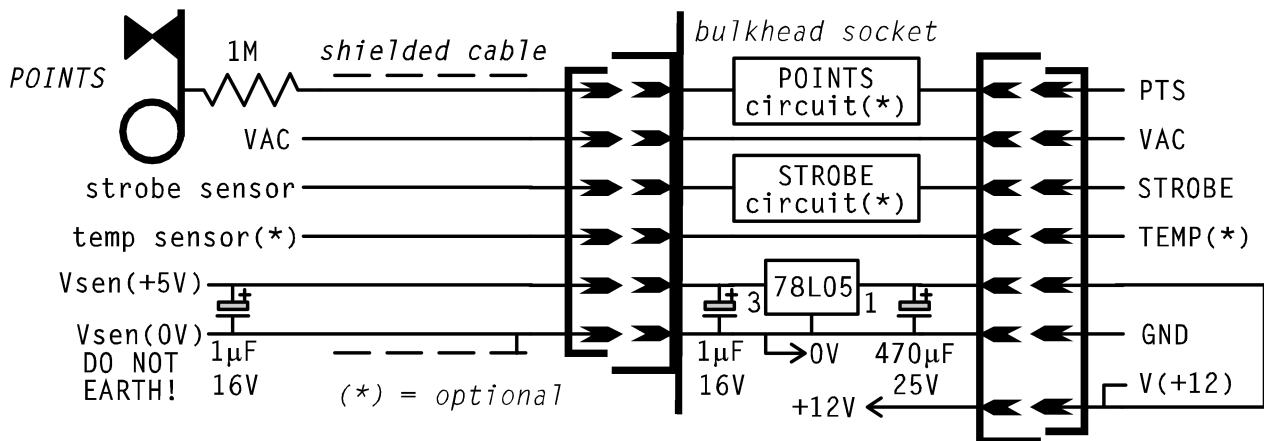
The large transient voltages and currents present within the distributor necessitate complete electrical isolation of the timing meter circuits from the ignition system apart from the single connection to the points, which must not interfere with the coil discharge circuit. This is achieved by placing a 1M resistor in the distributor between the points connection and the buffer transistor circuit shown in section 8.2. The points buffer circuit should be located within 1m of the distributor to minimise the effects of cable capacitance. Note that it is not sufficient to make the points connection to the points terminal of the ignition coil as there may be (but ideally should not be) sufficient resistance in the connection to the points for a significant voltage to persist at the coil terminal when the points are closed. The strobe sensor buffer circuit may be located anywhere in the chosen layout unless customisation to a particular installation dictates separation of the circuit from the timing meter to retain commonality of the latter to other vehicle installations.

The buffer transistors and our sensors only require the regulated low-current 5V supply given in section 8 which may be located either in the distributor or in a bulkhead interconnect located at the engine-bay firewall. In either case **sensor GND MUST BE fully insulated from the distributor**. Three cabling options are possible within this scheme and each has advantages and disadvantages:

Option 1: Buffer transistor(s) and sensor supply at engine firewall (recommended)

Placement of the MID-installation specific components at a bulkhead-interconnect location isolates the timing meter circuits from any unique modifications for noise reduction or signal amplification required for a particular distributor if the timing meter is intended for use with multiple vehicles and/or ignition systems. It also minimises component count in space-constrained distributors without undue degradation of the sensor signals. The diagram below shows a recommended cabling layout using a pair of multiple-pin panel connectors (IP65 rated) to make a double-sided socket containing the sensor supply, the buffer transistor circuit(s) and large 470 μ F capacitor. For conventional negative-earth vehicles the connections shown for +12V and 0V are made to *IGN* and

chassis earth respectively. By wiring the +12V supply to the 5V regulator through the accessory socket, removal of the timing meter cable will de-power the buffer(s) and sensor supply. The *IGN* connection should be made either to an existing max 2A fused accessory line or via an added 1A inline fuse. In this case the shielded cable to the distributor carries *Vsen* (+5V) and the cable to the timing meter carries V(+12). This layout permits easy removal of the distributor and dashboard timing meter cable and should be used even if the buffer circuits are located elsewhere. A single shielded cable can be used to supply both signals and power to the timing meter – *STROBE*, *PTS*, *VAC*, V(+12) from the *IGN* circuit, and *GND* via the remaining leads and cable shielding (see also section 13 if a *TEMP* reference line is used with *VAC*). Obtain a 3m length of *low impedance / low capacitance* 6-lead shielded digital cable to run to both the distributor and timing meter. Allow enough accessory cable length to reach the engine bay from the socket inside the vehicle, up to 2m.



Option 2: Buffer transistors and/or sensor supply in the distributor

The sensor supply and/or either buffer circuit may be located within the distributor if sufficient space exists either between the points plate and cent mechanism or below the cent plate. These components are 125C working-temp rated and reliable if well secured and screened from electrical noise. To minimise size, the components may be soldered together lead-to-lead as shown below. This ugly-but-effective module is then connected to the sensors, points and cable via leads insulated with 3mm heatshrink tubing after which the module is encased within a piece of (previously threaded!) 9mm heatshrink tubing. An ideal arrangement is to sling the module between the vac sensor and cable boss under the points plate, fixing it in place above the rotation arcs of the cent mechanism with a nylon clip. This fiddly arrangement is of most advantage where a distributor and matching ignition system are swapped out (e.g. for competition use) with another unit having different noise suppression or other sensor / buffer circuit customisations for use in the same vehicle, thus isolating both the timing meter and bulkhead interconnect from these differences.



Option 3: All components in the timing meter

All the buffer and supply circuits presented will function adequately if placed within the timing meter instrument alone. This arrangement may be preferable where a “test-only” or competition-spec distributor is modified to include the sensors only and fitted with a fixed length of cable ending in a plug which can be fed through the engine bay firewall directly to the timing meter. In this case the sensor supply may be dispensed with and the sensors powered directly from the timing meter’s 5V regulator. A +12V supply connection to the timing meter is made to *IGN* from the distributor-end of the cable and another line carries +5V back to the sensors, which still should have at least 1µF of local supply filtering. The specific buffer circuits deployed within the timing meter may be only suited to the distributor and ignition system under test. In particular, cable capacitance is likely to well exceed the minimum required for source noise filtering, resulting in a large negative dynamic dwell gradient with increasing RPM of magnitude 2DD/KRPM or more *before* the

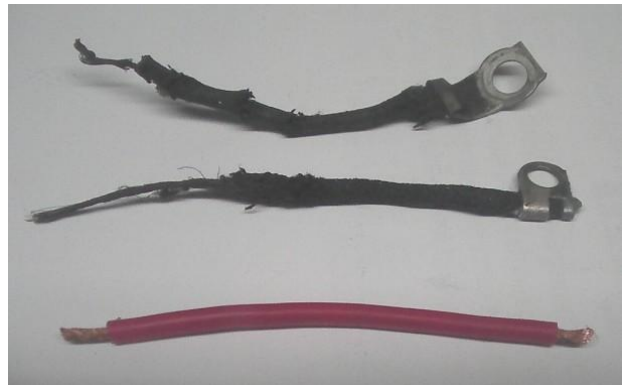
contribution from the ignition circuit. The indicated dwell at engine idle may be 2DD below the extrapolated points-gap equivalent value at 0RPM. In this case the filter capacitors in the buffer circuits may be omitted entirely.

8.7.1. Points buffer and strobe buffer noise filtering

The locations chosen for the buffer transistors dictate the values required for the line filtering capacitors C_{PTS} and C_{STR} . Sufficient capacitance is necessary to exclude high-frequency ignition primary circuit “ringing” voltages at ignition discharge from the buffer transistor inputs. The points buffer capacitor C_{PTS} will delay the detection of points closure, adding to the inrush current delay, so its value must be minimised to allow observation of ignition primary circuit current behaviour in the reported dynamic dwell curve. A total of 200pF is found to be sufficient for a bulkhead-located points buffer circuit used with a Bosch “Red” GT40R coil, resulting in a fixed contribution to the dwell curve gradient of $-0.35DD/KRPM$ to which normal coil primary inrush current will add a similar amount. A distributor-fitted buffer transistor may permit a smaller amount provided as a discrete capacitor, but a bulkhead-interconnect location requires this value *less* the cable capacitance to the distributor. A typical screened digital cable may exhibit 150pF/m. In contrast, the strobe buffer capacitor C_{STR} only needs to suppress any induced ignition “spike” voltage below the detection amplitude of the strobe sensor pulse. Its value should be minimised conservatively to reduce current drawn from the sensor at high RPM and typically is provided wholly by cable capacitance if the strobe buffer transistor is located in the timing meter.

8.7.2. Points plate grounding

In cabling the MID for the timing meter it is important to verify the state of the ignition circuit. The image at right shows two points plate ground wires in the condition found typically in an unrestored period MID. These were made of a soft-copper compound wire to withstand continual movement of the points plate without work hardening, as are the points connection wires. At 0.6mm core diameter these were never good enough for the high-amperage coil primary circuit and should be replaced immediately with a modern soft-core copper wire rated above 10A continuous current (lower wire in image).



8.7.3. Positive earth installation

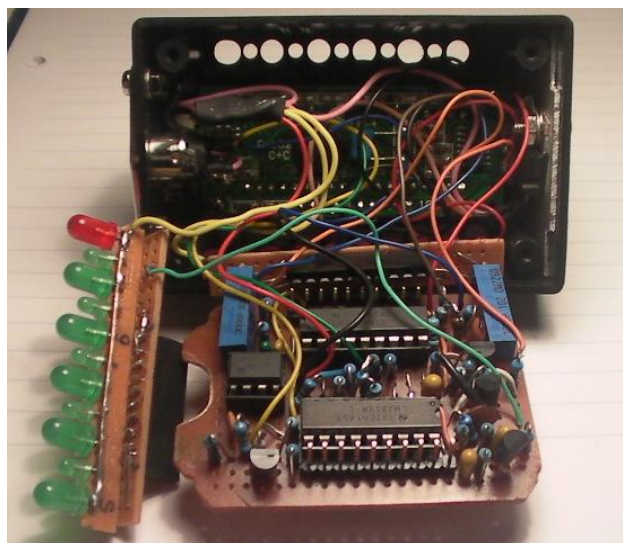
It is understandable that classic vehicle owners may want to retain absolute workshop-manual originality, including the positive chassis polarity employed in many UK-built vehicles. This configuration frequently presents problems when integrating modern electrical components or equipment with the vehicle’s electrical system. However, in many cases the underlying assumptions for retaining positive earth are based in folklore rather than electronics. Unless a positive-earth alternator is fitted or a specific dashboard instrument is known to be unipolar, reversing the vehicle’s polarity only requires reversing the connections to the battery and the ignition coil (which are marked (+) to *IGN* and (-) to the points in conventional negative earth). If a dynamo (generator) employing a field coil is being used, the latter must be re-polarised magnetically after reversing polarity by connecting a jumper lead to its field (F) terminal and brushing the other end against the battery (+) terminal a few times with the ignition off. In this case, the voltage regulator calibration should be checked after a few hours running. Note that a positive-earth alternator cannot be used in a negative-earth system.

To use the timing meter in a positive-earth system, all parts of the circuit board and components must be isolated from accidental contact with the vehicle’s metal surfaces. No external grounded

screw heads or grounded cable socket surfaces may be exposed on the timing meter. All parts of the cabling, including the sensor power supply, sensors and connecting wires must be fully insulated from the distributor body and chassis. In this case, the bulkhead connections for +12V and 0V (or their equivalent implementation) shown in the cabling guide in section 8.7 are connected to the chassis and *IGN* respectively. As the points voltages are inverted in the positive earth scheme, the timing displays will be inverted (timing shown = 180CD – actual, dwell shown = 90DD – actual) unless the inverter transistor in the points buffer circuit (section 8.2) is added to the bulkhead socket or equivalent location. This permits a negative-earth timing meter to read correctly from a positive-earth ignition system. Note that the PTS output also may be used to measure (90DD *minus*) the dwell angle with any voltmeter. A positive-earth ONLY version of the timing meter may be produced by omitting both the inverter transistors from the points buffer circuit and latch SET input.

8.8. Timing meter assembly

The image at right shows the completed timing meter. The bar-graph LEDs are fixed to perf-board strips and wired to headers mating with the pins at the top and bottom edges of the PCB. The DVM is secured at the front of the jiffy box (internal dims L78 x W48 x H28mm) behind the visible wiring and the voltage regulator and its heatsink line the right-hand side of the box. Visible on the PCB are the blue *SCALE* and *OFFSET* trim pots, accessible after assembly through a hole in the bottom-side of the box. When assembled, the PCB is held in place by the bar-graph LEDs protruding through the front of the box. The on/off and timing/dwell slide switches are located at either end of the DVM.



8.9. Calibrating the timing meter

Once assembled and tested, the timing meter must be calibrated to time correctly. This consists of first setting the timing display *SCALE* adjustment, which is then permanent for all distributor installations conforming to our sensor scheme, and then setting the display *OFFSET* adjustment against a specific distributor installation. The dwell meter requires no calibration.

8.9.1. Setting the display *SCALE* adjustment

This procedure is carried out at the test bench. First, switch the timing meter display to timing (not dwell). Power the timing meter via its +12V and *GND* connections with the *PTS* and *STROBE* lines connected to *GND* via patch leads. The timing meter should now display a static figure near zero (90 indicates dwell is selected). Adjust *OFFSET* until 0.0 is displayed then connect the *PTS* line to +12V momentarily. The timing meter display should read near 180. Adjust the *SCALE* potentiometer until the display reads exactly 180.0, then reconnect *PTS* to ground and de-power the unit. Repeat the process to ascertain both values are observed consistently. This completes the *SCALE* calibration and it should never require adjustment regardless of distributor installation.

8.9.2. Setting the display *OFFSET* adjustment

Connect the timing meter to its cable in the vehicle and attach (for example) a timing gun to the engine. **Ensure the points gap setting is correct** (manually or using the dwell meter option) and run the engine up to normal temperature until a stable slow idle is achieved. Check the timing meter shows zero vacuum advance (disconnect the vacuum line if necessary) and that the static timing at the crankshaft pulley is the expected figure, or adjust the distributor position to correct it. When the

correct static advance figure is observed, adjust the *OFFSET* potentiometer with the engine running until the displayed timing value matches the static timing figure obtained at the crankshaft pulley. Cross-check the two values against each other in case the centrifugal weights move. The timing meter is now calibrated against *this specific* distributor position, and changing the static timing angle (by changing the points gap or points plate rest position) will be reported correctly in the timing meter display. Note that the figure now shown on the timing meter when the points remain continuously closed is the actual offset angle, in (negative CD BTDC =) CD ATDC, of the strobe sensor for this specific distributor installation. This figure should be recorded for future reference (see section 9.2).

8.10. Testing and troubleshooting

The simple circuit design of the timing meter makes a number of assumptions about the MID it is connected to, as well as the electrical environment in the engine bay. It is prudent to first bench-test the assembled circuit on a breadboard with the distributor mounted on a motor-driven platform and the ignition system stripped-down to a bare set of points as described below at section 8.11. A dummy current load is necessary to overcome any contact resistance in the points caused by arc oxidation and attention from the points file is indicated if the dummy load draws too little current for steady timing measurement. The same arrangement may be used to analyse the centrifugal advance curve accurately at controlled motor speeds when “re-curving” the distributor.

The given circuits for the timing meter should operate as shown using the testing circuit. Individual components that may cause problems are the latch transistors (which should have roughly equal h_{FE} values) and the NE555 timer IC, which should be socketed on the finished PCB as all ICs should be. The latter should be checked for output-voltage low / high states of zero / $\sim 11.5V$ for static input voltages above / below $(V(+12) / 3) = 4V$, and stability of the output-high voltage for loads of at least 10mA. The sensors and magnets in the distributor are temperature-sensitive and signal loss at engine running temp indicates insufficient signal amplitude when hot. This may be corrected by altering the strobe input bias resistors or improving sensor / magnet proximity in the distributor. Similarly, the vac bar-graph range setting resistors should be calculated against the vac sensor output range at running temp.

Assuming the timing meter circuit produces a stable and accurate output *using the test circuit* to simulate the anticipated range of engine speeds and timing range, a failure to perform similarly when connected to the MID (either on the test-bench or in the vehicle) may be due to one of the following factors:

Static 0DD dwell angle: The points voltage never falls below 2 volts, even when the points are closed. Either the points plate is poorly grounded or the ignition circuit between the points connection and contacts (or the points contacts themselves) have significant resistance. Note that the coil primary circuit may draw 6A continuously through the points, so a 1-ohm resistance in this circuit would produce a 6-volt potential drop. The timing display will show 0CD in this case.

Static 90DD dwell angle: The points voltage never rises above 3 volts. If the engine is starting, this suggests the connection to the points circuit is faulty or the timing meter *GND* connection is offset significantly above the points ground voltage level. The timing display will show 0CD in this case.

Static 180CD timing display: The latch RESET input is not receiving the sensor signal. Check that the tachometer (if used) is active; if not check that the output of the STROBE inverter transistor is falling sufficiently low to trigger the timer IC (or timing latch if the two-transistor amplifier/filter circuit is used). If the sensor is producing pulses but the input transistor is not triggering the timer, a significant ground potential difference may exist between the sensor and timing meter.

Timing frequently rises by a multiple of 25%: The latch RESET input is occasionally missing a sensor pulse. If this occurs in bench-testing the MID without a coil in the circuit (so that no high-voltage discharge is present) and dwell is unaffected, then one or more of the cent plate magnets is

producing a weaker signal than the rest, particularly if the problem worsens with increasing engine speed. If fitted, the tacho display will also drop in concert with the timing rise. This situation may be alleviated by increasing the coupling capacitance in either sensor-input amplification circuit; otherwise the physical positioning of the affected magnets must be corrected. These may be identified by their lower static sensor output voltages when positioned directly in front of the sensor.

Timing frequently drops by a multiple of 25%: The latch SET input is occasionally missing a points opening signal. If this behaviour is observed in concert with an engine misfire then the ignition coil is not receiving charge. This may be due to a faulty coil, points capacitor or eroded points and is confirmed as an ignition system fault if the dwell display also rises similarly. Otherwise, a contemporaneous momentary rise in the tachometer level indicates an induced EMP in the *STROBE* line (see below). If this problem occurs in the absence of an active high-tension coil connection (so that the points are only active as a low-voltage mechanical switch) then there is an intermittent fault in the points circuit – either a grounding of the coil-connection side of the points, contact failure of the points or loss of grounding to the points plate.

Unstable timing at all engine speeds: The most likely cause of random instability in the timing display only with the high-tension circuit active is RF noise interference in the *STROBE* line. Ensure the connection leads in the distributor are as short as possible or shielded and no contact exists between sensor GND and the distributor. If the buffer transistor or sensor power supplies are present in the distributor, they should be located under the points plate away from the HT terminals.

Unstable timing at low engine speeds: Observation of drift, cyclic or unstable timing over a small range, only at engine speeds above idle, is most likely a genuine measurement of distributor timing error, typically due to mechanical vibration of worn parts. However at idle speeds ignition timing and dwell will both cycle sinusoidally over a small range precisely with the beat frequency between the sector time and DVM sample integration time. This is known as *Nyquist noise*. The time-average of this cycle is the correct value. At low engine speeds the points and sensor signals are large and well defined, and a stable reading at higher speeds indicates that the timing circuit is operating correctly. A potential cause of instability at low engine speeds is the use of a high-discharge-voltage coil, where RF noise is conducted to the timing meter (see below).

Unstable timing at high engine speeds: The timing display should reach a static upper limit of cent advance under continuous acceleration in the vehicle. The observation of erratic or unstable timing output from the timing meter only at successively higher engine speeds indicates either points bounce (float), rotor-shaft vibration or, in the absence of any disturbance to the engine's behaviour, a weakening signal from the points (evinced by a falling timing) or a weakening signal from the strobe sensor (evinced by a rising timing and falling tacho display). The latter case may be rectified by reducing ground offset voltages or correcting magnet alignments (see above). A deteriorating points signal only observed at high engine speed suggests a potential problem with the points or coil; either a slow coil charge-rate through worn points or a high closed-points voltage. Check the dwell angle reading on the timing meter - if the points offer resistance to the coil primary circuit when closed this will be observed as an artificially low dwell angle value, which would also decrease with rising engine speed at more than $\sim 2DD/KRPM$ in this case.

Tachometer reads double actual engine speed: The *STROBE* line is inducing a coil discharge EMP resulting in a second “ghost” trigger pulse to the tachometer circuit. This will also disrupt the timing output. Ensure the wires from the sensors in the distributor are well shielded (e.g. under the points plate) and the timing meter cable is routed away from any high-tension leads. Increasing the filter capacitance in the *STROBE* sensor input circuit should be performed only as a last resort.

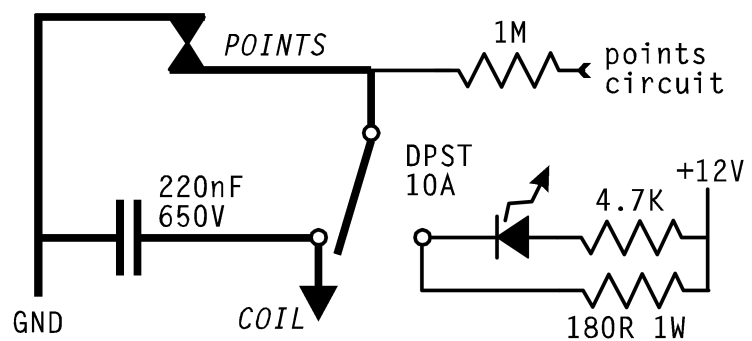
Timing unstable at high engine temperatures only: If neodymium magnets have been used to produce the strobe signal, their reduction in magnetic field strength at high temperature may have reduced the strobe pulse amplitude below the trigger level of the timing meter *STROBE* input for the implemented sensor-magnet geometry. A sensor-magnet geometry that produces a better signal is required (see also section 13).

8.11. A workshop MID analyser

The circuit designs presented for the sensor-in-distributor timing scheme may also be used to produce a workbench testing and analysis unit for unmodified MIDs. In this case the distributor is mounted on a frame and driven by an electrical motor with a variable speed control, the details of which are left to the designer. The motor's coupling to the distributor is a logical place to position a circular plate carrying the same array of magnets described for the cent plate around its circumference, with the sensor located alongside it on the frame. The relative orientation of the distributor to the sensor now sets the equivalent of static timing. A regulated 12VDC power supply powers both the timing meter circuit and the points through a dummy load in place of the coil, with a 1M resistor connecting the points to the buffer transistor circuit as before (see section 8.2). If using AC-mains sourced supplies for the motor, ignition and timing circuits remember to combine all the DC-side negative rails to avoid ground loops. In particular, points ground potential for the timing circuits must be sourced directly at the negative supply terminal of the ignition circuit to avoid positive closed-points offset voltages under high current load. Large filter capacitors and separated cable paths are required for a bench-test unit to exclude coil discharge noise from the timing and dwell circuits. Likewise, any dummy spark-plug circuit attached to the coil HT output must be fully enclosed in a solid steel housing and well grounded to the ignition supply.

If it is desired to test ignition system components under load together, it is convenient to have the high-current ignition test circuit switch-selectable with a low-current timing test circuit. The

suggested circuit at right uses a 10-amp rated double-pole, single-throw (DPST) switch to select either a dummy load resistor or a points capacitor and coil primary connection as the current source for the points. The second pole of the switch (not shown) disconnects the points circuit filter capacitor (C_{PTS}) when the low-current circuit is selected. The

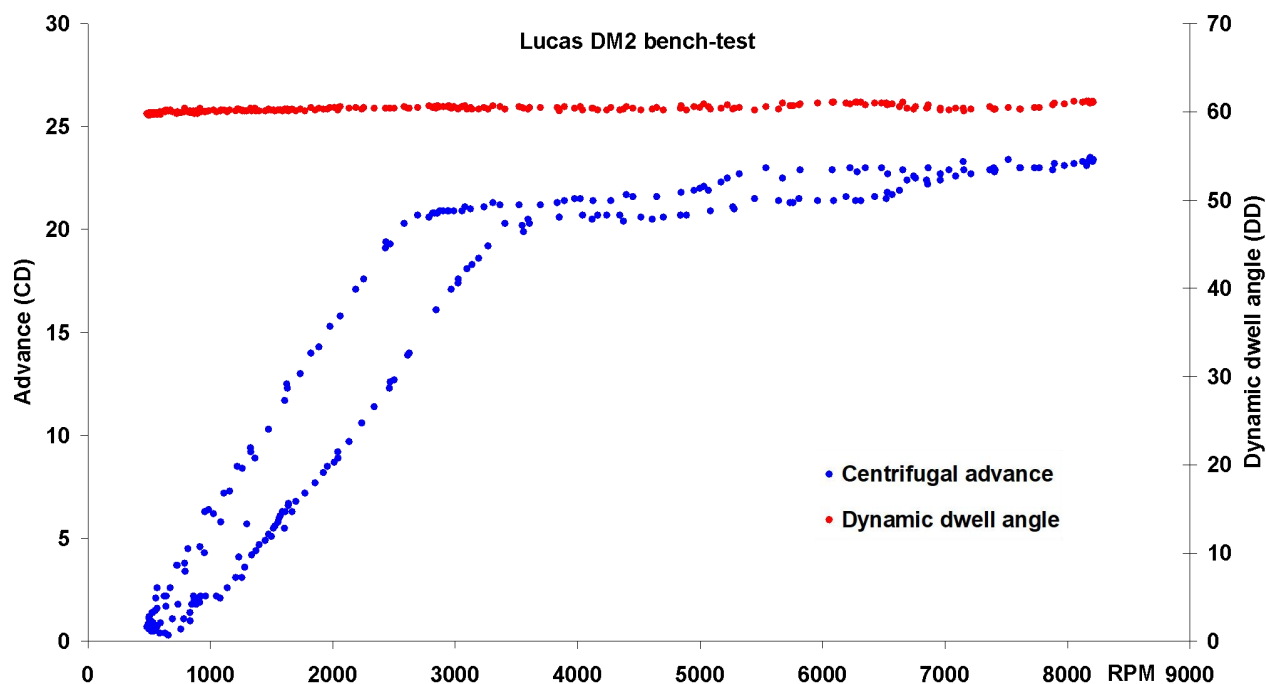


connections to the points, coil and capacitor must be made with 10A rated wires and the coil may be powered by a separate high-current supply. The rest of the circuitry is the same, and a road-going timing meter could be used with this workbench testing unit if a common-cabling scheme is adopted. Note that leaving the points capacitor connected to the points in the low-current test circuit results in a constant -1CD timing error at all speeds due to the capacitor delaying the rise in points voltage (to only 12V) upon points opening. If it is intended to garage-test an ignition system in a vehicle using this scheme (e.g. for high RPM ignition system discharge testing without engine involvement) such that its coil discharges across a single spark plug repeatedly in the stationary engine, it is important to disconnect the vehicle's distributor and disengage its gearbox to prevent any engine detonation from moving the vehicle. The distributor rotor in the vehicle can be located beside a discharge terminal reliably by manually rotating the crankshaft until the points open.

A workbench-only version of the timing meter may use a dial-calibrated instrument potentiometer for the *OFFSET* setting to obtain a zero timing figure at idle-equivalent RPM regardless of points gap setting. Further DVM modules for separate tacho and dwell displays may be used instead of the LED bar graph, or all of these may be replaced with analog meters to recreate the equivalent of the *SUN* distributor analyser that graced many auto-electrical workshops in the 1960s. The use of an analog meter instead of the DVM module would require the addition of an integration capacitor and op-amp to drive the meter. The capacitor can be quite small in value as the physical movement of the meter coil already provides "inertial" integration of the applied voltage and the high-impedance op-amp input provides the necessary isolation of the meter circuit from the latch. Note that the NE555 IC used in the tacho circuit provides sufficient output current to drive an analog meter directly through a voltage divider.

If the action of the vac-unit is also to be analysed at the workbench, a calibrated source of vacuum such as a small electric vacuum pump could be attached to the vac-unit through a vacuum tap to control the level of applied vacuum. A vacuum gauge would also be necessary at the coupling to the vac-unit. The vac-unit position sensor used in the distributor modification can be replicated easily in a workbench instrument by a potentiometer mounted on the frame beside the distributor with a clip-on linkage between it and the points plate to transmit motion under the action of the vac-unit. This potentiometer would then replace the sensor directly in the distributor vac-meter modification circuit and its motion calibrated in DD to measure the vac advance as a function of applied vacuum. This degree of instrumentation is only necessary if the intention is to check the proper action of the vac-unit quantitatively, as the timing meter alone will indicate the extra advance produced by the vac-unit under any source of external vacuum (such as sucking on a tube attached to its vacuum port).

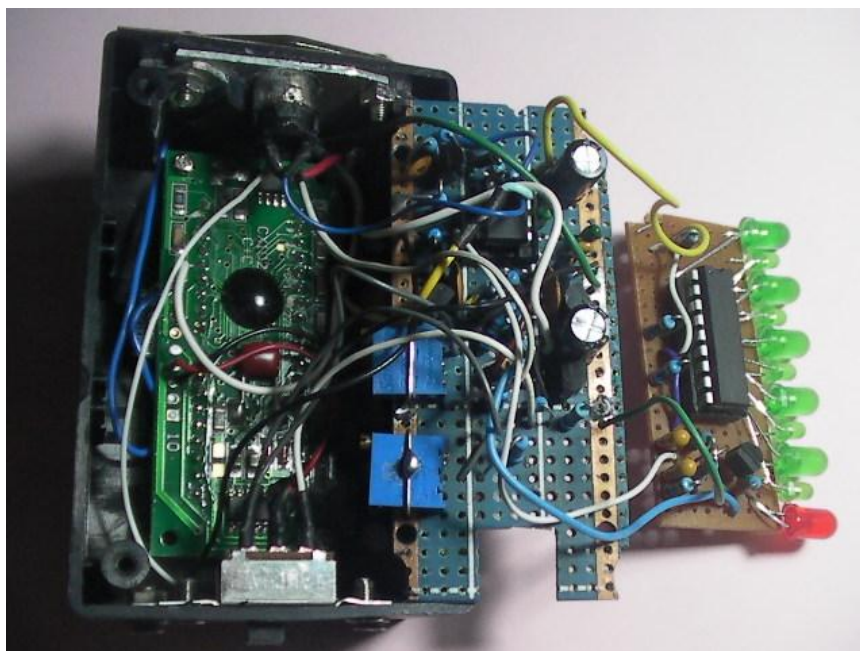
A bench-test MID analyser also permits the study and optimisation of distributor behaviour safely at far higher equivalent engine speeds than are desirable for in-vehicle testing. Such analysis is prudent for the mandated use of period MIDs in historic vehicle racing to protect high-performance engine builds from ignition-error induced damage. The timing meter tacho circuit will require a smaller *RC* constant (see section 8.1) to operate correctly at these speeds. The plot shown below, collected using the data logger (see section 9) from the bench-test rig at low points current, shows the measured cent advance and dwell curves up to the vehicle-equivalent of 8100RPM for an unrestored DM2 distributor restricted to 10DD max cent advance over a single transition from idle to max RPM and back to idle. Points on the plot represent values that would be observed on the timing meter set to zero timing offset. The lower cent curve corresponds to the acceleration phase and the upper curve to the deceleration phase. Note the key feature that the dwell curves are identical in each case.



It may have been expected that points “bounce” would be observed before 8K RPM as a drop in dwell duration. Instead, the slight increases in dwell duration near 6K and 8K RPM indicate a minor resonant shift of the rotor cam rotation axis away from the points cam-follower, highlighting an important consideration for bench testing of worn MIDs – thermal state. Instability of the rotor shaft and cam common rotation axes that may be evident at room temperature will often reduce or disappear at engine working temperatures where thermal expansion and thinner bearing surface oil films act to better stabilise these parts. It is worth considering the inclusion of a heating element (as a sleeved wire coil around the rotor shaft spindle) in the MID bench-test rig to attain a reasonable approximation of engine temperature during testing.

The cent curve shows an advance limit value of 20CD being reached at 3300RPM which then increases further in steps as play in the (cold) cent weights and rotor connector pins is taken up by increasing centrifugal force overcoming friction at these junctions, as well as a minor contribution to the cent advance from lateral “pitching-over” of the cent weights at high speeds. A final limit of 23CD is reached by 7K RPM and remains sustained by static friction until the rotor shaft speed drops to 5K RPM, below which the cent weight springs regain control of the lateral geometry of the mechanism. Static friction in the cent weight and rotor pivots then keeps the cent mechanism fully advanced until the rotor shaft speed drops below 2500RPM, producing the characteristic hysteresis in cent advance timing typical of this simple low-performance distributor design. (*Aside:* later performance MIDs typically featured two stacked cent plates with the rolling weights fixed between them, thus preventing the weights from pitching over at high RPM). Again, these features would be far less pronounced or absent in a well-lubricated distributor running at engine temperature. The observation of these effects at room temperature is a useful adjunct for condition assessment, fault diagnosis and potential performance improvement.

The image below shows a workshop bench-tester implementation of the timing meter. The same DVM module, timing and tachometer bar graph circuits have been used, although the latter has been built on a separate circuit board and the LEDs soldered directly onto the IC pinout for simplicity. Additional filter capacitors have been added to the DVM board 5V supply and timing PCB for the 12V and 5V supplies from the 7805 voltage regulator located at the top-end of the case. The sliding-switch at the bottom of the case selects between timing and dwell displays on the DVM. As before, the *SCALE* and *OFFSET* trim pots are accessible through holes in the case to permit the meter to be recalibrated against different distributors after assembly. Instead of a bar graph, the *VAC* output from the distributor is simply connected to a terminal on the side of the unit, alongside a *GND* terminal, for connection to an external DVM. This arrangement permits accurate measurement of the *VAC* sensor output voltage for calibration (see 9.4) or fault analysis. The image on the first page of this treatise shows a DM2 where the vac unit has been replaced by a potentiometer for bench testing. The pot body is fixed to a rod replacing the vac unit spindle and the pot sweep spindle is attached to the points plate via a lever and linkage. This arrangement provides an independent points-plate angular position reference for vacuum sensor calibration checking.



9. Data logger MID-mapping

While providing a quantitative measurement of ignition timing visually, the timing meter produces a great deal of information *sequentially* that is better analysed as a data set. The workbench MID analyser is sufficient to map the centrifugal advance curve alone, but the correct action of the vacuum advance is not ascertainable outside its connection to a working engine. In particular, the interplay of the two timing advance mechanisms in specific driving conditions cannot be determined without logging their respective states in real time under actual road use. To collect this data we can use the same sensor scheme presented for the timing meter to provide input for a microprocessor-controlled data logger module. We will then examine how the collected data can be reconciled with engine state under specific applied load and how the resulting analysis can inform engine tuning.

Choosing a data logger module (DLM) has been simplified greatly in recent years by the commercial production of single-board microcontrollers including multiple analog inputs and a Wi-Fi, Bluetooth or USB personal-computer interface port. As a simple, low-cost introductory example we will adopt the Arduino Nano v3.0 as our DLM. This “open-source” architecture platform has the added benefit of being extremely well supported by the worldwide electronics community with compilers and documentation freely available on the internet.

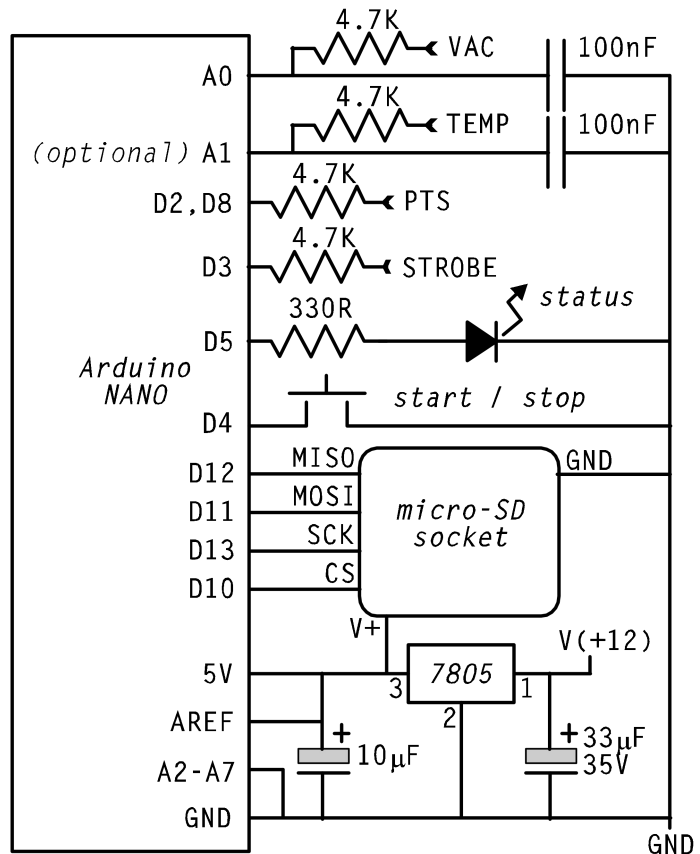
The Atmel ATmega328 microcontroller used in the Arduino Nano possesses two key features that obviates *all* the signal-timing circuitry of our analog timing meter: a real-time clock with 4 μ s resolution and configurable external *hardware interrupts*. The clock permits accurate timing of discrete events which are registered by a change in voltage applied to a digital input pin configured to suspend the microcontroller’s current process instantaneously and execute an *interrupt service routine* instead, after which the microcontroller returns to the previous task. We can use these hardware interrupts to register the opening and closing transitions of the PTS signal and the STROBE pulse from our timing sensor. By noting the times at which these events are registered by their respective interrupt service routines we may calculate the ignition timing and dwell angle easily in terms of measured real-time intervals. We can use the PTS and STROBE buffer transistor circuits from the timing meter to produce digital logic levels to trigger the interrupts.

The microcontroller also includes an 8-channel, 10-bit wide analog-to-digital converter (ADC). Each channel can encode a voltage in the range 0-5VDC linearly into an integer in the range 0-1024, equating to a voltage resolution of 4.9mV per ADC level. The output from our vacuum advance sensor VAC is within the ADC encoder range, but may only occupy 1V within it depending on specific magnet-sensor positioning. Without scaling, this resolves to $(1V / 4.9mV) = 204$ ADC levels corresponding to the full range of vacuum advance. As vac advance units typically have a range up to 20CD, this still provides 10 ADC levels per CD on average which is sufficient for quantitative analysis of the vacuum advance component of our timing signal. However, the non-linearity and (optionally) temperature dependence of our VAC signal must be corrected numerically. Fortunately, the microcontroller has sufficient processing capability to perform this task prior to recording vacuum advance values in the log file. The analog inputs must be protected from points noise with filter capacitors.

By taking advantage of these features of the Nano microcontroller, the program required for logging our timing data simply collects vacuum advance values continuously over a fixed sample period, during which the interrupt service routines collect timing data independently. At the end of each sample, the collected data are averaged over the sample period and stored as an entry in the log file before the sample accumulators are cleared and the process starts again. Note that this scheme is not limited to data logging alone – the Arduino component catalogue includes digital and analog accessory displays which would permit a fully-digital version of the timing meter to be constructed.

9.1. Assembling the data logger

Microcontrollers typically omit large amounts of non-volatile memory due to space and cost issues, and the Nano is no exception. To provide a medium for the DLM to write its timing log data to, we must attach a suitable solid-state memory card socket. The simplest form is the micro-SD card socket which connects to the Nano through five wires and is treated as a removable file device by the DLM. The data logger circuit should be assembled to be plug-compatible with the existing timing meter cable (see section 8.7.3 for positive-earth vehicles). The same LM7805 5VDC-1A voltage regulator should be used to power the DLM, as well as the sensors if the 78L05 5V regulator is not present in the distributor circuit. Note that the 5V input/output pin of the Nano board is used to power the unit rather than the *VIN* pin, which is not rated for connection to an automotive (12V-15V) supply. This also provides an analog voltage reference at the *AREF* pin for the analog inputs.



Once switched on in the vehicle, the data logger will attempt to initialise communication with the micro-SD card and pulse the status LED slowly if no card is present or card I/O fails. Otherwise, it will wait for a low signal from the push-button before commencing data acquisition at the rate of five log entries per second, indicated by the status LED changing state for each completed entry. An entry will not complete until at least one strobe signal is registered, as indicated by the status LED change rate. If data acquisition is commenced before the engine is started, no log entries will be made before engine cranking begins. If the engine is running, acquisition will continue until the push-button is pressed again at which time the status LED is unlit and the log file is closed.

The C-language Arduino program provided in section 11 operates the DLM. This code should be copied into a file called “timing.ino” and configured in the Arduino integrated development environment (IDE) as described below. The program is run by a generic “bootloader” kernel program which is permanently loaded (“burned”) into the Nano microcontroller first.

IMPORTANT: An ISP (in-circuit serial programmer) or microcontroller “burner” device is required to install the bootloader (another Arduino board can also be used). Purchase of such a device may be avoided by obtaining an Arduino Nano “clone” board from another manufacturer with the bootloader pre-installed, e.g. the Gravitech Nano v3.0. As the Arduino architecture is open-source, there are many such clones available. Check the microcontroller board specifications for the presence of a bootloader before purchase.

Details of bootloader installation depend on the ISP used and there are ample tutorials available on the internet to guide this process if required. After establishing the presence of the bootloader in the microcontroller, the compiled program may be uploaded to the device’s flash program memory. The data logger unit is now complete and ready to test using the timing meter test circuit presented previously.

9.2. Configuring the data logger program

The program code listed in section 11 assumes the default circuit specifications given for the timing meter sensor circuitry. It is anticipated that different distributor sensor installations will require alteration of the calibration constant definitions used by the data logger to characterise the timing and vacuum sensor inputs. These definitions are found at the top of the program code as labels representing each constant numerical quantity used to define characteristics of the data logger DLM itself and calibration factors for the input signals. Only numerical values should be changed in these definitions, and then only within the range permissible by the device constraints given below. Other labels are described in the operating scheme (section 9.6) and *VAC* temp correction (section 13.1).

VAC_CH and **VAC_TR** are respectively the analog input channels for the vacuum advance sensor and (optional) temperature reference sensor. These must match the circuit diagram shown above.

COM_SPD is the COM port baud rate for communication with the host PC through the integral USB port. This figure must match the serial port baud rate configured in the Arduino IDE.

ADCbits defines the ADC channel width used in the Nano board – other boards may differ.

AREF_V is the measured voltage at the *AREF* pin. This is the ADC input-range reference voltage. If this is found to be more than 5.05V place a small-value fixed resistor between *AREF* and the supply to reduce this voltage to 5.0V.

TACH_CAL is the tachometer calibration, converting stroke-microseconds to RPM.

TIME_CAL is the timing calibration, scaling stroke-fraction to CD.

DWEL_CAL is the dwell calibration, scaling stroke-fraction into dwell angle in DD.

STAT_ADV is the static advance angle of the distributor, in CD BTDC. This is subtracted from the measured ignition timing to calculate the centrifugal advance timing component (CENT).

VAC_OFS is the offset in DD from the first element of the **VAC_DD** array to the zero vac advance position, or the rest position of the vacuum advance unit. This value is zero if the first element of the array is the zero vac advance position. However, it is prudent to include at least -1DD of range in the array to permit observation of timing error caused by movement of the vac unit rest position or points plate over-travel on sudden vacuum drop, as well as detecting thermal drift in the vac sensor. The zero vac advance position within the array will also be offset significantly for combined advance/retard vacuum units.

TIME_OFS is the offset angle of the timing sensor in the distributor, in CD ATDC. This figure will change according to where the sensor has been located around the distributor body. It is subtracted from the measured timing value in the log file analogously to the timing meter *OFFSET* voltage, which is displayed on the timing meter when the points are continuously closed. In the absence of the timing meter value, upload the program with **STAT_ADV** and **TIME_OFS** both set to zero and observe the engine timing at steady slow idle using (e.g.) a timing gun whilst simultaneously collecting a dataset using the data logger. Ensuring the logged **VAC** advance values are (correctly) zero at idle, substitute the observed static advance value from the timing gun for **STAT_ADV** and substitute the data logger's observed timing value minus **STAT_ADV** for **TIME_OFS** in the program (see also 8.9.2).

PTSDELAY is the delay time (in whole microseconds) added to each dwell interval by input line capacitance in the points circuit (see sections 5.1 and 8.7). It corrects the reported dynamic dwell duration such that the dwell is constant at all engine speeds *unless* it is affected by ignition primary circuit current (see 10.3.1). This value is set by the combination of fixed capacitor value and cable capacitance (if any) between the points connection resistor and the points buffer transistor input resistor, at 0.5µsec/pF (see also 9.3 if no capacitance meter is available). Reported dwell durations are *increased* by 3.5DD/KRPM/msec to offset the decrease due to capacitive input delay.

VAC_TFAC and **VAC_TOFS** specify the gradient and origin of the linear function used to calibrate the **VAC_TR** analog input if a measured temperature correction is used with the vacuum position sensor. A correction function must be defined as shown within the `loop()` procedure in this case (see section 13.1.5).

VAC_DIAG enables diagnostic output of the measured vacuum sensor voltage level and temp reference sensor voltage level (if present) in each log entry. Set to `true` to enable diagnostics.

The **VAC_DD** array sets the calibration curve correction for the vacuum sensor. As noted earlier, the sensor output is not linear with movement of the magnet on the points plate toward it. The values shown in the array are monotonically-increasing static voltages at the sensor for points plate positions between minimum (first array value) and maximum vacuum advance (array value before **MAX_DD**) in 1DD increments, as measured at the test bench after reassembly of the distributor and using the exact same sensor supply voltage as used in the vehicle (see 9.4). *Note:* a more sophisticated translation algorithm has been omitted due to the typically small range of vac advance units and the limited DLM memory available for a large inversion array. The DLM has ample spare processing capacity for the simple serial array lookup and interpolation method used.

T_MIN defines the data logger reporting interval in msec. When activated, the data logger collects values continuously and averages successive samples within the collection period **T_MIN** before recording them in the log after any current timing intervals have concluded. The default period of 200ms should be short enough to observe any transient MID timing phenomena in real time.

Timer log files will be located in a data logger-created directory named “TimeLogs” in the root directory of the SD card. These will be named `Timennnn.log` where the number *nnnn* indicates the order in which logs were collected. New log files will be numbered starting after the last *consecutive* log file found on the card from `Time0001.log` onwards. Any existing files matching this numbering will be overwritten. The default log file format consists of seven tab-spaced numerical values per sample, with no headings (see section 9.5 regarding vac sensor diagnostic output):

1. TACH – Engine RPM;
2. TIMING – Ignition timing in CD;
3. CENT – Centrifugal advance in CD;
4. VAC – Vacuum advance in CD;
5. DWELL – Points “dynamic” dwell angle in DD;
6. PTSERR – Points opening event error count;
7. STRERR – Strobe sensor event error count.

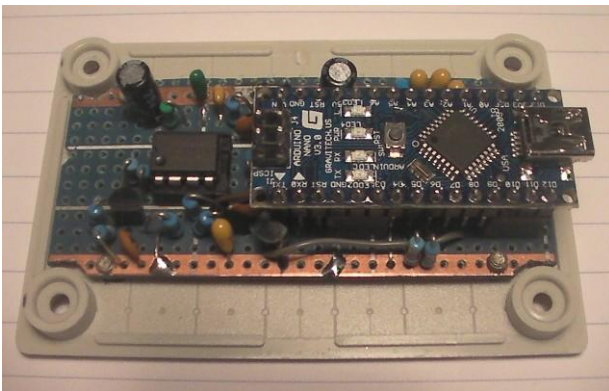
The column delimiter may be changed to (e.g.) a comma by altering the definition of **DELIM** to `,`. The timing-signal error detection counts per sample interval are provided as a diagnostic to isolate any faults that may lead to disruption of the timing signals such as electrical noise or mechanical vibration. For example, a missed points-opening signal is indicated by an unmatched strobe signal, and vice-versa. Faults indicated by these counters are detailed in section 10.4.

Host PC log output through the USB serial port is activated when SD card initialisation fails (e.g. if no SD card is present) and a character is sent from the host to initiate communication. From within the Arduino IDE, connect the unpowered data logger to a USB port. Check the status bar connection message to ensure that the IDE is using the correct serial port. The data logger may now be connected to an input source such as the test circuit or a bench-test analyser. Open the serial monitor window in the IDE. Press any key to commence serial I/O with the data logger, which should respond by turning off its status LED. Pressing the data logger start/stop button then produces log entries in the serial monitor until the button is pressed again to terminate the log. The serial monitor display may be saved by cutting-and-pasting the window contents into a text editor. *Note* – all the serial monitor output within a connection session is retained and may be accessed by scrolling back the window using its right-hand slide bar after stopping data logger output.

The data logger program omits intentionally any means of reading the micro-SD card through the Nano's mini USB port, which is too flimsy for repeated connection and should only be used for programming and testing the DLM unit unless it is integral to a bench-testing analyser incorporating a PC (in which case the SD card slot may be omitted). After data logging, retrieve the log files by placing the micro-SD card into an SD slot or USB adaptor for analysis using a PC.

Uploading the data logger program into the DLM is accomplished by leaving the SD card slot empty and connecting the Nano's USB port to the PC *without* the DLM being separately powered beforehand. This permits the PC to perform a power-up handshake with the Nano board and establish a temporary COM port for it, which should appear as a new port option in the Arduino IDE tools selection panel. After selecting this port in the IDE, click the upload icon to compile and upload the program to the DLM. When the upload has completed, you may connect the timing meter test circuit to the data logger and open the serial monitor window in the IDE (see above).

The following is shown in the images below: At left is the Arduino Nano module socketed on a strip of Vero board beside an (optional) accessory serial port IC, prior to the attachment of wiring to the SD card socket, cable socket and power supply. At right: the completed data logger connected to the timing meter tester (see section 8.3) via its input cable socket common to the timing meter; at the opposite end of the case the USB cable plugged directly into the Nano board for host communication and programming; the status LED and red data logging start/stop pushbutton beside it; the small micro-SD memory card which is inserted into the slot above the cable socket for in-

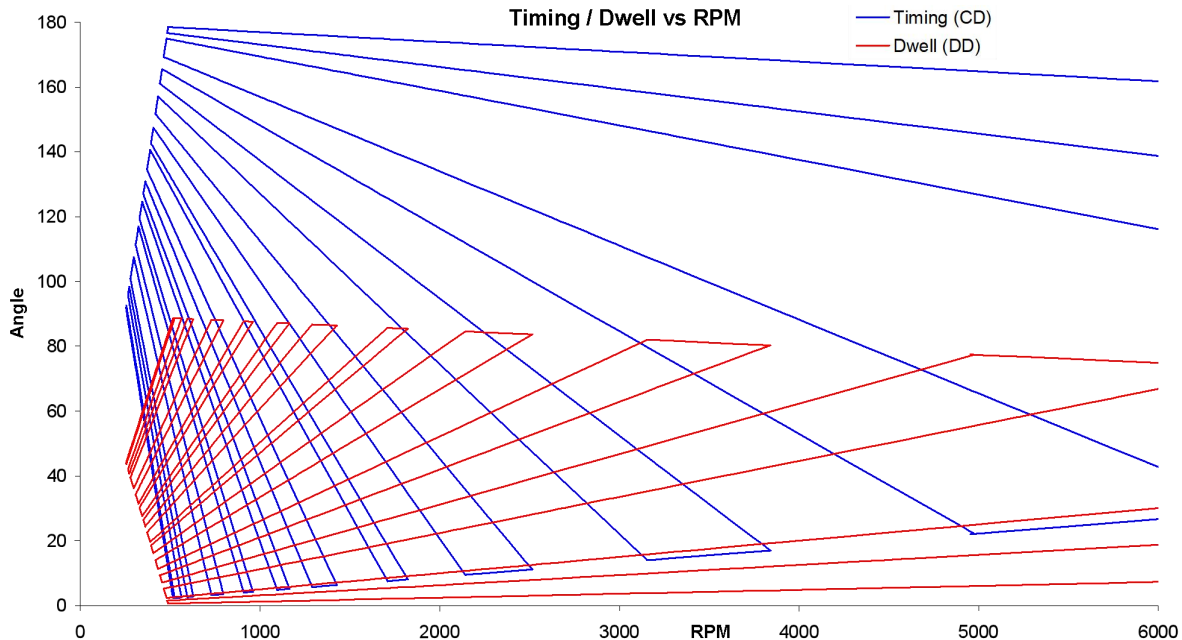


vehicle data logging and the USB adapter necessary if a micro-SD slot is not present in the host data analysis computer.

Not visible in the above images is an extra socket below the Nano's micro-USB socket for an accessory serial cable connection, in this case a D9 socket for an RS-232 port. If the data logger is to be used frequently in a bench-test configuration with direct host connection, it is recommended that the existing serial communication pins (RX and TX) on the Nano board be used together with a serial interface IC instead of the flimsy included micro-USB socket, or at least wiring the latter to a larger USB socket mounted on the instrument case. Generic circuits for serial port communication with Arduino boards are widely available on the internet.

9.3. Testing the data logger

As the data logger uses an accurate real-time clock to time distributor ignition events, it requires no calibration other than that for the vacuum advance sensor given below. The timing meter test circuit described previously may be used to ascertain the correct operation of the data logger and characterise its output, as is shown here.

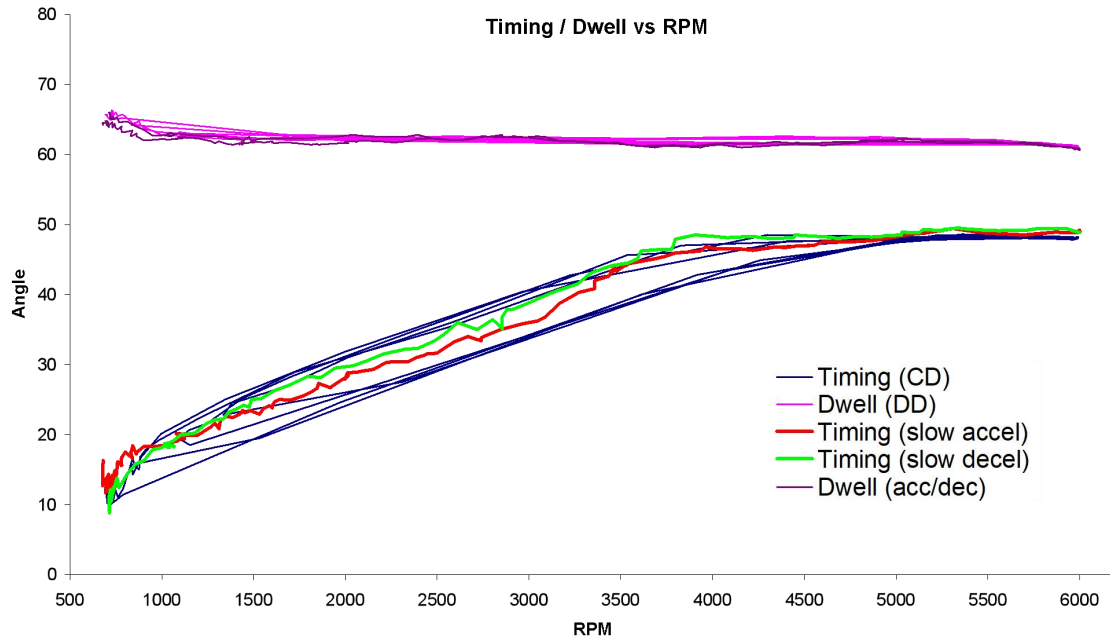


The MS-Excel graph above shows the result of logging the output of the timer test circuit whilst continuously adjusting the Q_LOW pot over its entire range for increasing increments of the Q_HIGH pot. For each position of the latter, the blue (CENT) timing curves represent decreasing Q_LOW time with increasing frequency (RPM) resulting in a greater ratio of Q_HIGH to Q_LOW durations, which simulates the open-points interval and scales as the timing angle in CD. The fall in max timing with increasing RPM reflects the greater contribution of the test-circuit 5.6K current-limiter resistor to Q_HIGH as the two pots go to zero. Although the plot has been truncated arbitrarily at 6K RPM as this represents the typical range of interest for distributor timing events, the data logger will function correctly beyond 30K RPM - unlike the analog timing meter, whose tacho circuit was intentionally limited to 6K RPM to ensure optimal engine speed readout over the working range of the timing circuits. Also shown as a set of red curves in the graph are the measured dwell angles for each point on the timing curves with $PTSDELAY$ set to 0. These approach 90DD as the ratio of Q_HIGH to Q_LOW durations approach zero. This ratio Q_T may be measured for any given setting of the two pots using a DVM via dividing the voltage on the tester T_MON output by 12V. The timing log should show $180CD \times Q_T - TIME_OFS + STAT_ADV$ and the dwell log should show $90DD \times (1 - Q_T)$. A more exact method would be to sample the test circuit's output waveform using a digital storage oscilloscope while logging it and calculating Q_T for several noted positions of the pots. The resulting stored waveforms would also furnish an accurate measure of the simulated engine speed. Actual tests of the data logger circuit performed in this fashion show accuracies below one significant figure (error < 1RPM, 0.1CD, 0.1DD) to beyond the equivalent of 10K RPM. Accordingly, any logged data not conforming to expected values must represent an unexpected *electrical* state of the ignition system low-tension circuit, which in turn may result from a mechanical fault in the distributor.

The event-handler error detection counters should remain zero until the Q_LOW pot nears zero, corresponding to unrealistically low dwell values. The simulated points closed period eventually becomes too short to be registered as a valid PTS signal, leading to unmatched strobe signals increasing the $PTSERR$ counter and no log file output until a valid low PTS level signals the start of

a timing cycle. Further reduction of Q_LOW leads to cessation of the strobe signal as well, resulting in no further PTSERR count increment. However, in actual distributor data logging there are several possible situations in which various combinations of the event-detection error counters indicate specific problems with the ignition system and these will be detailed in section 10.4.

A slew-rate response test may be conducted by sweeping the Q_LOW pot rapidly over low duration values with Q_HIGH set to minimum and logging the output from the timing test circuit. The log should show engine speed changes that stabilise within one entry (200ms) of the sweep ending, for observed speed variation of at least 2000RPM per log entry, or a slew-rate of 10K RPM per sec.



Attaching the data logger to our points-only (no ignition coil or points capacitor) DM2 bench-test rig set to 10CD static and zero vac advance, and running the rotor speed from the equivalent of idle to 6000RPM and back rapidly (within 2 seconds) produces the graph above. As this distributor is fitted with conventional points, the dwell angle is seen to be a near-constant value of 62DD across the RPM range, reflecting the physical points-gap setting of about 0.015". The timing curve shows the huge centrifugal timing advance produced by this DM2, increasing from zero at idle to 40CD after 5000RPM. Also evident in this graph is the approx. 6CD timing hysteresis between increasing (lower curves) and decreasing (upper curves) equivalent engine speed below 5000RPM due to the inertia of the centrifugal weights and friction at their pivot and linkage pins resisting rapid changes in rotation speed. Superimposed on this plot is a single slow acceleration timing curve (red) followed by a single slow deceleration curve (green). Although the hysteresis is reduced, the irregular *but reproducible* trajectory of the timing curves betrays the resonant harmonic vibration produced by a worn rotor shaft bush. The corresponding peaks and dips in the dwell curve at equivalent RPM indicate the resulting movement of the rotor cam axis respectively away from and towards the points, particularly at engine idle speeds where the pressure of the points spring on the cam is sufficient to overcome the rotor shaft's angular momentum and push it away across the distributor axis.

In the absence of a capacitance meter, the above configuration also may be used to derive a PTSDELAY value for a bulkhead-located points buffer transistor. By interposing the intended distributor cable between the points connection resistor and bench tester's points buffer input resistor, dwell values reported by the data logger at high RPM will include a capacitive delay due to the cable. These may be compared to equivalent values observed without the cable but with a known-value capacitor connected to GND at the same point to gain a capacitance ratio for the cable. The same technique could also be applied to the test circuit by interposing the resistors and cable between the NE555 output and the inverter transistor instead of the existing 100K resistor.

9.4. Accurate calibration of the vacuum advance sensor

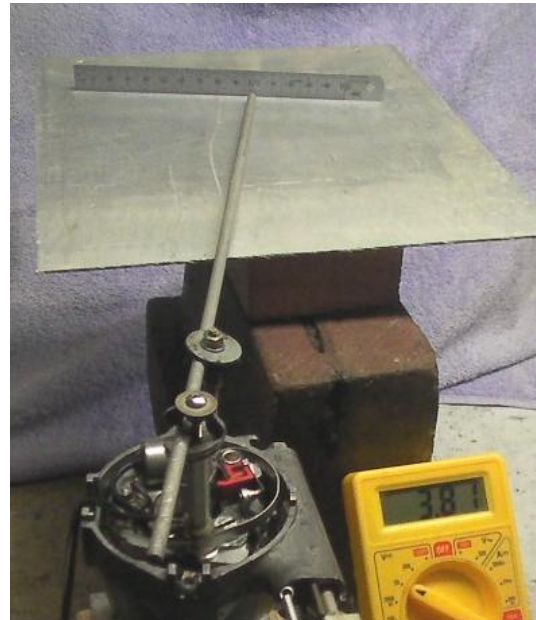
Having chosen and characterised a sensor/magnet pairing as described in section 13 and assembled them into the distributor, it remains to calibrate the sensor. To produce an accurate vac-sensor response curve for the data logger `VAC_DD` array it is necessary to manually “degree” the sensor output for a sequence of points plate positions exactly 1DD apart between the rest position of the vac unit and its full advance position. As this response curve is totally a function of the specific placement of sensor and magnet in the distributor, the measurement must be made at the workbench with the sensor *in situ* in the distributor. If a thermal-drift compensation scheme has been deployed for the vac sensor that permits calibration at room temperature, the method given below is sufficient for accurate calibration. Otherwise, it is necessary to maintain the distributor body at its normal running temperature using a heat gun, hairdryer or soldering iron clamped to the distributor spindle and monitoring the temperature by means of a digital thermometer and thermocouple with the latter attached as closely as possible to the magnet on the points plate. The system has reached thermal equilibrium when the sensor output has stabilised for a non-zero incident flux from the magnet.

Clamp the distributor in a vice and attach a makeshift pointer to the points plate. This should consist of a rigid rod with a pointed end attached to a bracket made to fit over existing screw holes on the points plate such as that for the points capacitor bracket. The pointer rod must be held *radially outward* from the rotor shaft axis, such that their axes cross, and the length from the rotor shaft axis to the end of the pointer rod should be 286.5mm. Clamp down a sheet of mild steel under the end of the pointer and position a steel ruler held by a magnet at the end of the pointer arc. Adjust the ruler to denote the rest and max advance positions of the pointer. For the given pointer rod radius, each DD is exactly 5mm apart. If it is anticipated that the rest position or max rotation of the points plate *with respect to the sensor* may change later (e.g. if the vac unit is replaced or modified), it is prudent to measure sensor voltages at extra DD positions either side of the marked range for future reference.

If the sensor and magnet have been located directly beside the vac-advance linkage pin (as is the case in our DM2 example) it will be necessary either to leave the vac unit connected to the points plate or replace its linkage with an identical loose equivalent to retain a representative local magnetic field distribution. Use a wooden or plastic implement to push against the linkage pin whilst taking readings in this case. Otherwise, the vac unit may be disconnected from the points plate.

Power the sensor using a regulated 5VDC supply (preferably using the intended 5V supply for the distributor sensors in the vehicle) and monitor its output voltage using a bench DVM. Record the sensor voltage seen at each DD position several times and for both rotation directions of the points plate, being careful to avoid touching the pointer or its bracket when rotating the plate. When a consistent set of sensor voltages are recorded, replace the entries in the `VAC_DD` array

starting with the minimum vac advance sensor voltage up to the max vac advance sensor voltage, all of which must be less than `AREF_V`. It is prudent to include at least one DD below the rest position of the vac unit in the array to permit observation of timing error caused by movement of the vac unit, momentary points plate over-travel on sudden vacuum drops or thermal drift. Record the vac unit rest position offset from the first array element at the `VAC_OFS` label in DD. Ensure the number of entries in the array at least corresponds to the total vac advance range in DD of the vac unit, followed by the `MAX_DD` end-of-range sentinel element. Re-compile the DLM program and upload it to the microcontroller.



While the distributor vac-sensor “degreeing” rig is still assembled on the workbench, the accuracy of the linearity-correcting interpolation function may be determined by attaching the data logger to the vac-sensor *VAC* output line from the distributor and powering the data logger from a 12VDC supply. With the points plate position indicator at the rest position, activate the data logger and slowly rotate the points plate to rest at each DD position for several seconds. The resulting log file will report the vac advance (in CD) corresponding to the DD positions within 0.1CD if mapped correctly. If an error is found, the *VAC_DD* array entry may be corrected, the code re-compiled and uploaded to the data logger for verification. Note: if all vac advance values reported by the data logger are out by the same (small) amount, it is likely that the 5V supply used for mapping the sensor does not match the data logger’s 5V supply exactly. If this is the 78L05 already present in the distributor circuit, correct the sensor map by scaling each entry by the ratio of the two supply voltages.

9.5. Verifying the vacuum sensor calibration using logged data

Accuracy of the vacuum advance measurement scheme may be verified by careful study of the cent advance values reported in the data logs. These values are produced by subtracting both the fixed static advance and the measured vac advance from the measured total timing advance. As the latter includes the vac advance as applied to the timing by the points plate position, subtraction of our measured vac advance and the static timing should produce the cent advance curve accurately *unless* mechanical timing error is imposed by the distributor or our vacuum sensor calibration is erroneous. The most common cause of the latter is a shift of the vac sensor output due to thermal effects upon both it and its reference magnet at engine running temperatures. Schemes to correct for thermal effects on the vac sensor are presented in section 13.1. Conversely, a shift in the rotation axis of the distributor upon engine heating may offset the total timing advance from its equivalent values when cold, resulting in a shift of the calculated cent advance curve. This is observable as multiple parallel cent curves if the logged timing data is plotted as a function of engine speed in a spreadsheet. In most cases, a mechanical timing shift can be discerned from a vac measurement error by checking equivalent engine-speed cent values where vac advance is zero or by the observation of multiple corresponding dwell curve tracks (see section 10.3.1). Note that small (<2CD) timing shifts due to thermal expansion of the points contacts and rotor parts within the first ~10 mins of engine running from cold are the norm for period MIDs.

Where a vac sensor calibration error is suspected, it is useful to collect timing data together with the corresponding sensor output values under the relevant test conditions. This may be performed by setting the *VAC_DIAG* flag to `true` in the data logger program script before compilation and upload to the DLM. Subsequent logged data will include two extra columns corresponding to the vac sensor voltage and reference sensor voltage (if present, see section 13.1.5) as measured by the DLM. Remember that these voltages are referenced from *Vsen* for the sensors and *AREF* for the DLM’s analog inputs. After importing the log file into a spreadsheet program, the sensor voltages may be used to recreate the vac advance measurement for each log entry using the same function employed in the data logger program, but referenced from a vac sensor calibration array encoded within the same spreadsheet. Likewise, the reference sensor corrections given in section 13.1.3 may be applied using spreadsheet formulas. The vac sensor calibration array interpolation is not straightforward in MS Excel as no array-based linear interpolation function is available, but it may be performed by interpolating each 1DD-equivalent sensor voltage interval into a separate column and then summing across rows to obtain the vac advance conversion. For example, assuming a data-log derived (and temp-corrected) sensor voltage column *V1:Vn* and a sensor calibration array *S1:Sm* such that each sensor voltage value is 1DD apart and *Sm* equals *MAX_DD*, the formula

$$= (V1:Vn >= Si) * (V1:Vn < Sj) * ((V1:Vn - Si) / (Sj - Si) + k) * 2$$

produces a column containing vac advance values in CD corresponding to sensor voltages between *Si* and *Sj* assuming that *Si* corresponds to *k* DD. The *S1:Sm* array values are adjusted to correct for the observed differences between timings with vac present and equivalent timings with vac absent.

9.6. Technical: Data logger operating scheme

This section details the operating scheme of the data logger at the device level as an introductory tutorial on event-driven microcontroller programming and may be omitted. The material covered here may inform any functional extension of the data logger program and electronics.

Fixed static advance: In principle, the data logger could identify a specified engine state at which to calculate static advance rather than using a supplied constant value. This would reduce progressive systematic error in the cent advance calculation as the points gap changes with wear. Such a strategy is not included in the DLM program due to the risk of the timing data being biased opaquely by transient conditions in the engine and ignition system.

Asynchronous processing: The main loop procedure `loop()` runs continuously in the DLM once power-up initialisation is complete. When data acquisition is activated by the `DOAcq` flag being set, the procedure accumulates vac advance readings and writes log file entries periodically before clearing the measurement accumulators for the next acquisition cycle. The event timing measurements are not performed by this procedure, but by hardware interrupt service processes that operate *asynchronously* to the main loop. Upon a designated change in voltage level on one of the monitored input lines *PTS* and *STROBE*, a corresponding hardware interrupt is generated in the DLM microcontroller. This suspends execution at the current instruction in the main loop and executes the designated interrupt service routine instead. Once completed, execution of the main loop continues at the suspension point and with the original processor state preserved. The interrupted code cannot ascertain any action of an interrupt service routine other than by examination of flags and data it leaves modified upon exit. In our case, the sequence of timing events that cause hardware interrupts dictate when a measurement cycle begins and ends. The main loop must defer creating a log entry until a later iteration if a timing measurement is in progress at the end of a sample period, and it does so by checking the `timing` and `ptsopn` flag states. As these flags will always be false if the engine is not actually running, the code also checks that the strobe count `strCt` is non-zero in the current sample before reading out the timing accumulators.

Interrupt handling scheme: The Atmel ATmega328P microcontroller used in the Arduino Nano furnishes only two edge-triggered external interrupts, which may trigger on either rising or falling voltage levels on their respective input pins. As the data logger must identify the points opening, points closing and strobe events unambiguously and precisely in time to produce accurate timing data, ideally we would adopt a strategy of triggering interrupts on the rising and falling edges of the *PTS* signal and the rising edge of the *STROBE* signal. Monitoring both the points opening and closing events using the same interrupt and ascertaining which event has occurred by testing the logic state of the *PTS* line from within the corresponding interrupt service routine is bad practice as noise on the input line may lead to an instantaneously false state report compared to the expected transition that prompted the interrupt, causing a points-state misidentification timing error. Likewise, flipping the programmable trigger edge sense between interrupts may introduce noise triggering or degrade the acuity of the edge discrimination scheme. Fortunately, the ATmega328P microcontroller also offers a number of *pin-change* interrupts (supported by the Arduino IDE as part of its AVR library) which trigger on a logic-level change on an input pin. As it is preferable and far more accurate to use an electronic method to identify transient voltage phenomena in real time, we may use one (falling) edge interrupt line to monitor our inverted points opening signal, the second (falling) edge interrupt line to monitor our inverted strobe pulse and then use the fact that a points closing event *must follow* each points opening event to enable a pin-change interrupt tied to the *PTS* line only in anticipation of a points closing event. This interrupt handling scheme precludes multiple sampling of the input lines and extraneous interrupts for the same physical event.

Event sequence initialisation: If the data logger is activated before engine start or the engine stops during sampling, upon engine start the interrupt service routines execute an initialisation sequence over two distributor rotation sectors before any (further) data logging is performed. Points interrupts are ignored during initialisation. The initialisation is led by the first strobe interrupt to occur, which

registers the sector start time. The second strobe event attempts to establish the current sector duration to enable data acquisition and error logging. If successful, the sample period is restarted by the main loop and subsequent events contribute to timing data accumulation. Otherwise, the initialisation sequence is repeated until a valid sector period is established. The initialisation routine is also performed if the sector timing register is corrupted by repeated missed strobe events, indicated by a sample period in which fewer valid strobe events than missed strobe events occur. Note that such a sample period will not be logged but adjacent log entries would show missed strobe counts (see section 10.4.2).

On-the-fly data logging: Conventionally, when using asynchronous interrupt-driven data acquisition routines it is necessary to temporarily suspend interrupts while the relevant event data accumulators are read out to prevent further interrupts from corrupting the data during access by the main loop. However, suspension of interrupts will lead to event timings being delayed and/or timing events being missed by the DLM, as well as a loss of event sequencing. Fortunately for our case, the extreme speed of the microcontroller processor compared to the distributor's fastest possible ignition event sequence permits data collection from the interrupt-driven accumulators within a calculated "window" of time in the event sequence *without* suspending interrupts. Any single iteration of the main loop only has the `timing` and `ptsopn` flag states to ascertain what period of the timing cycle that it occurs within. When both these flags become false, no timing event is in progress but a new timing cycle may commence at any moment with a points-opening event. Assuming that this is the case, the main loop read-out and reset code has *at most* the distributor rotation time to reach the next points opening event at maximum engine speed. Our conventional 6K RPM upper limit on engine speed equates to a distributor sector time of 5ms, so a full-advance ignition at 50CD BTDC prior to a strobe pulse at 30CD ATDC allows 50DD or 2.8ms. The processing time for the main loop read-out / reset code marked within comments in the program script is just 170 microseconds (μs), or 6% of the time available at 6K RPM. In electronic ignition systems where the dwell duration is dynamically controlled in response to engine speed, short dwell duration rather than the strobe-limited timing duration becomes the readout time constraint. However, short dwell durations ($\sim 10\text{DD}$) are applied at low RPM only such that the dwell *time* remains extended at about 5ms.

Vac advance sampling: The high processing speed of the DLM also results in a massive oversampling of the vac advance level in each log entry, as the main loop has little else to do between log entries. This permits restriction of vac level sampling to main loop iterations with `ptsopn` true to ensure no current is flowing through the points circuit in the distributor. The vacuum advance sensor positioning scheme given for the timing meter in section 8.5 specified locating the sensor clear of any magnetic field disturbance from the points circuit as the timing meter monitors vac level continuously. As the DLM monitors the points state in real time, any potential bias of measured vac advance level due to points circuit current may be precluded at no functional cost in the data logger by making these measurements only when the points are open.

10. Using the timing meter and data logger

Having established an accurate method of determining actual ignition timing it remains to interpret the observed behaviour and efficacy of the dynamic timing program produced by the MID. Optimal values of ignition timing for the various states of engine load are highly specific to individual engine, induction and exhaust system parameters. Data on target timing profiles for any given configuration *using modern fuels* will be found online in vehicle-specific or motor-racing forums where experts have analysed equivalent implementations. In particular, any retrofit customised camshaft must be supplied with recommended ignition timing curves. Likewise, a distributor re-curved to a specific engine configuration by an expert automotive electrician should be provided with a paper record of the timing calibration for reference. In this section we will consider general observations made with the timing meter and relate them to specific engine states. It is also assumed that the correct operation of the timing meter has been established previously with the specific engine components under test (see 8.10). Also remember that period MIDs exhibit small timing instabilities or offsets normally when cold.

10.1. First check - the dwell meter

Dwell angle measurement is independent of static and dynamic timing controls within the MID and affords a basic check of the points electrical circuit and points cam rotation axis stability. This may be performed either during engine starting or running. Some faults indicated by the dwell angle measurement include:

Unstable dwell during engine cranking only

High dwell values indicate low coil primary circuit voltages, suggesting a weak battery or poor supply to the coil. Conversely, low dwell values indicate a failure of the points circuit to sink sufficient current to charge the coil effectively due to resistance in the path to engine ground.

Oscillating dwell value at engine idle speeds

If the dwell figure exhibits a *continuous* sinusoidal oscillation over a small angular range at engine idle speeds that does not repeatedly stabilise for short periods (i.e. not Nyquist noise), either the rotor cam is worn asymmetrically, its spindle is bent or the driveshaft bush is worn. The behaviour may persist at higher engine speeds but remain unobservable due to sample averaging over a larger number of ignitions by the timing meter.

Increasing reported dwell with increasing RPM

The dwell meter is failing to detect points opening at high engine speed. If engine misfire occurs in concert with this observation then an electrical fault in the coil primary circuit is indicated. Otherwise, the most likely cause is a higher ground potential at the PTS circuit than at the points plate (check engine grounding).

Decreasing reported dwell with increasing RPM

A linear decrease in the reported dwell with increasing engine speed of $\sim 1\text{DD}/\text{KRPM}$ indicates normal coil primary circuit charge and *PTS* line delays (see section 5.1). Larger drops in dwell with increasing RPM suggest the *PTS* circuit ground potential is lower than that at the points plate, extending the apparent points open duration. Where points grounding is known to be adequate, parasitic resistance across the points contacts is maintaining a positive voltage briefly after points closure (see section 10.3.1).

Anomalously low (or zero) dwell angle

The points voltage never falls below 2 volts, even when the points are closed. Either the points plate, distributor or engine block is poorly grounded or the points themselves have significant electrical resistance. Note that the coil primary circuit may draw 6A through the points continuously, so a 1-ohm resistance in this circuit under load would produce a 6-volt potential drop.

Anomalously high (or 90DD) dwell angle

The points voltage never exceeds 3 volts. If the engine is running, the *PTS* line connection is faulty or the *PTS* circuit / timing meter ground connection is floating. Check that the timing meter operates correctly with the test circuit.

Increasing constant dwell angle over mileage

The points gap setting is decreasing due to insufficient lock screw tension or a worn contact-set points cam follower. Replace the screw or points plate if either has a worn thread and ensure the points cam is lubricated correctly after fitting a new contact set.

Decreasing constant dwell angle over mileage

Arc-erosion of the points is increasing the effective points gap (even if the gap as measured by feeler-gauge seems correct). Also check the points capacitor and points plate grounding.

Erratic dwell angles at low RPM only

Suspect a worn points cam, worn rotor shaft bush or play in the cent advance mechanism. Increasing rotor angular momentum with rising engine speed may force these parts into a more stable configuration against friction forces. Cyclic dwell “beating” over a small range at low RPM is ascribable to Nyquist (sampling) noise between the dwell duration and DVM integration periods.

Erratic dwell angles at high RPM only

If this phenomenon coincides with similarly erratic timing, the likely cause is points “float” or “bounce”. If this is the case, the engine running will also be “rough” at the same observed speeds.

Reproducible nonlinear dwell curve over engine speed range

This is typically caused by harmonic vibration of the distributor rotor shaft in a worn bushing, confirmed by observation of the same resonance curve in the bench-test rig with no coil attached to the points. Otherwise a problem with the coil or points capacitor is indicated.

Random dwell angle transients

Brief increases in dwell angle indicate an intermittent short in the points circuit. Likewise, brief decreases in dwell angle indicate an intermittent circuit interruption, typically caused by arc-eroded points or poor electrical connection. Engine misfires will be observed where such transients are of sufficient duration to hinder charging of the ignition coil.

Breakerless ignitions

If a breakerless ignition is employed, the conventional dwell angle is replaced by an increasing linear relation between dwell angle and engine RPM. The dwell angle may be as low as 10DD at idle and increase to more than 30DD at max RPM. More than a full distributor rotation may be required for the ignition module to commence applying dwell periods to the coil circuit at engine start. The behaviour of a specific ignition module in correct operation should be noted for reference comparison in future fault diagnosis. Any departure from normal operation that cannot be attributed to electrical connection, heat dissipation or attachment stability most likely indicates a failing power transistor in the ignition module. A fault in this unit may also be diagnosed by replacing it temporarily with a set of breaker points and monitoring the other ignition system components for correct operation. Note that a defective (or reversed-polarity) ignition coil may operate satisfactorily with breaker points but damage a breakerless ignition module over time.

10.2. Using the timing meter

Having observed correct function of the points and ignition charge circuit using the dwell meter, we can use the timing meter to check the MID timing behaviour in garage testing and also observe and diagnose specific on-road engine ignition states.

10.2.1. Engine starting

During engine cranking the timing meter should show the static ignition timing only. If the dwell meter display shows the expected figure correctly, small departures from static ignition timing only observed during cranking suggest a mechanical fault in the distributor cent mechanism that is stabilised by higher engine speed. Large errors or loss of timing signal during cranking suggest a flat battery or bad battery connection to the coil circuit (such that the coil is running on the alternator / generator / dynamo after starting). Another common ignition fault indicated by drops in displayed timing and RPM during cranking is a voltage drop on the *IGN* line due to an intermittent connection in the ignition switch mechanism during twisting of the ignition key to the start position.

10.2.2. Static ignition timing check

A primary function of the timing meter is to monitor the condition of the points over extended use, particularly as this is the one MID component intended for regular testing, maintenance and replacement. After running the engine to working temperature and achieving a stable low-speed idle, the timing meter will display the static ignition timing in the absence of any vac advance. If vac advance is present at idle, the amount indicated by the vac meter display may be multiplied by two and subtracted from the timing display to obtain the static ignition timing. An alternative method (and a good test of the vac mechanism) is pressing the accelerator briefly at idle to extinguish vac advance, observable by the absence of the vac meter display. The timing meter display should drop to the static ignition timing value briefly before engine RPM increases sufficiently to activate the cent advance mechanism.

10.2.3. Centrifugal advance curve

In the absence of a manifold-direct driven vacuum advance unit, the timing response of the MID to rapid changes in engine speed is controlled by the cent advance mechanism. By observing the timing meter at various speeds in specific driving situations (and when safe to do so) such as acceleration, coasting, cruising under power, ascending or descending an incline, decelerating and upshifting or downshifting, a degree of familiarity with the MID's particular cent advance program may be attained. Key features to note include a rapid timing response to sudden large changes in engine speed, a reliable drop to static advance timing upon return to engine idle, an identifiable and repeatable upper timing limit value corresponding to max cent advance and a timing figure that is stable to within a few CD at constant cruising speed. Note that the rate of engine speed reduction at throttle closure is dictated by flywheel inertia, not ignition timing.

As the cent advance mechanism is purely mechanical, salient forms of observable timing error will include:

Sudden jumps in timing without simultaneous changes in engine speed

This may be caused by stick-slip friction in the rolling-weight mechanism or rotor cam and only requires lubrication to correct. Alternatively, wear in either the rolling-weight pivot posts or drive shaft bush may produce a discrete set of stable rotation modes in the distributor that it jumps between in response to engine speed rather than a continuous timing curve.

Slow "wandering" of timing at constant engine speed (above idle)

Unstable timing produced in conditions of constant engine speed and load where the vac unit is certain not to be active indicates significant wear in the cent mechanism components if similar wandering is not also seen at a smaller proportion in the dwell curve (otherwise the drive shaft bush is worn).

Erratic timing at a particular engine speed only

Where the timing is observed to vary rapidly over a fixed range of values at a particular constant engine speed, a harmonic resonance is present in the timing mechanism. Either the drive shaft is vibrating within its bushing, the cam rotor is vibrating on its spindle or the points are floating /

bouncing (at high engine speed only). In such cases, the same behaviour must be evident proportionally in the dwell meter display at the same engine speeds.

In the absence of any such discernable timing errors, the appropriateness of the cent advance produced at a particular state of engine speed and load may be inferred from the following:

Engine “pinking” or detonation under load

The observation of engine “pinking” or “pinging” (a metallic rattle from the cylinder head region) under load indicates an over-advanced ignition for that particular engine state, assuming that the engine is not excessively over-gearred or the engine speed too low to produce the required power.

Engine overheating at cruising speed / “white” spark-plugs

Where the fuel *is known* to have sufficient octane rating for the engine’s compression ratio and the fuel mixture supplied to the engine *is known* to have correct stoichiometry at cruising speeds, over-advanced timing will cause engine inefficiency and high cylinder temperatures. Either the max cent advance is set too high or the additional vac advance results in too much total ignition advance.

Breakerless ignitions

In general, a points-replacement ignition module should replicate the make/break behaviour of points accurately as far as the ignition coil primary circuit is concerned, and do so without the issues of timing drift due to wear and vibration. The timing advance curve remains under the control of the cent and vac mechanisms only. As the coil-primary discharge path through the points contacts is replaced by a power transistor in any breakerless ignition system, a small potential drop must exist across the transistor’s conduction path during its “on” state (equivalent to points closed), necessitating a commensurate heat-sink for the power dissipated by the module. In comparison, the points offer negligible resistance to the coil primary circuit current once the contacts have fully closed (see 10.3.1). Accordingly, use of a breakerless ignition necessitates a reliably consistent low-resistance current path to ground through the other coil primary circuit components to prevent weakening of the ignition discharge from the coil. Any parasitic resistance present may lead to weak or missed ignitions, indicated by drops in timing and jumps in dwell on the timing meter.

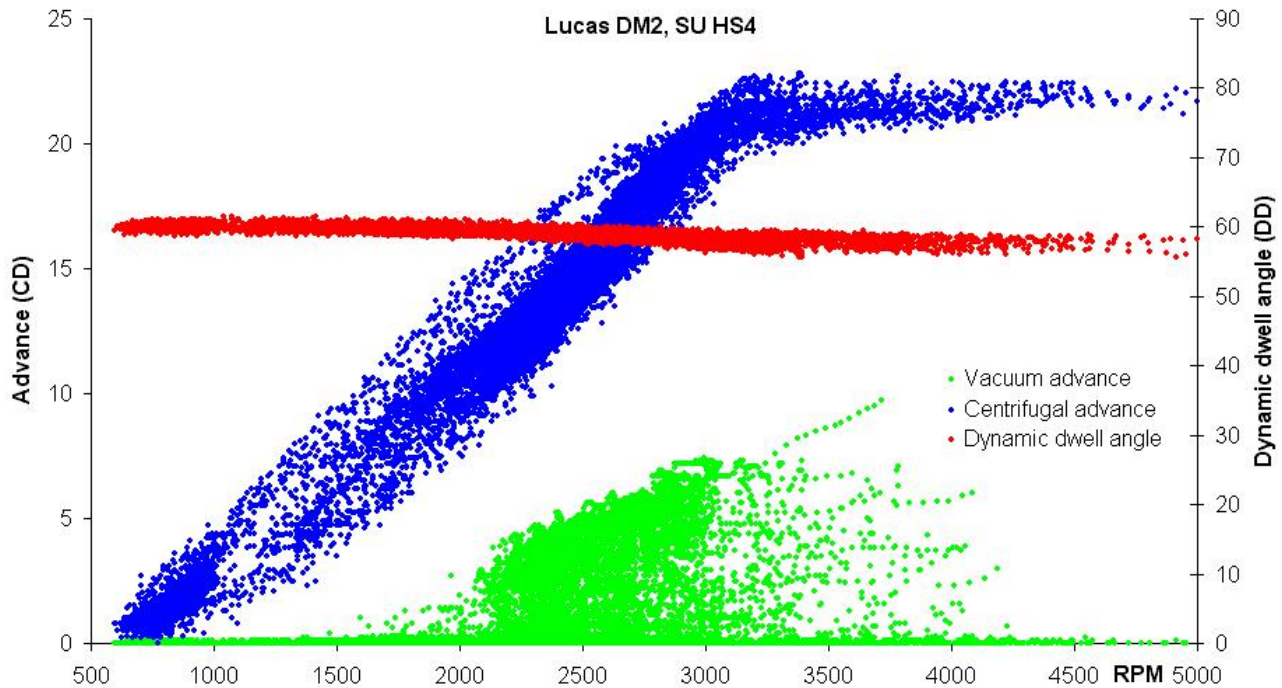
10.2.4. Vacuum advance optimisation

The primary function of the vac advance display on the timing meter is to ascertain that the vac advance unit is operating correctly. Firstly, the lack of any displayed vac advance in any engine state generally indicates a failed vacuum unit diaphragm, ruptured vacuum line or blockage in the vacuum pick-up point at the carburettor or inlet manifold. Secondly, sudden discrete jumps in vac advance rather than smooth changes with throttle position indicates stick-slip friction in the points plate bearing in response to applied torque from the vacuum unit. If this friction cannot be reliably eliminated by lubrication alone, the points plate assembly needs to be repaired or replaced. Finally, the degree of vac advance observed should be compared to the stated figures for the vac unit under the relevant engine states and any discrepancy due to poor maintenance, wear or vacuum leaks eliminated before embarking on any detailed study of vac advance efficiency optimisation.

The correct behaviour of vac advance is key to efficient highway cruising. By observing the vac advance display on the timing meter safely under cruising conditions at various steady road speeds, the degree of vac advance being added to the cent timing curve may be established. Assuming that the cent advance curve is considered correct for the vehicle, the vac timing component may then be correlated with fuel consumption data collected over the same conditions. A consideration of optimal vac advance must not just maximise total advance but also make allowance for variable engine load at cruising speed due to changes in terrain, vehicle load factor, headwinds or altitude. An over-advanced ignition due to excessive vacuum advance is evidenced in such engine load states by engine “pinking” or detonation that decreases or disappears as *more* accelerator is applied, unlike excessive cent advance. In this case, the increase in throttle aperture increases the mixture density slowly but decreases the total advance rapidly as vac advance is extinguished.

10.3. Using the data logger

An example of an extended road data logging session is shown the MS Excel plot below, which is collected from a points-driven Lucas DM2 (40624A) distributor fitted with an 11DD max cent advance restrictor plate and a (5-14-8.7) customised vac advance unit. In this case vacuum advance is driven by (one of two) SU HS4 carburettors, which employ the throttle-flap venturi depression port method of vacuum production. The ignition system under test includes a 0.15 μ F points capacitor, a Bosch “black” SU12R ignition coil and matching ballast resistor. A PTS delay correction of +0.35DD/KRPM has been applied to the measured dwell curve by the data logger.



Examining the broad features of this graph in turn, first we observe that the dwell plot shows a slowly decreasing dwell angle across the engine speed range from 60DD at idle to ~57DD at 5000RPM, indicating a small coil primary charging delay to the dwell duration. Lower points in this plot correspond to higher ignition system component temperatures after extended running. The vacuum advance plot displays the anticipated behaviour for a carburettor-venturi driven vacuum advance mechanism, with no advance produced before ~1500RPM and a linear increase in observed max vac advance (corresponding to the throttle flap being held at the exact angle for max depression at the venturi outlet) up to about 10CD at 3800RPM. At each engine speed, values of vac advance between zero and the observed maximum correspond to adjacent throttle-flap positions producing intermediate amounts of vacuum. The paucity of vac data in the 1500-2200RPM region reflects the absence of time spent cruising at low speed in second gear, whilst the excursion tracks present above 3000RPM represent second and third gear part-throttle acceleration phases. Higher values of max vac advance would be observed cruising at potentially illegal road speeds. The zero-vacuum values in the plot correspond to either to full-throttle acceleration or closed-throttle deceleration.

The centrifugal advance plot betrays a key characteristic of mechanical distributors: the *trajectory-dependent* relationship between mechanical advance and engine state. The upper curves are closed-throttle rapid engine speed drops out of gear and the lower curves are full throttle accelerations in gear. This hysteresis in cent advance as a function of engine speed is due to the inertia of the cent weights resisting rapid changes in engine speed. For this reason, performance tuning a mechanical distributor for competition centres on the response curve of the cent advance mechanism under hard acceleration only and ignores the other cases. A common fault identifiable by multiple parallel cent-plot trajectories is a “sticky” points plate which rotates only once sufficient vacuum is developed to overcome static friction in its collar bearing.

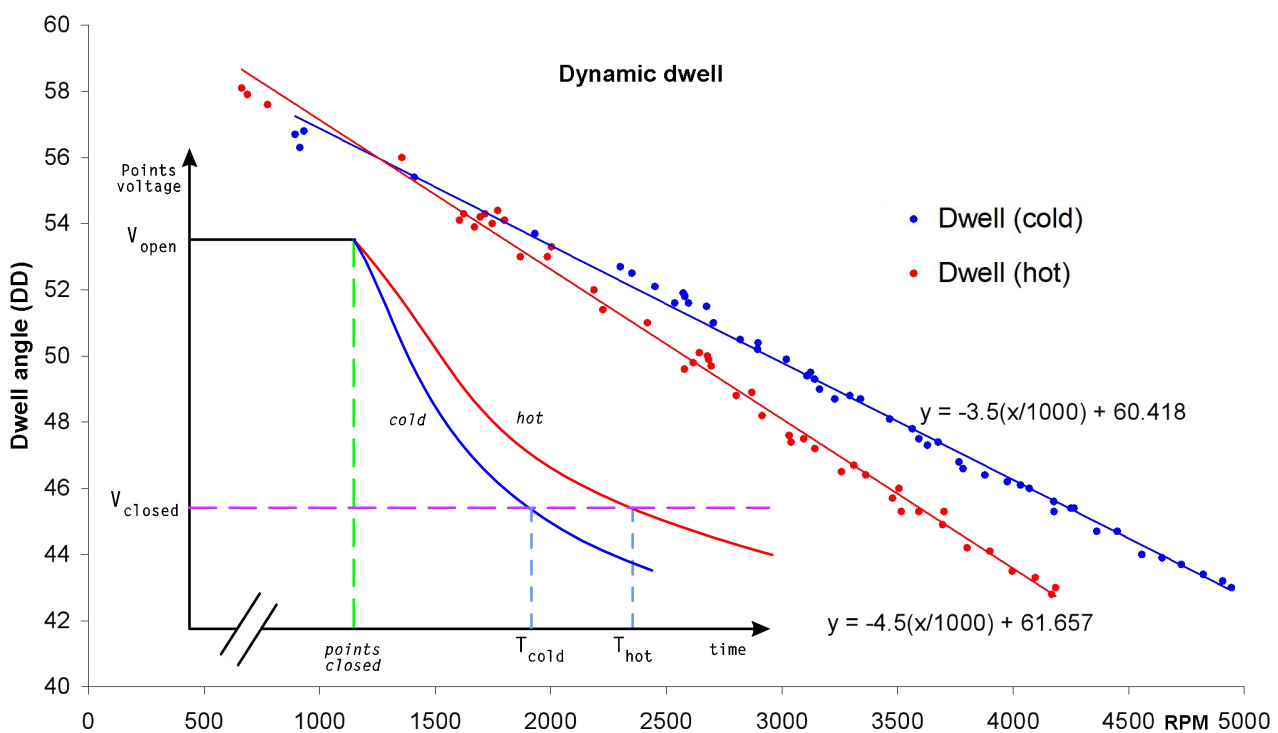
10.3.1. Dwell curve analysis

The dynamic dwell “curve” as a function of engine speed can furnish information about the distributor mechanism and coil primary circuit. The graph in section 9.3 illustrates the effect on dwell angle due to vibration of a worn rotor shaft bush and similar reproducible dwell-curve artefacts can be produced by worn rotor cams or their pivot posts, worn points sets, worn points plate collar bearings or unbalanced cent mechanism parts. Dwell-related electrical faults described in section 10.1 will manifest either as discrete events such as sudden jumps in dwell value or as continuous states such as drift of all or part of the dwell curve over time. The normal dwell-curve behaviour for an otherwise functional ignition system is a $\sim 0.5DD$ per 1000RPM linear decrease in observed dwell angle with increasing RPM from the (extrapolated) conventional points-gap value at zero RPM. This behaviour indicates a *constant* short delay time to the apparent points closure in each ignition cycle, as detected by points voltage. Unlike the actual rotor-cam dwell angle, each ignition cycle will add exactly one extra points closure delay event to our dwell measurement, such that it decreases linearly with rising RPM.

As was detailed in section 5, inrush current through the coil primary circuit upon points closure can maintain a non-zero potential across the closed points briefly due to parasitic contact resistance. The data logger will not detect the points as having closed until the points voltage falls below 2V. The time T_i taken for the points voltage to meet this criterion may be calculated from a plot of dwell angle D vs engine speed ω as the gradient $dD/d\omega$ expressed in DD per 1000RPM. Dimensionally,

$$\frac{1DD}{1000RPM} = \frac{1DD \times 1min}{1000 \times 1rev} = \frac{1DD \times 60 \times 1000msec}{1000 \times 180DD} = \frac{1}{3} \text{ msec, so } T_i = -\frac{1}{3} \frac{dD}{d\omega} \text{ msec.}$$

We may consider T_i as the coil primary circuit “inrush” charge time at points closure. A value of T_i greater than 0.3ms not attributable to inadequate common electrical grounding of all ignition system components and the data logger suggests significant points resistance due to either eroded points contacts or poor connection to the ignition primary circuit. Prematurely arc-eroded points contacts can be caused by a failed points capacitor. Other possible causes include a partial short in the ignition coil primary windings or just the use of a high discharge-energy coil without adequate wiring. Provided that T_i is less than the geometrically-defined dwell time (such that the reported dwell angle does not drop toward zero at high RPM) the coil will be sufficiently charged to function correctly. An additional indicator of the coil primary circuit state is given by any observed variation of T_i with increasing engine temperature and operating time.

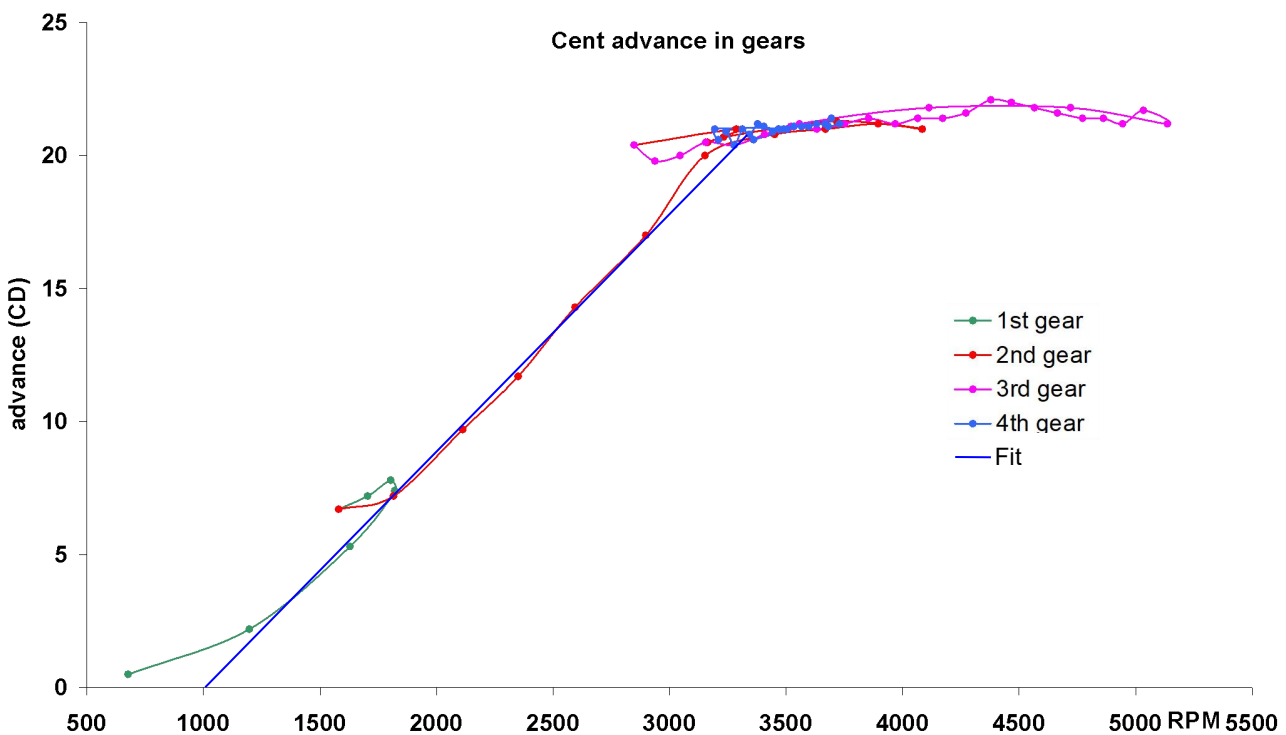


The graph shown above shows the effect of insufficient points ground current capacity on coil charge time. The *reported* drop in dwell angle increases from 3.5DD/KRPM after engine start to 4.5DD/KRPM after an hour's use, corresponding to an increase in T_i from 1.17ms to 1.5ms. Note that the extrapolated value of dwell angle at zero RPM is the expected 60DD within statistical errors. The apparent delay in points closure detection due to inrush current is illustrated in the inset plot. From the instant of points closure, the voltage at the points terminal drops to the product of coil primary circuit current and points (or grounding) resistance. The points will not be detected as closed by our electronics until the points voltage drops to V_{closed} . The parasitic resistance of the points contacts, coil primary, wires and connections will increase generally with temperature.

Shifts of the *entire* dwell curve by a constant dwell offset between cold and hot engine states are produced by thermal expansion both in the points contacts and (potentially) the rotor shaft bearing. The presence of multiple parallel dwell curves *only* over the active vac advance engine speed range *and* at equivalent engine / ignition system temperatures indicates a variation of dwell angle with points plate orientation. In this case, sequences of log entries having similar vac advance values will exhibit similar dwell angles at equivalent engine speeds. This behaviour is caused by an eccentric points plate location with respect to the points rotor due to either a badly worn points plate collar bearing or mispositioned points baseplate in the distributor. The cent advance plot will also exhibit multiple parallel tracks where this eccentricity also affects the points opening angle with respect to the points plate.

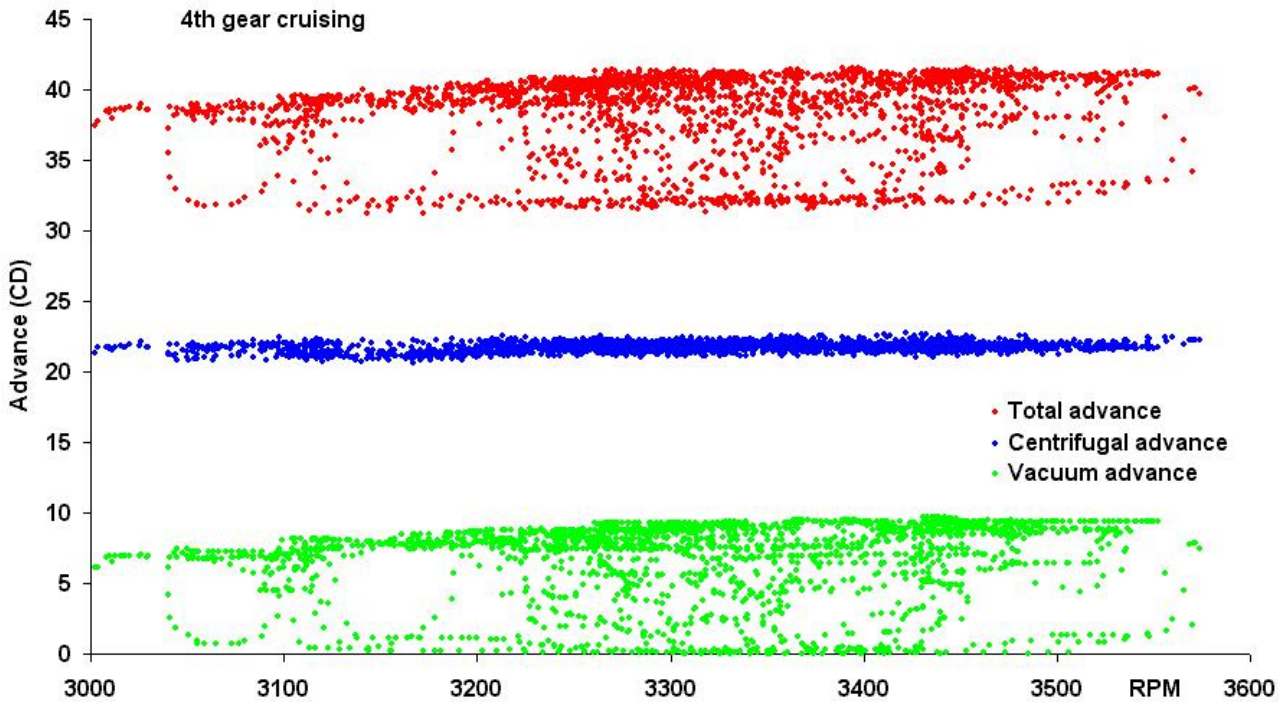
10.3.2. Acceleration through gears

The extended-session logging example is provided to motivate a more context-specific analysis of logged timing data corresponding to the identification of engine-state phases in the log files. In addition, the provision of a start/stop button in the data logger is made to permit the collection of timing data specific to a particular situation as a single log file. For example, by identifying the acceleration phases in the log file by selected drive gear, the conventional cent advance curve may be identified from the overall trend of timing advance against RPM in each gear. The single cent curve corresponding to the hardest acceleration sequence from rest (lowest cent advance points of the session plot) is shown below. A linear fit to the highest engine-load points of the timing curve suggests nearly 10CD per 1000RPM cent advance between 1000 and 3200RPM, with the expected restrictor-plate cent advance limit of 22CD beyond this range. The curve is surprisingly linear although some minor vibrational play in the mechanism is evident above 4K RPM.



10.3.3. Highway cruising

If we consider instead a region of a log file corresponding to cruising at highway speeds, we obtain timing plots corresponding to a small region of engine speed as in the following figure. The cent advance plot indicates the correct behaviour of the mechanism, producing a constant 22CD accurately over the engine speed range above max cent advance. The vac advance is seen to vary from 0 to 9CD, described by successive loops between different engine speeds corresponding to throttle “trimming” by the driver to maintain a constant road speed in response to changes in road direction and terrain. The total advance plot shows the advance actually applied to the ignition timing, ranging from 31 to 41CD but mostly maintained at 39CD (static advance = 10CD). The



appropriateness of this timing programme for the vehicle is determined by the combined specifications of the engine, induction and exhaust systems as described in section 3. This data should be considered as part of any restoration or maintenance of a period vehicle having revised engine specifications, being retrofitted with modern components and, in particular, using modern fuels. It is also worth noting that the total and vac advance data in the above figure are separately measured quantities, whereas the cent advance plot is calculated from their difference. The evident accuracy of the latter indicates the veracity of both the DLM timing acquisition scheme and the vac position sensor scheme, the latter consisting of a thermally-uncompensated UGN3503 and neodymium magnet calibrated at engine running temperature in this case.

10.3.4. Using overdrive

Vehicles possessing an overdrive or 5th gear for high-speed cruising can reduce fuel consumption by maintaining road speed at significantly lower engine RPM when high torque is not required. This assumption is valid only at sufficiently high road speed and marginal engine torque loading such that the throttle is either maintained or reduced upon overdrive engagement. An increase in engine throttle required to maintain speed indicates insufficient initial torque for the selected final-drive gearing and potentially higher fuel consumption. Such over-gearred cruising is likely to result in ignition timing cent and vac advance both being reduced, further decreasing engine efficiency. It is possible to identify cruise-speed gearing in the log files by calculating road speeds from the engine RPM shown in log entries using the equation

$$V = \frac{RPM \times 60}{(gear) \times (axle)} \times \frac{2 \times \pi \times R_e (mm)}{1,000,000} \text{ km / h } (\times 0.625 \text{ mph})$$

where *gear* and *axle* are the drive ratios of the gearbox and axle differential respectively and R_e is the effective road wheel radius at cruising speed, typically a few mm more than the axle centre height above the ground when stationary (and *not* half the horizontal tyre diameter). As overdrive gear ratios are typically 80% of the 1:1 gearing produced conventionally in 4th gear (where the gearbox input shaft is coupled directly to the output shaft), the equation above will yield the anticipated value of road speed correctly with a value of (say) 0.8 for *gear*. The identification of an up-shift to overdrive in a log file together with a drop in cent and/or vac advance is suggestive of either too low a road speed, too high an engine loading (due to vehicle weight, road grade, headwind, altitude etc) or inability of the engine to maintain the expected torque in its present state of tuning and wear.

Note that the above equation may also be used to check the speedometer calibration by creating brief log files at specific indicated road speeds using a known final-drive gearing. Remember to check tyre pressures beforehand and correct for their thermal expansion after some road use.

10.4. Log file error indicators

The “points error” PTSERR and “strobe error” STRERR indicators in the log files are provided to diagnose unexpected timing phenomena registered by the data logger control program. They are incremented as necessary in units representing the different types of timing error identified by the program within each sample period and cleared after a log entry is made. Such errors should be infrequent (a few per hour of engine operation) in a well-maintained ignition system. As the event handlers are invoked in response to specific changes in voltage levels on the *PTS* and *STROBE* lines from the distributor, it is possible for rapid small changes around the trigger voltage levels to cause spurious or unmatched events where the signal voltage transitions are not clearly defined. In particular, the mechanical make/break switching performed by the points may occasion rapid electrical noise transients that are detected erroneously as additional timing events. Resistance in the data logger’s *GND* path will also diminish the *PTS* and *STROBE* signals. Similarly, an intermittent open-circuit on the *IGN* line may momentarily halt DLM execution and cause timing errors. The hardware signal discrimination scheme employed in the DLM may trap only some signals or misreport others in this case. The frequency and confluence of these errors may be used to diagnose the underlying cause and potentially isolate a fault with the ignition system. Some of the error conditions reported by these indicators are common to the timing meter display errors detailed in section 8.10 and would be observed on the latter under the same test conditions. Here we will investigate the timing phenomena and instrumental error conditions made discernible by the DLM’s more sophisticated signal processing abilities.

The data logger event discrimination scheme is configured to permit collection of ignition data during engine starting by commencing a logging session with the ignition on prior to cranking. Similarly, if the engine stalls during active data logging (but the data logger remains powered), logging will resume when the engine is cranked. This feature facilitates analysis of the coil primary ignition circuit when cold and during high battery loading, as well as the diagnosis of circuit faults from errors indicated in the associated log entries. The data logger’s status LED will not change state while the engine remains stationary.

Note that the collected timing data are *not* corrected upon the detection of an error condition. The detection sequence and interval between events are used only to perform a most probable identification of the error type. A more sophisticated error-handling scheme is possible where the current RPM and physical limits on engine speed change can be used to discern invalid timing periods between sectors of the distributor’s rotation and correct the timing values accordingly in real time. Such a scheme is omitted in the data logger program for reasons of simplicity and the intention to detect and report real timing phenomena in the MID transparently.

It is possible to confirm specific types of error by correlating a non-zero error indicator with timing data from the same log entry, particularly at low RPM where the number of ignitions per sample is

small. Comparison of timings with unaffected log entries other than at engine idle must include consideration of acceleration / deceleration inertial effects on the cent advance mechanism as well as vac advance state.

10.4.1. Points event error (PTSERR)

A points opening event is triggered upon detection of a rising-edge voltage above 3V at the points. Likewise, a points closing event is detected upon a falling-edge voltage below 2V. Fluctuating voltages on the *PTS* line around the trigger voltage levels for detection of a points event may cause several spurious events to be triggered in quick succession. Voltage fluctuations may arise from a poor *PTS* connection or electrical interference from the high-tension circuit if electrical shielding of the *PTS* line is insufficient. Alternately, badly arc-scorched points, a failed points capacitor or poor points plate grounding may result in slow or multiple signals, as may points “bounce” at high engine RPM. The PTSERR counter registers two types of points event error:

Spurious points opening events (PTSERR values below 100)

These are detected as points-opening events within a timing interval already in progress. They are only registered as timing events if the previous timing interval exceeded a distributor sector period, indicating that a strobe signal was not registered. Frequent spurious points events at installation indicate insufficient filtering capacitance at the PTS buffer transistor input (see section 8.7). Otherwise, if the associated log entry shows normal timing and dwell for the given engine state, the spurious event indicates make/break noise upon the points either opening or closing, potentially due to a worn rotor cam or vibrating rotor shaft (particularly if seen only at low RPM). The presence of such noise near the level of the coil primary voltage upon points opening would adversely affect correct discharge of the ignition coil. If the event occurs outside the nominal open-points duration the corresponding sample dwell duration will be biased downward. Timing will be biased upward if the spurious events occur after the strobe pulse and before the next correct ignition angle. Spurious points events also may be caused by points bounce upon closing (at high RPM) or an intermittent break in the coil primary circuit. Points contact resistance in low-current distributor bench testing using the data logger may produce spurious points events, even at low rotation speeds.

Missed points opening events (PTSERR values in multiples of 100)

These are detected as strobe events that occur outside a valid ignition timing interval, more than half a distributor rotation sector after the last strobe event. The ignition timing accumulator is not updated in this case. Failure to detect the points opening will decrease the ignition timing and increase dwell values in the affected log entries, most notably at low RPM. A weak PTS signal caused by poor connection at the distributor, intermittent short in the coil primary circuit, scorched points contacts or a low open-points voltage in the coil primary circuit may be indicated. Conversely, a continuously high points voltage even with points closed will result in a failure to trigger any points events, in which case the affected log entry sample period will be extended until the points voltage falls sufficiently to cause a points closing event. Infrequent missed points events may be caused by momentary “arc filament” shorts across the points and may indicate a failing points capacitor.

10.4.2. Strobe event error (STRERR)

As the strobe pulse is not produced by the ignition system, any strobe signal errors detected by the DLM must originate in the strobe sensor circuit. Strobe event errors may be caused by electrical-noise induced spikes on the *STROBE* line or missing strobe pulses caused by a weak STROBE signal. If our distributor bench-test timing rig is available, faults in the strobe pulse circuit may be ascertained out of the vehicle. There are two error conditions registered by the STRERR counter:

Spurious strobe events (STREERR values less than 100)

These are detected as strobe events occurring within half a distributor rotation sector of the last valid strobe event. In this case, no change is made to the timing accumulators and the strobe signal is ignored. No effect will be observed on the timing data unless further spurious strobe events occur during valid timing periods, in which case the timing data will be corrupted, and potentially in log entries showing no strobe errors if the noise is frequent and random. Such undetected errors will be indicated by log entries with large increases in TACH value compared to adjacent entries. Frequent spurious strobe errors most likely indicate insufficient electrical screening of the *STROBE* line in the distributor or engine bay, or electrical noise in the *GND* connection path of the data logger. Avoid increasing the value of the filter capacitor on the *STROBE* input transistor unless improved electrical screening fails to exclude ignition noise from the circuit.

Missed strobe events (STREERR values in multiples of 100)

These are detected as strobe events occurring more than 1.5 sectors after the last one. TACH values in the affected log entries will be lower, in proportion to the ratio of detected to actual strobe events. If missed strobe counts increase with RPM, the strobe magnets in the distributor may be misaligned (see 8.10) or producing insufficient magnetic flux when hot. Otherwise, the *GND* connection either to the strobe sensor, its power supply or the data logger may be poor, or the power supply to the sensor is faulty.

10.4.3. Specific error combinations

Certain observed errors occurring in combination within a log entry are indicative of a common cause rather than a chance coincidence of discrete error events. Such error-indicator combinations may be used to identify more general faults in the ignition system. Known cases include:

Equal number of spurious strobe and missed strobe events in a log entry

Strobe signals are being misinterpreted as spurious and discarded due to corruption of the sector timing register. In each case, the following strobe signal is considered late and a missed strobe is flagged. The most common cause of this error combination is induced points noise on the strobe sensor line, which may be reduced by increasing C_{STR} or the strobe buffer transistor filter capacitor (see 8.7.1). This error combination also may be caused by momentary low supply voltage to the DLM at normal engine speeds (see below) or to the strobe sensor, producing a missed strobe event. In the latter case, a subsequent power spike to the sensor causing a spurious strobe signal before the 1.5-sector missed-strobe time discrimination limit is reached will lodge an abnormally long sector period into the sector timing register. Unless reset by a change in engine speed, a sample period containing no valid strobe events will cause a (silent) timing system reset.

Equal number of spurious strobe and spurious points errors in a log entry

This error combination indicates uniquely that the DLM time clock has halted temporarily during data logging. The sequence of points and strobe events occurring during this interval appear contemporaneous and are rejected. This fault is caused by a transitory drop in supply voltage to the data logger from the *IGN* line, either due to poor connection or momentary short to ground. This reaction of the data logger to a supply voltage “brown-out” may be unique to the Nano board. Observation of this error combination in log entries associated with engine starting indicates a fault in the ignition switch, typically an instantaneous open circuit as the ignition key is twisted to the start position. This may be ascertained by “hot-wiring” *IGN* to the battery, starting the data logger and cranking the engine briefly. Absence of the error combination from the resulting log file localises the fault to the ignition switch.

10.5. Breakerless points replacements

Removing the points from the MID and replacing them with a magnetic or optical sensor-driven transistor switch is a popular method of averting their maintenance issues and rotation-speed

limitations. Whilst being a generally beneficial upgrade to the MID (provided that the points are retained in the vehicle's toolbox in case the module's power transistor fails) there is one typically neglected factor in their design: the friction of the points cam follower against the oncoming rotor-cam rotation helps to close the centrifugal weights completely at low engine speeds near idle, where the action of their counter-springs is weakest (particularly if these parts are worn or dry). In the absence of this friction, the weights may remain always partially open unless the distributor is re-curved in the absence of spring-loaded contact breaker points. This phenomenon may be noticed as an anomalous drop in engine RPM after a period at idle, where the centrifugal weight counter-springs have overcome some static friction to close the weights completely and so further retard the timing.

The behaviour of the timing data collected using the data logger will broadly resemble that seen with breaker points, with the exception of the dwell curve. The control module of the breakerless points unit will produce dwell durations that increase in proportion to engine speed, starting at a much lower dwell at idle speed than that produced by points. This feature reduces ignition coil heating at low engine speeds and also reduces power consumption by the power transistor that emulates the points. The variation in coil charge time between hot and cold states of the ignition system primary circuit will still be evident in plots of the dwell curve (see 10.3.1) but will now include a delay contribution from the power transistor, which may or may not be negligible. The performance characteristics of the control module should be documented for future reference or fault diagnosis.

If the data logger is enabled before the engine is started, a short series of missed ignitions may be reported in the first log entry during initial engine cranking. This is due to the ignition module requiring a series of its own timing signals to establish a minimum dwell duration period. A full rotation of the distributor at the equivalent of 300RPM may be required before the ignition module will trigger its power transistor coil-discharge circuit for the first time. Such behaviour will make cold starting with a weak battery difficult and totally precludes the use of an emergency hand-crank starter in early vehicles. This "setup phase" of the module also makes it particularly vulnerable to disruption from momentary *IGN* line voltage dropouts during starting due to worn contacts in twist-key ignition switches.

11. Data logger program script

```
/* copy text from here ... */
/* TIMING.ino : MID Timing data logger. Copyright Frodo Irrxsom, 2015-2023 */
/* Distributed under the terms of GPL v3. See https://www.gnu.org/licenses/ */
#include <SPI.h> // compile in Arduino IDE
#include <SD.h> // version 1.0.3 or later
/* SEE SOURCE DOCUMENT FOR CONSTANT AND ARRAY DEFINITIONS BEFORE ALTERING */
#define VAC_CH A0 // VAC ADC channel
#define VAC_TR A1 // VAC temp ref ADC ch
#define PTSOPN 2 // D2 pin - points open
#define PTSCLS 8 // D8 pin - points close
#define STROBE 3 // D3 pin - strobe
#define PBTN 4 // D4 pin - pushbutton
#define STATUS 5 // D5 pin - status LED
#define COM_SPD 9600 // COM port baud rate
#define SD_CS 10 // SD card chip select
#define T_MIN 200L // (msec) log period
#define DELIM "\t" // log column delimiter
#define ADCbits 10 // ADC resolution (bits)
#define ADC_RES ( 1 << ADCbits ) // ADC resolution
#define AREF_V 5.01 // (V) analog ref V
#define LEVS_V ( (float) ADC_RES / AREF_V ) // ADC levels per input V
#define TACH_CAL ( 30 * 1E6 ) // (RPM) tach scale factor
#define DWEL_CAL 90 // (DD) rotor sector angle
#define TIME_CAL 180 // (CD) stroke angle
#define TIME_OFS 21.5 // (CD ATDC) sensor offset
#define STAT_ADV 12.5 // (CD BTDC) static advnce
#define PTSDELAY 150 // (usec) PTS close delay
#define VAC_OFS 1.0 // (DD) vac array 0 offset
#define VAC_VI ( 2.5 * LEVS_V ) // sensor zero offset lev
#define VAC_TFAC ( 1.0 / ADC_RES ) // vac temp corr factor
#define VAC_TOFS 0.0 // vac temp corr origin
#define MAX_DD AREF_V // max vac sentinel value
#define VAC_DIAG false // log vac diagnostics
#define SPURIOUS 1 // spurious event err unit
#define MISSED 100 // missed event err unit
#define MAXLUNS ( (unsigned long) (-1L) ) // max unsigned long value
#define elapsed( a, b ) ( ( a ) < ( b ) ) ? ( MAXLUNS - ( b ) ) + ( a ) : ( a ) - ( b )

enum { HALT, FIRST, SECOND, RUN } volatile StrState = HALT;
enum LogVars { TACH, TIME, CENT, VAC, DWELL,
               PTSERR, STRERR, VACV, VACT, LOGVARS }; // logged data values
unsigned int PtsClsInt, LogNum = 0, vacLt = 0, vacCt, deg, var,
             LogPrec[LOGVARS] = { 0, 1, 1, 1, 1, 0, 0, 5, 5 }; // log file var precisions
float VacS, VacR, LogVar[LOGVARS], VAC_DD[] =
    { 2.79, 2.88, 3.00, 3.15, 3.32, 3.50, 3.69, 3.85, 3.99, 4.09, 4.14, MAX_DD };
#if VAC_DIAG // diagnostics enabled?
#define LOGLIM LOGVARS // record raw vac levels
#else
#define LOGLIM VACV // omit vac levels
#endif

char TimerDir[]="/TimeLogs", TimerFile[]="/Time0001.log", TFile[40];
File LogFile;
Print *LogLine = &Serial; // output device pointer
enum LogDevs { NoLog, Host, SDcard } LogTo = NoLog; // active log device
unsigned long currT, startT, opnT, clsT, evT, dT, ddT, strT, sect;
volatile unsigned long strCt, revT, timT, dwlT, ptsE, strE;
boolean DoAcq = false, Stat = LOW, trig = false;
volatile boolean timing = false, ptsopn = false; // read-onlyint flags

void IncLogNum() { // increment log file #
```

```

char buf[8];
unsigned int i = 0, j = 8;
itoa( ++LogNum, buf, 10 ); // do not use String class
while ( buf[ i ] ) i++;
while ( i-- ) TimerFile[ j-- ] = buf[ i ];
for ( i = 0; TimerDir[i]; i++ ) TFile[ i ] = TimerDir[ i ];
for ( j = 0; TimerFile[j]; j++ ) TFile[ i + j ] = TimerFile[ j ];
TFile[ i + j ] = 0;
}

void PointsOpenInt(){ // points open interrupt
evT = micros(); // event time index
dT = elapsed( evT, clsT ); // points closed duration
if ( timing ) // incomplete timing cycle
    if ( elapsed( evT, strT ) > secT ) opnT = evT; // missing last strobe?
    else ptsE += SPURIOUS; // spurious points event
else{
    opnT = evT; // valid open event
    dwlT += dT + PTSDELAY; // normal dwell duration
}
timing = ptsopn = true; // timing event begins
PCIFR |= PtsClsInt; // clear any pending ints
PCICR |= PtsClsInt; // enable pts close int
}

/* macro */ ISR( PCINT0_vect ){ // points close interrupt
clsT = micros(); // event time index
ptsopn = false; // dwell event begins
PCICR &= ~PtsClsInt; // disable pts close int
}

void StrobeInt(){ // Strobe interrupt
evT = micros(); // event time index
dT = elapsed( evT, strT ); // strobe interval
if ( digitalRead( STROBE ) == LOW ) switch ( StrState ){
    case HALT : // suspend handler
        strT = evT; // just reg sector start
        break;
    case FIRST : // first strobe event
        strT = evT; // 1st sector start T
        secT = dT; // 1st sector period
        timing = false; // clear timing state
        StrState = SECOND; // sequence next event
        break;
    case SECOND : // second strobe event
        ddT = dT * 2; // double strobe period
        strT = evT; // next sector start T
        if ( ddT > secT && ddT < secT * 3 ){ // strobe error trap
            secT = dT; // register sector period
            strCt = revT = timT = dwlT = strE = ptsE = 0; // clear all counters
            StrState = RUN; // error trapping on
            timing = false; // clear timing state
        }
        else StrState = FIRST; // re-initialise strobe
        break;
    case RUN : // engine started
        ddT = dT * 2; // double strobe period
        if ( ddT < secT ) strE += SPURIOUS; // spurious strobe
        else{ // valid strobe
            if ( ddT > secT * 3 ) strE += MISSED; // missed strobe check
            else secT = dT; // current sector time
            strT = evT; // next sector start T
            if ( timing ){ // valid timing event?
                revT += secT; // accum sector times
            }
        }
    }
}

```

```

        strCt++; // inc strobe count
        timT += elapsed( evT, opnT ); // accum timing interval
        timing = false; // timing event ends
    }
    else ptsE += MISSED; // missed points event
}
else strE += SPURIOUS; // points noise trap
}

void setup(){ // initialisations
pinMode( STATUS, OUTPUT ); // configure controller
pinMode( PBTN, INPUT_PULLUP );
pinMode( PTSOPN, INPUT ); // don't assume defaults
pinMode( PTSCLS, INPUT );
pinMode( STROBE, INPUT );
analogReference( EXTERNAL ); // use common 5V supply
*digitalPinToPCMSK( PTSCLS ) |= bit ( digitalPinToPCMSKbit( PTSCLS ) );
PtsClsInt = bit ( digitalPinToPCICRbit( PTSCLS ) ); // install int handlers
attachInterrupt( digitalPinToInterrupt( PTSOPN ), PointsOpenInt, FALLING );
attachInterrupt( digitalPinToInterrupt( STROBE ), StrobeInt, FALLING );
Serial.begin( COM_SPD ); // attempt host connect
while ( LogTo == NoLog ){ // find a log device
    if ( SD.begin( SD_CS ) ) LogTo = SDcard; // SD card initialised
    else if ( Serial.available() > 0 ) LogTo = Host; // Host handshake sent
    digitalWrite( STATUS, Stat = !Stat );
}
digitalWrite( STATUS, Stat = LOW ); // log device found
if ( LogTo == SDcard ){ // SD card selected?
    LogLine = &LogFile; // swap output to file
    if ( !SD.exists( TimerDir ) ) SD.mkdir( TimerDir ); // create dir if absent
    do IncLogNum(); while ( SD.exists( TFile ) ); // next available filename
}
else IncLogNum(); // output to serial port
while ( VAC_DD[vacLt] < MAX_DD ) VAC_DD[vacLt++] *= LEVS_V;
vacLt--; // convert DD to levels
}

void loop(){ // no heap var decs here!
if ( ( digitalRead( PBTN ) ) == LOW ){ // command detected
    do delay( 200 ); while ( digitalRead( PBTN ) == LOW );
    DoAcq = !DoAcq; // switch logging on/off
    if ( DoAcq ){
        if ( LogTo == Host ) Serial.println( TimerFile ); // report new log file
        else LogFile = SD.open( TFile, FILE_WRITE );
        StrState = FIRST; // reset timing scheme
        for ( var = 0; var < LOGVARS; var++ ) LogVar[var] = 0.0;

        VacS = VacR = vacCt = 0;
        startT = millis(); // set clock
    }
    else{
        if ( LogTo == SDcard ) LogFile.close(); // end of current log
        IncLogNum();
        digitalWrite( STATUS, Stat = LOW );
    }
}
if ( DoAcq ){ // logging event
    currT = millis(); // update clock
    if ( StrState != RUN ) startT = currT; // reset in progress
    else if ( ptsopn && !trig ){ // read vac @ I(pts)=0A
        VacS += analogRead( VAC_CH ); // avoid float casts
        /* uncomment following line for DLM vac temp correction (see text) */
        // VacR += analogRead( VAC_TR ); // get vac temp proxy
    }
}
}

```

```

    vacCt++; // inc vac sample count
  }
  if ( StrState == RUN && currT - startT >= T_MIN ){ // log entry period
    if ( strCt <= strE / MISSED ) StrState = FIRST; // engine running?
    else trig |= timing && ptsopn && vacCt; // log event trigger
  }
  if ( trig && !timing && !ptsopn ){ // wait for ints clear
    LogVar[PTSERR] = ptsE; // read/reset counters...
    LogVar[STRERR] = strE;
    LogVar[TACH] = TACH_CAL * (float) strCt / revT;
    LogVar[TIME] = TIME_CAL * (float) timT / revT - TIME_OFS + STAT_ADV;
    LogVar[DWELL] = DWEL_CAL * (float) dwlT / revT;
    strCt = revT = timT = dwlT = ptsE = strE = 0; // ...while ints are clear
    VacS /= vacCt;
    LogVar[VACV] = VacS / LEVS_V;
    /* uncomment following lines for DLM vac temp correction (see text) */
    // VacR /= vacCt;
    // LogVar[VACT] = VacR / LEVS_V;
    // VacR = VAC_TFAC * VacR + VAC_TOFS; // temp correction factor
    // VacS = ( VacS - VAC_VI ) / VacR + VAC_VI; // scale vac by temp fac
    deg = 0; // calc vac in DD
    while ( deg < vacLt && VAC_DD[deg + 1] < VacS ) deg++;
    VacS = deg + ( VacS - VAC_DD[deg] ) / ( VAC_DD[deg + 1] - VAC_DD[deg] );
    LogVar[VAC] = ( VacS - VAC_OFS ) * (float) TIME_CAL / DWEL_CAL;
    VacS = VacR = vacCt = 0;
    LogVar[CENT] = LogVar[TIME] - LogVar[VAC] - STAT_ADV;
    for ( var = 0; var < LOGLIM; var++ ){ // write log file values
      LogLine->print( LogVar[var], LogPrec[var] );
      if ( var == LOGLIM - 1 ) LogLine->println(); // end of log entry?
      else LogLine->print( DELIM ); // column separator
      LogVar[var] = 0.0; // zero log vars
    }
    LogLine->flush(); // save log entry to SD
    digitalWrite( STATUS, Stat = !Stat ); // signal activity
    startT = currT; // reset clock
    trig = false; // reset log trigger
  }
}
}
/* end of TIMING.ino */
/* ... to here, and paste into a file named "timing.ino" for compilation in the Arduino IDE */

```

12. Modifying / recalibrating the vacuum advance unit

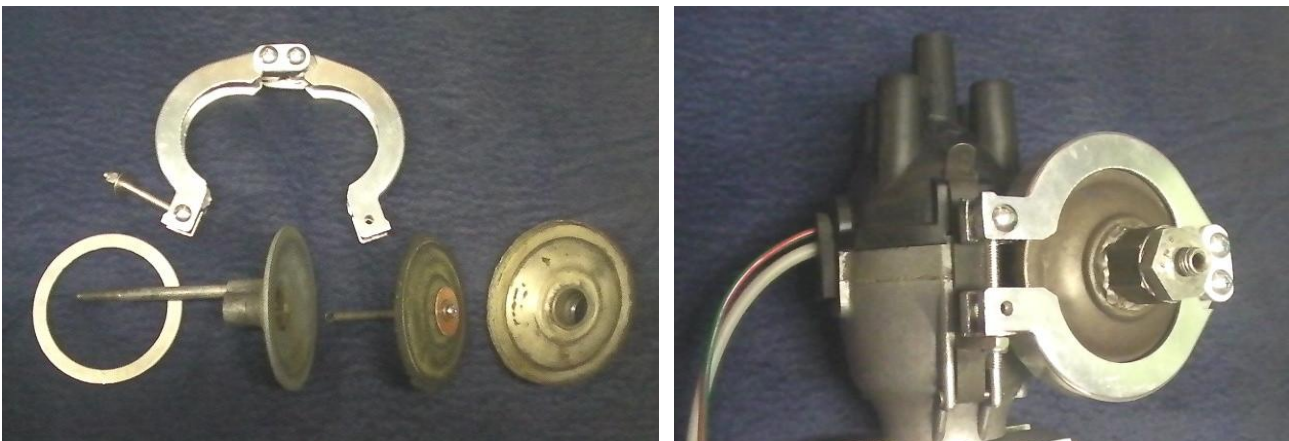
Should it be considered worthwhile or expedient to modify an existing vacuum advance unit rather than replace it, the design commonality of these simple devices permits a generalised discussion of their disassembly, reconditioning, recalibration and reassembly. As a representative example we again consider the Lucas DM2 vacuum advance unit.

12.1. Disassembly

The vacuum chamber is typically formed as a pair of round clamshells which both seal against the rubberised-cotton diaphragm sandwiched between their edges. One of these chamber-halves will have a collar around its outer circumference into which the other half seats, after which the collar is roll-formed into a seam over the opposite-half flange. This machine-pressed seam was not intended to be re-opened and must be prised open by securing the unit in a vice and gradually working around the seam, lifting its peened edge with a small flat screwdriver and pliers until (warning) the two halves pop apart under the force of the vacuum control spring compressed between them. If the seam cannot be opened in this manner, it may simply be cut through by placing the vacuum unit in a lathe and turning off the inner part of the seam.

12.2. Reconditioning

Once the vacuum chamber has been opened, remove and clean the internal components after noting their relative positions. The vacuum diaphragm may be replaced with a hand-cut piece of rubberised cotton sheet or industrial oil-compatible diaphragm stock. If the central attachment post to the points plate is fixed to the diaphragm using a rivet, drill this out and tap a thread in its place to fix the new diaphragm in place by a screw secured with some loctite. Finally, obtain a suitable vacuum flange clamp to re-secure the two halves of the vacuum chamber back together. Choose a size of the KF/NM style clamps intended for vacuum pipe flanges the same flange (not pipe) size or slightly larger than the outer diameter of the vacuum chamber flanges. These clamps have a wide groove and can accommodate a range of flange diameters and thicknesses – if the clamp is too wide for the vacuum chamber union, machine an aluminium packing-piece ring to add to either outer side of the chamber flanges under the clamp.



The images above show a KF vacuum flange clamp modified to fit the Lucas DM2 / 25D vacuum advance unit. As there is no good match in the clamp sizes to suit this vacuum chamber diameter, a clamp of the nearest size has been split and radiused internally to achieve a satisfactory fit. The aluminium ring at the left of the disassembled view is the packing ring that should be made just wider than the gap between the clamp and the rear of the vacuum chamber, so as to compress the vacuum diaphragm between the chamber halves as the clamp is tensioned. A well-made clamp and packing ring will require no sealant between the diaphragm and vacuum chamber halves, greatly simplifying replacement of the diaphragm or access to the vacuum control spring even with the distributor in

place on the engine. Remember to fit the packing-ring to the vac unit before the latter is fixed to the distributor.

12.3. Recalibration

The central controlling component of the vacuum unit is the (usually) single heavy spring that is compressed by the action of atmospheric pressure on the diaphragm in the absence of manifold pressure on the opposite side. It is highly unlikely that this heavy spring has lost its rating unless it has been badly corroded during extended storage outside the vehicle and may be assumed to conform to factory specifications otherwise. Similarly, if the centre-stop plug and seat (or equivalent detent limiter for maximum vacuum advance) have not been excessively worn they should be retained as-is. Any modification of the vacuum unit should be performed reversibly to permit recovery of original specifications should the need arise. For example:

12.3.1. Increasing the operating vacuum level

This may be achieved by placing a washer between the vacuum spring and its seat in the vac chamber top half. The washer must match the spring OD and have sufficient internal clearance to admit the detent plug held with the spring (or otherwise clear whatever detent device is used). In the DM2 unit this may be achieved without dismantling the vacuum chamber as the hexagonal end-cap of the chamber can be unscrewed to access the vacuum spring and detent plug.

12.3.2. Decreasing the operating vacuum level

This may be achieved by adding a spacer ring between the diaphragm and vacuum-side chamber flange to reduce the preload on the vacuum spring. This ring may be made of metal or plastic and sealed against the chamber flange with silicone sealant prior to the chamber halves being reassembled within a flange clamp of appropriate width. As this will add length to the vacuum unit, a correspondingly longer detent plug must be used to retain the same max vac advance. In the DM2 the same result may be achieved by placing a thicker gasket washer between the hex end cap and vac chamber top half.

12.3.3. Increasing / decreasing the max vac advance

This is achieved by either increasing or decreasing the length of the detent plug or equivalent device used to limit maximum compression of the vacuum spring.

12.3.4. Increasing / decreasing the zero vac advance position

Note that this is equivalent to changing the static advance position of the distributor. The zero vac advance (or points plate rest) position may be altered by changing the length of the linkage between the vacuum unit and points plate peg or changing the position of the vacuum unit on the distributor. In the Lucas DM2/23D/25D distributors this position is adjustable by means of a vernier adjustment screw (see Components of the MID). If it is absolutely necessary to alter this setting within the vacuum chamber itself, either add material (shim or washer) or remove material (file down) at the shoulder of the advance linkage coupling post on the atmospheric side of the diaphragm. Note that this modification will decrease the operating vacuum level (see above).

12.4. Estimating the vacuum spring calibration

The vacuum spring presents a linearly-increasing force against atmospheric pressure with decreasing manifold pressure. It is preloaded in the vacuum chamber to resist compression until a minimum vacuum level is reached, after which it compresses to add vacuum advance to the ignition timing up to a minimum compressed length at max vac advance. The vacuum levels corresponding to min and max vac advance are given in the vac unit's specifications, often stamped on the unit itself. After disassembly of the vacuum unit, measure the distance C_{min} occupied by the compressed spring as fitted between its seats on the diaphragm centre post and at the end cap of the

top vacuum chamber. Next, measure the length C_{max} of the max-advance detent plug within the spring (or whatever device is employed to limit the maximum compression of the vacuum spring) corresponding to maximum vac advance. The vacuum spring calibration is given by

$$K_{vac} = \frac{C_{min} - C_{max}}{V_{min} - V_{max}} \text{ and } L_0 = C_{min} - K_{vac} V_{min}$$

where V_{min} and V_{max} are the factory-specified manifold vacuum levels corresponding to min and max vac advance. To change the vacuum unit calibration, either or both the minimum and maximum compressed lengths of the vacuum spring are changed by altering the vacuum chamber components as described above. The spring compressions produced by target vacuum levels V^*_{min} and V^*_{max} are then given by

$$C^*_{min} = V^*_{min} K_{vac} + L_0 \text{ and } C^*_{max} = V^*_{max} K_{vac} + L_0.$$

In the above equations K_{vac} is the (negative) vacuum spring rate and L_0 is the spring free length. The calculated value of the latter may differ slightly from the measured free length of the spring either due to its duration under compression or the inclusion of the diaphragm elasticity in the factory vacuum calibration.

13. Magnetic sensor scheme selection guide

The Hall-effect magnetic flux sensor used for both the strobe and vac sensors in the timing meter and data logger instruments is the UGN3503UA, originally produced by Allegro MicroSystems. Although this device is now superseded, it is still produced and remains widely available as a generic (OEM) component. Many later improved versions of it have already ceased production at time of writing. In this section the limitations imposed by the choice of this IC are analysed and alternative devices investigated to mitigate measurement accuracy, thermal stability or geometrical layout issues. Depending on region, obtaining these devices may require an international order. Always source electronic components from reputable distributors with stated returns policies to avoid substandard, reject or fake parts. Obtain sufficient amounts to cover future distributor installations plus spares in case of discontinuance (a minimum order quantity of 10 ICs is common).

Two types of linear ratiometric Hall-effect sensor are presently available. The most common type is the *symmetric* linear sensor for which the ideal output function is given by

$$V_S = V_{SS} \times \left(\frac{B \times S}{V_{Sref}} + \frac{1}{2} \right), \quad |V_{SS} - V_{Sref}| < 1V \text{ (typical)}$$

for a supply voltage V_{SS} , an incident magnetic flux B (typically positive = facing south pole) and a device flux sensitivity S defined at a reference supply voltage V_{Sref} . The quiescent ($B=0$) device output level V_{NULL} is thus $V_{SS}/2$. Alternatively, an *asymmetric* linear sensor is defined by

$$V_S = \frac{B \times S \times V_{SS}}{V_{Sref}} + V_{NULL}, \quad |V_{SS} - V_{Sref}| < 1V \text{ (typical)}$$

where the quiescent output level V_{NULL} is a fixed constant independent of supply voltage. Such sensors are only used with one magnet polarity corresponding to their working output range.

The following table lists device characteristics at $V_{Sref} = 5.0V$ supply voltage and 0.1mA output current for a range of Hall-effect sensors listed as available from multiple distributors at the time of writing. Similar devices for which production has ceased still may be available as remnant stocks.

Part # (TO-92 package)	Manufacturer	Sens (mV/G)	dS/dV _{ss} (mV/G/V)	dS/dT (μV/G/°C)	V _{NULL} (V)	ΔV _{NULL} (mV/°C)	Magnet spec'd
UGN3503UA	Allegro	1.3	+0.5	+1.67	2.5	+1.0	none
SS495A	Honeywell	3.125	+0.625	+0.67	2.5	±1.5	none
A1321LUA	Allegro	5	+1.0	+2.5	2.5	+0.035	SmCo
DRV5056A1QLPG	Texas Insts	20	+4.0	+24	0.6	+0.1	Nd
DRV5056Z1QLPG	Texas Insts	20	+4.0	0	0.6	+0.03	none

Manufacturers warn that individual device characteristics may vary considerably from specified values, and are highly batch-dependent. Each device should be calibrated individually for precision measurement. For example, the UGN3503 only specifies a null-field voltage between 2.25V and 2.75V at $V_{ss}=5V$ and 25C for any given device. The ratiometric coefficient dS/dV_{ss} describes the change in device sensitivity with supply voltage for $V_{NULL} < V_{ss} < V_{Sref}$. The *nominal* sensitivity temperature compensation factor dS/dT and null-field output voltage shift ΔV_{NULL} shown for each device assumes increasing temp between 25C and 85C and are only applicable for device output voltages above V_{NULL} . Positive values of dS/dT indicate an increasing device sensitivity to compensate for the drop in magnetic field intensity with increasing ambient temperature for fixed magnets. The sintering process used to produce rare-earth magnets often results in multiple magnetic domains so a symmetry axis of the magnet should never be assumed to correspond to a similarly symmetric magnetic field. Any particular mutual arrangement of magnet and sensor should be marked for reference. Only three types of fixed magnets are available in the small sizes typically required for deployment inside a MID:

Magnet material	dB / dT (% / °C)	$\Delta B_T/B$ (% typ)	T_{max} (°C)	Package (small disc)	Relative Strength
Neodymium	-0.16 - -0.19	-10	85	Ni plate	High
Samarium-Cobalt	-0.05	-3	350	Sintered pellet	Medium
AlNiCo-5 ... -9	-0.03 - +0.01	-1	400	Ni plate	Low

The rate of magnetic field intensity change with temperature dB/dT is shown as a typical percentage change $\Delta B_T/B$ at 85C relative to 25C. The large field strength drop for the neodymium magnet makes it unsuitable as an *uncompensated* reference-field source for our vac position sensor, although it is ideal as our strobe-pulse field source due to its superior field strength (even when hot) and is available in both 2mm-diameter discs and high-temp variants if required. In contrast, an alnico-8 magnet is essentially temperature-independent and would be ideal as a reference-field source for our vac position sensor if the latter has sufficient sensitivity and the magnet track can be located close enough to the sensor. The Sm-Co magnet suits either application provided that it is not fitted by impact means if it is not hard-plated. The weaker magnets may require an aluminium fixing bracket to the points plate if they are unable to remain in place under their own attraction.

Several temperature factors must be considered in selecting combinations of sensors and magnets for our MID monitoring scheme. Firstly, insulating these components thermally against conductive heating will only delay radiant heating. The temp-compensated sensors must maintain thermal equilibrium with their reference magnets to produce an accurate flux measurement. It is preferable for them to achieve thermal equilibrium with their environment rapidly as the engine working temperature is maintained within a narrow target range. In most cases the location of the MID on the engine will afford some degree of air cooling such that the MID will operate at a slightly lower temperature than the engine block, but at a constant ratio. It is a good idea to clip a thermocouple to the distributor body (or points plate if possible), connected to a digital thermometer or temp-sensing multimeter in the vehicle's cabin, and monitor its temperature variation in actual road use with the engine at stable running temp in warm weather to establish a representative working temp range for the sensors and magnets. Secondly, the degree of measurement precision desired for our MID characterisation instruments across a specified temperature range dictates the degree of thermal compensation deployed to achieve it. This criterion dictates that the selection of magnetic sensor should be based on the precision required of the vac position sensor, as the strobe sensor specification is more tolerant of thermal drift. It is expedient to source one type of sensor for both tasks, even if the strobe sensor is used with neodymium magnets.

13.1. Thermal compensation correction

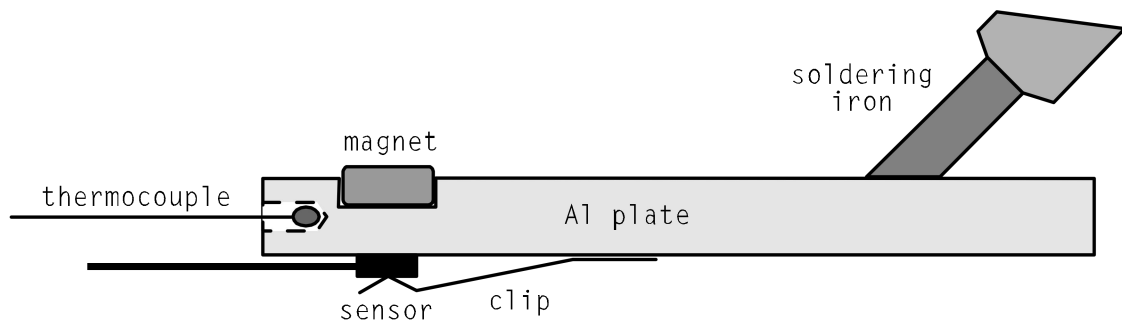
Any individual pairing of Hall-effect sensor and magnet must be characterised across the temperature range intended for accurate measurement. If accurate MID data logging is only required at normal engine running temperatures, the vac position sensor and magnet may be fitted to the MID and calibrated directly (in DD) with the distributor maintained at engine running temp using the method given in section 9.4. For an ideal compensated sensor and magnet combination the sensor output for each magnetic flux density should be constant at all required temperatures. As our vac position measurement scheme may use less than 100mV of sensor range to encode each DD of vac advance, thermal deviations should be limited to less than 10-20mV per DD to retain accuracy. Where the sensor and magnet pairing output diverges from its value at normal engine temp, the ratiometric property of the sensor may be used to apply a linear voltage correction to the device and recover acceptable thermal stability. The resulting corrected sensor output as a function of magnetic flux density will differ from that observed at any given temperature for the bare device. Also, more than one correction method may be needed if the device exhibits multiple significant thermal drift dependencies. Note that all such corrections necessarily reduce the output voltage range of the sensor – resolution is sacrificed for accuracy.

If the intention is to produce an accurate vac level measurement for the data logger, a unipolar sensor such as the DRV5056 offers a greater output voltage range and magnetic sensitivity,

producing superior position resolution from the data logger's ADC. Thermal compensation of the "A"-suffix device types (intended for a particular NdFeB magnet "recipe", which remains undisclosed) will largely reduce the degree of correction required, and hence output range compression, compared to relatively uncompensated sensors such as the UGN3503. However, its inbuilt temp measurement compensation makes common thermal contact with the magnet critical and thus unsuited to MID locations other than the points baseplate. An uncompensated "Z"-suffix type sensor used with a high thermal stability magnet is preferable. The following correction schemes may be employed with any linear ratiometric sensor type, including the DRV5056.

13.1.1. Sensor / magnet thermal characterisation

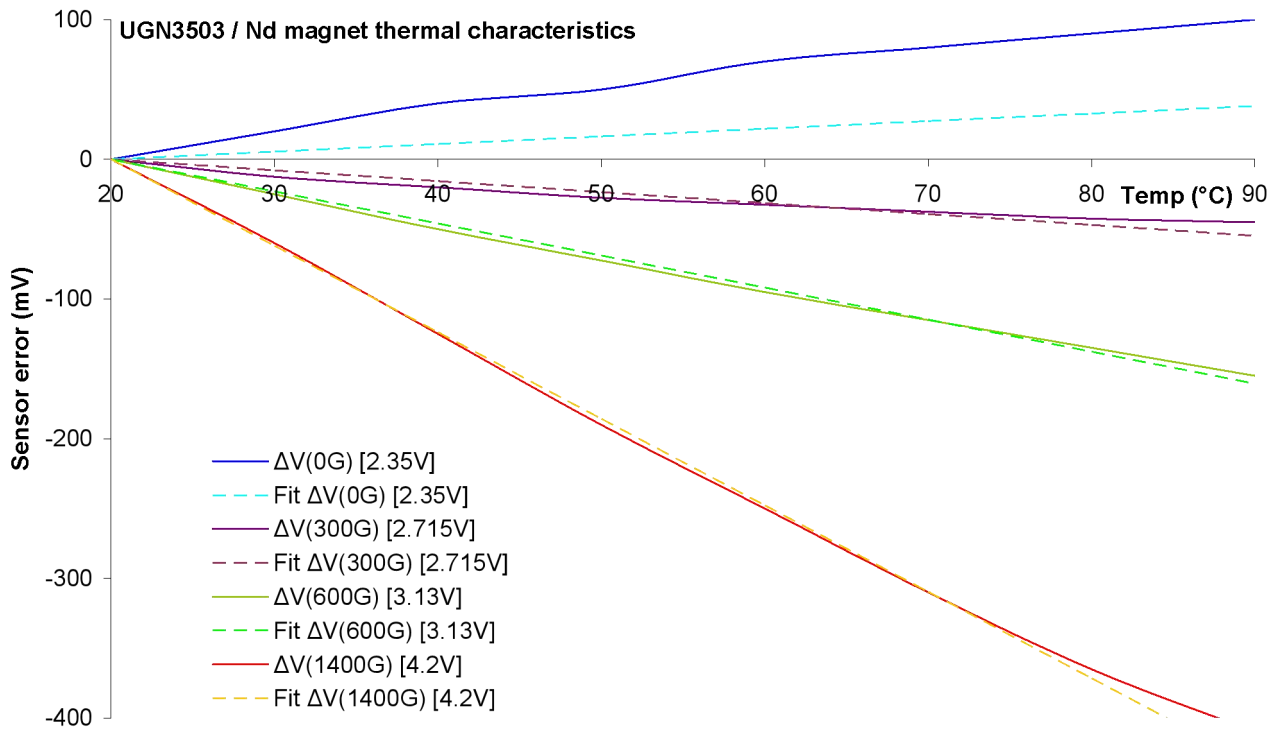
Thermal characterisation of the magnet / sensor pairing is performed most conveniently prior to their integration with the MID. To achieve a reproducible characterisation, the magnet and sensor must be heated together in common contact with a heat reservoir. This can be made from an aluminium plate with a recess drilled into it to retain the magnet and a non-ferrous metal or high-temp plastic clip on the opposite side to hold the sensor. A thermocouple attached to a digital thermometer should be located in a drilling in the plate near the magnet. All the parts should be assembled together using heat transfer compound. The sensor output voltage is measured incrementally whilst **slowly** heating the aluminium plate continuously across the desired temp range with a clamp-supported soldering iron before switching off the iron in-place and recording the sensor voltage across the same temp range as the assembly cools and taking the average of the two sets of measurements. This process should be repeated for low, medium and high magnetic flux densities through the sensor, as well as for zero flux with no magnet present. If a 3.5-digit voltmeter is being used, it is prudent to reference its negative input to a suitable fixed-resistor V_{ss} voltage divider so the $\pm 2000\text{mV}$ voltmeter range is available at each sensor output voltage. No output current load must be placed on the sensor other than the voltmeter impedance.



The above method should be sufficient to characterise the thermal response of the sensor / magnet combination where these are attached respectively to the points baseplate and moving plate. In other configurations where a thermal gradient is observed between the two components in the MID at engine running temperature, it may be necessary to perform the thermal characterisation with the sensor and magnet *in situ* in the MID at the test bench, with the latter heated via its driveshaft and spindle to mimic actual engine heating and a cooling fan applied to its exterior to achieve the thermal gradient observed previously. Sensor response instabilities due to variable thermal gradients can be minimised by using the most thermally stable magnet possible.

Example: UGN3503UA with a neodymium magnet

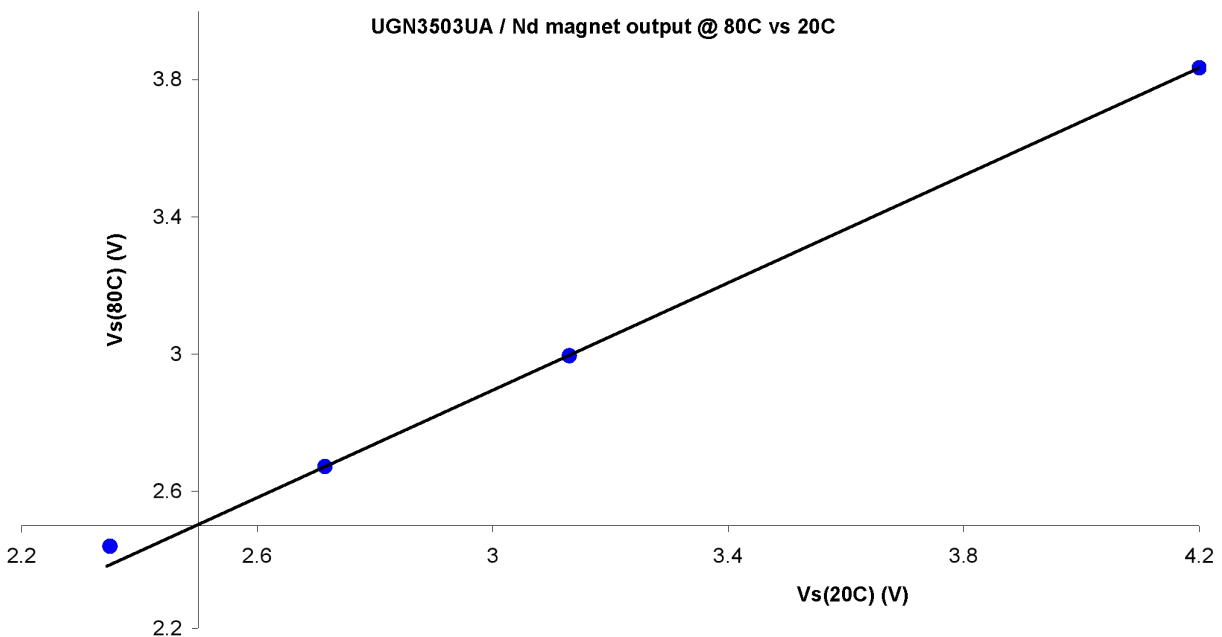
As a worst-case example, consider the pairing of the UGN3503 sensor with an Nd magnet. Collecting sets of sensor output voltages $V_s(T)$ across 20C to 90C temperature ranges for various magnet-sensor spacings and plotting these as drift voltage $\Delta V = V_s(T) - V_s(20C)$ versus temperature for the pairing of a UGN3505UA sensor and a neodymium magnet produces the solid curves in the graph below. The value of $V_s(20C)$ for each plot is shown in brackets in the graph legend. On inspection the voltage drift for each sensor position relative to the magnet evidently is close to a linear decrease with increasing temperature, apart from the zero-field case which displays a linear increase with temperature. The latter observation indicates a departure from the



manufacturer's specification for the sensor of zero temp drift at V_{NULL} (see below). We may calculate linear fits to the sensor voltage drift plots according to the function

$$\frac{V_S(T) - V_S(20C)}{V_S(T_{max}) - V_S(20C)} = \frac{T - 20C}{T_{max} - 20C} \equiv L_T(T)$$

where $L_T(T)$ is the fractional gradient referenced between 20C and a specified upper temp $T_{max} = 80C$ taken as a linear-range reference endpoint common to all the plots. Linear fits to the observed thermal drift plots using this function (not shown) are within 10mV across the 20C-80C working temp range for *all* of the sensor voltages, which is within measurement error. If we plot $V_S(T_{max})$ vs $V_S(20C)$ for each sensor-magnet spacing, we observe a linear relationship between the two sensor voltages for each applied field state, indicating that the sensor output at T_{max} has decreased by the *same* fixed fraction of its output at 20C. Next, we note that the projected value of V_S for which the sensor output is identical at 20C and T_{max} is equal to 2.5V, the nominal null-field output voltage V_{NULL} for this sensor. Finally, the actual null-field sensor voltage ratio is observed not to conform to the linear relationship of the applied-field sensor states.



The above analysis permits us to derive a simple characteristic function for this sensor-magnet pairing for all applied-field states at all temperatures in the specified range. If we define the temperature-invariant sensor output voltage as $V_I = 2.5V$ and the gradient of the $V_S(80C):V_S(20C)$ sensor output ratio plot as $(1 - K_S) = 0.785$, then some algebra yields

$$V_S(T) - V_S(20C) = K_S (V_I - V_S(20C)) L_T(T)$$

which is the function used for the linear ΔV fits shown as dashed lines in the sensor thermal drift graph. As expected, the null-field sensor output curve is not fitted by the function. Rearranging the fit function to obtain $V_S(20C)$ in terms of $V_S(T)$ produces

$$V_S(20C) = V_I + \frac{V_S(T) - V_I}{1 - K_S L_T(T)}$$

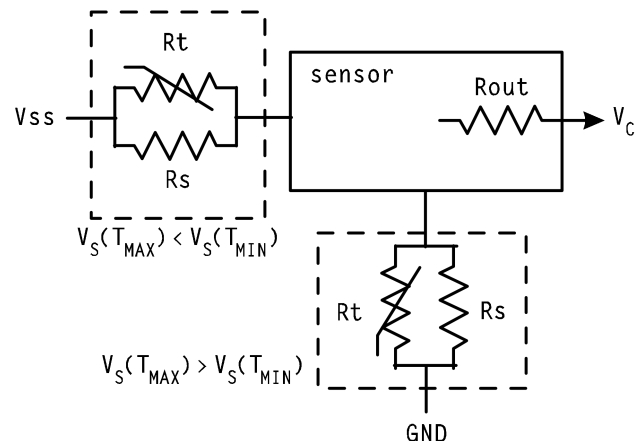
as the correction function for the sensor / magnet combination at the observed system temperature and sensor output voltages above V_I . This fortuitous result is not accidental – it indicates an underlying property of the sensor’s design. The observation that V_I is equal to the nominal null-field output voltage V_{NULL} for this sensor suggests that the sensor’s ratiometric divider is operating correctly but the field sensor transistor is offset with respect to it. This would explain why the actual null-field plot at $V_S(20C) = 2.35V$, below V_I , is not corrected by the same linear fit factor. The fact that one constant value of K_S satisfies all the remaining cases (rather than being some pathological function of V_S) also indicates that the sensor’s thermal characteristics are essentially independent of applied magnetic field, so that the observed drop in output voltage with rising temperature is wholly due to magnetic field decay from the neodymium magnet. Crucially, this characteristic of the UGN3503 permits thermal drift correction using just a few electronic components.

13.1.2. Thermistor compensation

One method to correct for thermal drift is to use negative-temperature-coefficient (NTC) *thermistors* to adjust input and output voltages from the device as a function of temperature. These devices exhibit a logarithmic resistance decrease with increasing temperature and should only be used as low-current reference resistors. They are only produced in widely-spaced room temp resistance values and are intended for pairing with parallel shunt resistors to achieve specific thermal circuit voltage corrections. The temperature dependence of a thermistor’s resistance is given conventionally in terms of the *B* or *beta* (β) parameter:

$$R_T = R_0 \exp\left(\frac{B}{T} - \frac{B}{T_0}\right)$$

where T is the device temp in Kelvin ($^{\circ}C + 273.15$) and R_0 is the device resistance at $T_0 = 298.15K$ (25C). The thermistor(s) must be fixed in close thermal contact (e.g. using heat transfer compound) to the sensor on its carrier. An additional complication *and feature* of ratiometric sensors is that their sensitivity to magnetic flux varies linearly with supply voltage over a small range (typically $\pm 1V$), so offsetting the sensor from either supply rail can be used to correct both its gain and V_{NULL} for thermal drift. These factors make a-priori calculation of specific voltage-divider and shunt resistor values difficult and considerable trial-and-error component selection is required. Effort may be reduced by encoding voltage-divider equations in spreadsheet formulas and applying these to tables of measured device outputs over the working temperature range to model corrections.



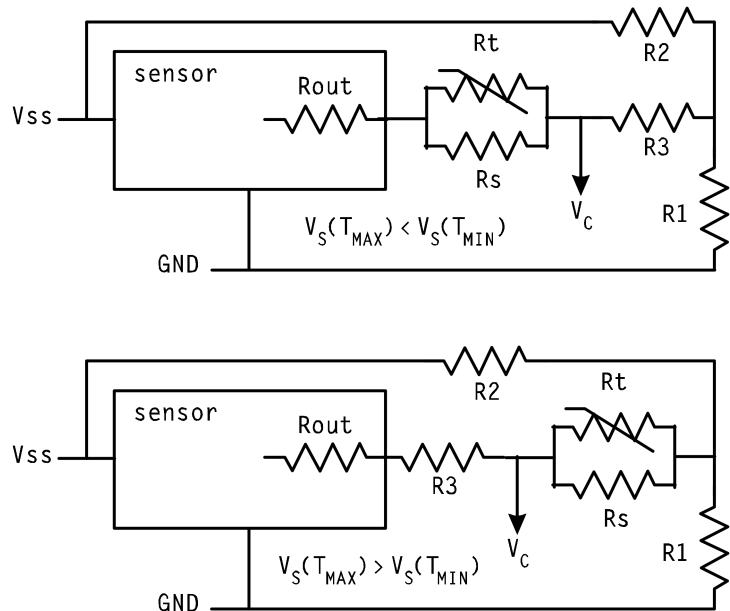
Minor sensor voltage drift: If the sensor voltage is observed to vary by less than 1mV/°C across the desired temp range at high intercepted magnetic flux levels it may be corrected by placing a parallel combination of low-value (<100Ω) NTC thermistor Rt and shunt resistor Rs in either the sensor’s GND path (for rising sensor voltage with rising temp) or VSS path (for falling sensor voltage with rising temp). The shunt resistor (typically <100Ω) is selected to render the sensor output constant across the temp range. The correction may be modelled using the equation

$$V_{SS}^* = V_{SS} - I_S \frac{R_t R_s}{R_t + R_s}$$

where the current through the sensor I_S for negligible output current is kept constant by the device’s internal voltage regulator for small changes in V_{SS} , typically around 6mA for most sensors. The actual circuits used should be characterised by using various fixed resistors in place of the thermistor/shunt pairing and measuring both I_S and V_S as a function of temperature to find a resistance-temperature relation to reproduce using the thermistor. The adjusted supply voltage V_{SS}^* is then used in place of V_{SS} in the sensor definition function and $(V_{SS} - V_{SS}^*)$ added to V_C if the sensor has been offset from GND.

Significant sensor voltage drift: If the sensor output voltage V_S is observed to drift by more than a few mV/°C at high applied field levels or the device output thermal-drift $\Delta V_S(T)$ increases with rising applied magnetic field intensity, a linear correction to the output voltage may be applied using a voltage divider that includes an NTC thermistor and shunt-resistor pairing in one division. The orientation and values of the three resistors are selected to negate $\Delta V_S(T)$ at the divider junction, which becomes the new sensor output. This “reactive” voltage divider is referenced to a “passive” voltage divider that produces the reference voltage equivalent to V_S at $\Delta V_S(T) = 0$, which ideally should equal V_{NULL} . This arrangement minimises current drawn from the sensor output, which may add to thermal drift or (in the case of the UGN3503) degrade the device with continuous use near the upper end of its operating temp range. As with the previous thermistor correction strategy, the orientation of the V_S output voltage divider with respect to the sensor depends on the type of error the sensor exhibits with increasing temperature: for falling V_S levels the thermistor / shunt pair connect to the sensor and for rising V_S levels they connect to the reference divider (see circuits).

Modelling of this correction is best performed using a spreadsheet in which the correction can be applied numerically to sets of observed values of V_S as a function of temperature at various magnet-sensor spacings. As this correction involves loading the sensor output, the device internal resistance R_{out} must be included in circuit calculations. Large-value (KΩ) resistors should be used to minimise drawn current from the sensor and the voltage drop over R_{out} . Defining $R_{1||2}$ as the parallel combination of R_1 and R_2 , and $R_{t||s}$ as the parallel combination of R_t and R_s , we can write the corrected sensor output V_C as

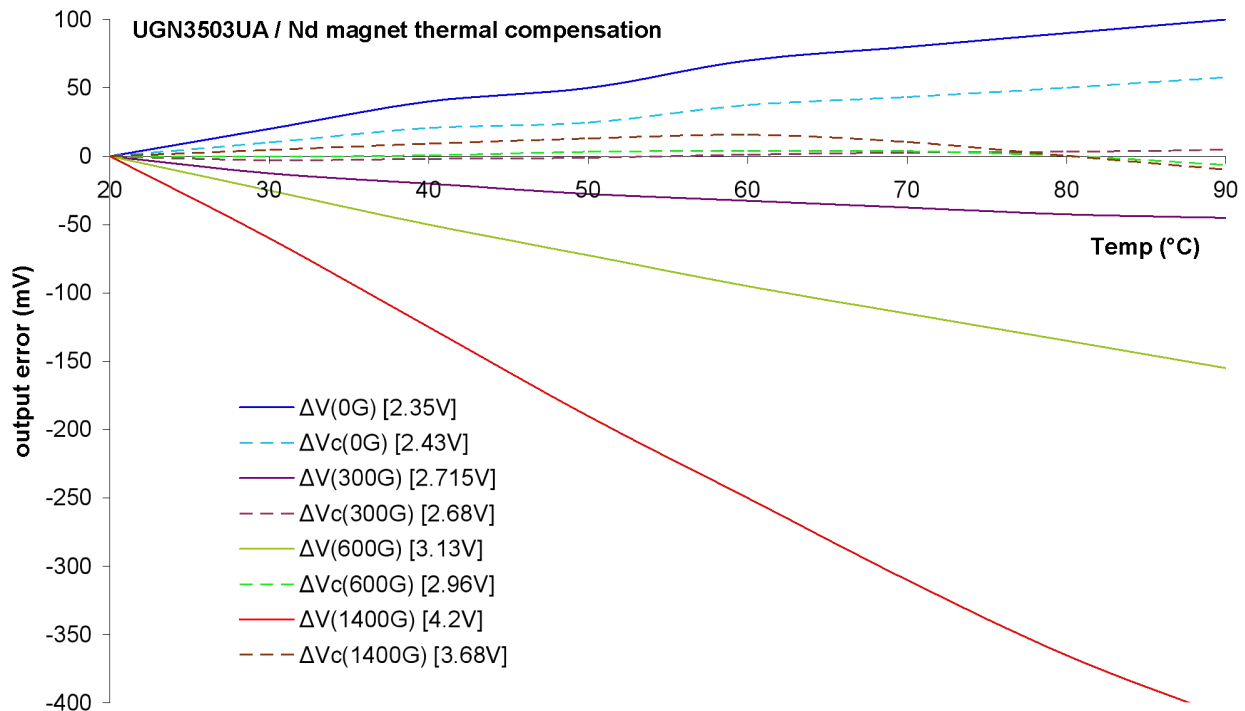


$$V_C = \frac{V_S R_2 (R_L + R_{1||2}) + V_{SS} R_U R_{1||2}}{R_2 (R_U + R_L + R_{1||2})}, \text{ where } \begin{matrix} R_U = R_{t||s} + R_{out} & \& R_L = R_3 & V_S(T_{MAX}) < V_S(T_{MIN}) \\ R_U = R_3 + R_{out} & \& R_L = R_{t||s} & V_S(T_{MAX}) > V_S(T_{MIN}) \end{matrix}$$

Values of the resistors can then be determined by minimising calculated values of $(V_C(T) - V_C(20C))$ simultaneously across the temperature and magnetic flux ranges. The thermistor should have a nominal value around 10K. In cases where the thermistor/shunt pairing resistance alone is insufficient to correct the sensor output in the rising- V_S circuit, an additional series resistor between it and the reference divider can be used and added to the definition of R_L .

Example: UGN3503UA with a neodymium magnet

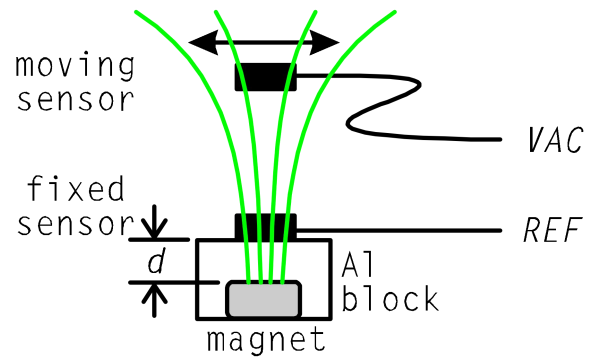
Returning to the sensor/magnet pairing characterised earlier, applying the above analysis to the observed sensor voltage drift plots produces the following set of predicted correction curves for the sensor using the falling- V_S correction circuit, plotted as $\Delta V = (V_C(T) - V_C(20C))$. The corrected output levels at 20C are shown in brackets in the graph legend, and indicate that the correction circuit compresses the uncorrected sensor output voltage range at 20C by 70%. Values of the resistors used are $R_1 = R_2 = 5.1K$, $R_3 = 4.7K$, $R_t = 10K @ 25C$ ($\beta=4100$), and $R_s = 4.3K$. The output resistance of the sensor is found experimentally to be $\sim 180\Omega$ for output currents below 0.25mA. Setting $R_1 = R_2$ produces 2.5V as the reference divider voltage to match the sensor's output level V_I at minimum applied-field correction, so that $V_C = V_I$. The worst-case predicted correction of the sensor at its maximum incident flux level is within 15mV of the 20C value across the temp range, and within a few mV for applied field levels below that down to V_I . As this circuit effectively implements electronically the correction function found previously for this sensor/magnet pairing, the same failure to correct the null-field sensor output curve is observed. In practical terms, the selection of components to render the corrected sensor output at 80C equal to that at 20C is made to match the two most relevant states of engine temperature at which calibrations and measurements are made using our timing meter and data logger. Subsequent testing of this circuit using the same sensor/magnet pairing found good agreement with modelling.



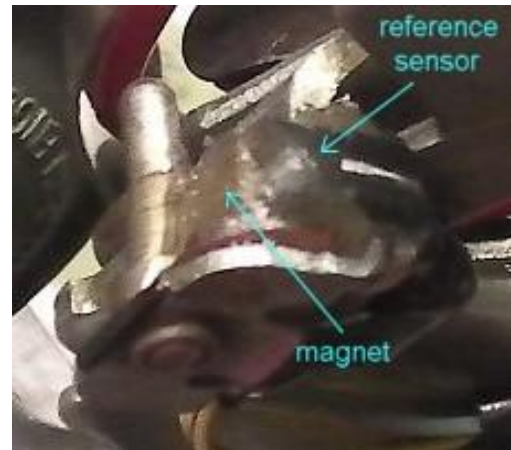
13.1.3. Reference sensor thermal compensation

A superior method of thermal drift compensation is to fix a second identical magnetic sensor adjacent to the magnet to provide a motion-independent measurement of its magnetic flux and sensor thermal drift. The *ratio* of the fixed-sensor output to that of the sensor that moves relative to the magnet is thus fully corrected for thermal drift across the working temp range, irrespective of magnet and sensor type. The analog electronics required to perform this correction are too complex to fit in the distributor so the two sensor outputs must be supplied to the data logger for digital

conversion and numerical processing. This will require an additional line in the cable from the distributor and an additional socket pin which is either left unconnected in the timing meter or connected to the bar-graph vac display IC R_L or R_H terminals via a high-impedance voltage divider to bias its display range. As this method adds the complication of a moving electronic component on the points plate, careful consideration must be given to magnet/sensor locations, wire routing and wire flexibility rating to cope with continuous movement.



This configuration assumes that the reference sensor produces a maximum thermal voltage drift at the upper end of its output range, and that the observed drift may be used to scale the output from the moving sensor numerically to obtain the correct equivalent sensor voltage at room temperature. The distance d shown in the diagram is the thickness of the (solid) aluminium bracket between the magnet and reference sensor fixed to it, and is chosen to produce a near-maximum output voltage from the reference sensor that remains below saturation at all temperatures. The thickness d for an Nd magnet would be about 2mm for the UGN3503UA but greater for the higher-gain sensors unless an off-axis position or a weaker magnet type is used. The bracket locates the magnet and reference sensor together either on the points plate or distributor body, with the (relatively) moving sensor located on the opposite distributor component. The sensor may also be located beside the magnet provided that a similarly high magnetic flux value is observed with the intended sensor orientation and location. In MID configurations where a thermal gradient is unavoidable between the two sensors, attach the reference sensor and magnet to the MID component that is hotter at engine running temperatures (e.g. points baseplate). An alternate mounting method where space constraints dictate an odd-shaped layout of the magnet and reference sensor, particularly where the magnet requires support to prevent movement, is to embed the magnet and reference sensor together in epoxy resin to create a “module”, as was performed for the vacuum sensor (see section 15). This may include some rigid spacers through which holes may be drilled to fix the module in place with screws in the distributor or the module may be formed-in-place by dripping epoxy resin onto the components held in place in the distributor, as in the image at right in which the sensor is located beside the magnet on the points plate vac pin pedestal in a DM2 with its leads wrapped around behind the latter. It is prudent to perform such an assembly with the sensor wired to a power supply and voltmeter to ensure that the magnet is correctly oriented within its external symmetry range to produce the expected magnetic field value, particularly if the reference sensor is located off the magnet’s symmetry axis.



Example: Two UGN3503UA sensors and a neodymium magnet

To illustrate the correction scheme using a reference sensor where a large thermal gradient exists between the two sensors, such as may be seen where the relative-motion sensor is fixed to the distributor body and the reference sensor and magnet positioned on the points plate, a mock-up of this arrangement was assembled on the test bench where the two sensors are separated by a thin aluminium plate which is also fixed to the heated plate separating them from the magnet. The “sandwich” plate will be cooler than the heated plate in proportion to its rate of radiative heat loss relative to its rate of conductive heating. Accordingly, the sensor located on top of this plate will suffer less thermal sensitivity degradation than the sensor in direct contact with the heated plate and

will report a lower magnetic flux measurement error with increasing temperature than the latter. Collecting sets of sensor output data from the two sensors in this arrangement for increasing temps between 20C and 90C and for several positions of the relative-motion sensor with respect to the magnet produces sensor output error values shown as the solid curves shown in the graph below, with the sensor voltage at 20C in each case shown in brackets in the legend. The error curve for the reference sensor is identical for each position of the relative-motion sensor so it is shown as a single plot of ΔV_{ref} vs temp.

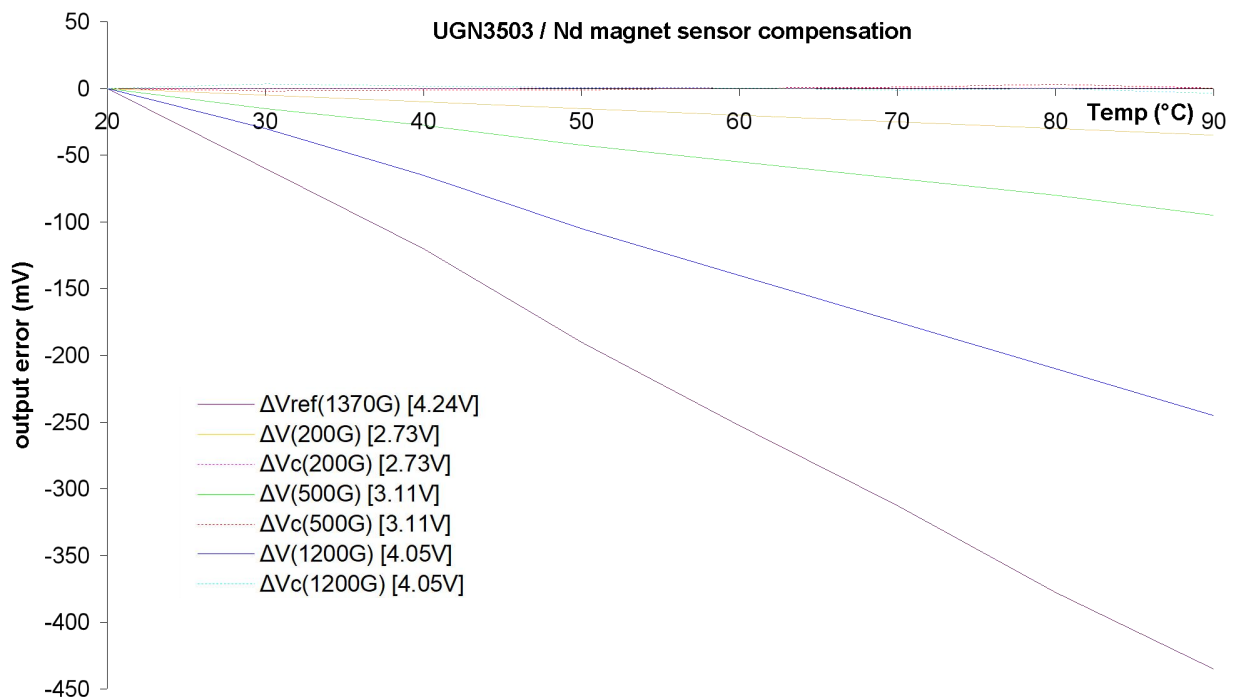
Applying the same thermal characteristics analysis used previously for the UGN3503UA, we find that the relative-motion sensor exhibits a common error scaling factor K_M for its output as a function of temperature at each position relative to the magnet but the reference sensor possesses a different scaling factor K_R . The ratio of these two factors is directly proportional to the temperature gradient between the two sensors and thus may be used to effect a correction between them. Remembering that the UGN3503 output voltage is temperature-invariant at a single value $V_I = V_{SS}/2$ (not V_{NULL}), we may define sensor output functions $M(T) = V_M(T) - V_I$ and $R(T) = V_R(T) - V_I$ where $V_M(T)$ and $V_R(T)$ are the sensor output voltages of the moving and reference sensors respectively, and for both greater than V_I for all temps in the working range. As we found that the voltage drop for the UGN3503 sensor with increasing temp from its value at 20C was directly proportional to its value at 20C multiplied by a linear thermal factor $L_T(T)$, we may write

$$M(20C) - M(T) = M(20C)K_M L_T(T) \text{ and } R(20C) - R(T) = R(20C)K_R L_T(T)$$

and then calculate appropriate values of the linear scaling constants K_M and K_R from the gradients of the sensor output error plots below. Dividing these equations by each other eliminates the thermal factor L_T , effecting our scaling of the moving sensor output against the reference sensor. Rearranging the resulting equation

$$\frac{M(20C) - M(T)}{R(20C) - R(T)} = \frac{M(20C)K_M}{R(20C)K_R} \text{ we obtain } M(20C) = \frac{M(T)}{1 - \frac{K_M}{K_R} \left(1 - \frac{R(T)}{R(20C)}\right)} \equiv \frac{M(T)}{R_C(T)}$$

such that the moving sensor output $M(T)$ is divided by a reference-sensor correction factor $R_C(T)$ to obtain the equivalent moving sensor output at 20C. Differences between the observed value of $M(20C)$ and that calculated at each temperature using the above equation are plotted as the dashed curves in the graph, showing that thermal effects have been eliminated.



The addition of a temp reference component to the distributor will incur wiring effort, particularly if the temp sensor moves with the points plate. The image at right shows a magnetic reference sensor installation in a DM2 with all components located below the points baseplate. The sensor is fixed beside the magnet in an epoxy resin module with its flexible leads secured to the rear of the vac pin platform. A nylon clip is fastened to the baseplate to retain the wiring above the rotation plane of the cent mechanism. The flexible leads must be much longer than the movement range of the points plate without drooping into the cent mechanism.



In distributors such as the DM2 where the two sensors are located on separate assemblies, a flexible thermal bridge consisting of soft copper wire braid may be attached to the two sensor supports to reduce their mutual thermal gradient. Even without this aid, the reference sensor correction reduces total vac error below 0.2CD between 0C and 80C and below 0.05CD over the cruising temp range.

13.1.4. Engine temperature thermal compensation

The number of components added to the distributor may be reduced if the engine temperature is already measured electrically. Sourcing a voltage-level signal representative of engine or distributor temperature to the data logger, scaling it to 5V using a voltage divider and measuring it via an ADC channel in the DLM at the same point in the acquisition cycle as the vac sensor level would allow immediate software thermal correction of the latter upon collection. This correction would be applied as a thermal scaling factor $L_T(T)$ in the vac sensor output function shown in section 13.1.1:

$$V_S(20C) - V_I = \frac{V_S(T) - V_I}{R_L(T)}, \text{ where } R_L(T) = 1 - K_S L_T(T).$$

In cases where such linear thermal correction to the vac sensor voltage produces insufficient accuracy, an array of correction offsets indexed by temperature may be employed with linear interpolations between array entries similar to the method used to translate sensor voltage to CD using the **VAC_LV** array. Such a scheme is simplified if a representative engine temp measurement is already available as a voltage level within the vehicle dashboard or from an electrical temp sensor attached elsewhere on the engine. Otherwise, addition of a thermocouple or reference thermistor to the distributor body requires the addition of a *TEMP* line in the cable to the data logger and altering plug compatibility with the timing meter. A basic correction to the simple bar-graph vac display in the latter may be performed simply by applying the temp level voltage to either the R_L or R_H terminals via a high-impedance voltage divider as required. Unfortunately, the dynamic dwell angle / RPM gradient thermal variation cannot be used to correct the vac sensor as it is dependent on the ignition system (mostly ignition coil) temperature rather than the engine temperature.

13.1.5. Data logger program temperature correction function

An outline function for temperature correction is included in the data logger program script. This assumes a 5V-scaled temperature reference voltage is present on the ADC channel labelled **VAC_TR** in the program header and is sample-averaged into the variable **VacR** as for the measured vac-sensor voltage **VacS**, both in ADC levels. The reference level **VacR** is applied to the vac-sensor level **VacS** as a linear correction with coefficient factor **VAC_TFAC** and offset **VAC_TOFS**. The code appears in the `loop()` function as comment lines and should be modified to implement the type of correction selected from the previous sections. Note that the correction is applied before

the $VacS$ value is scaled into distributor advance using the VAC_DD array. This assumes that the vacuum unit calibration is performed at the target temperature (e.g. 20C) of the thermal correction.

For example, choosing values of VAC_TFAC and VAC_TOFS such that the correction function equals zero at 20C and one at T_{max} yields $L_T(T) = VAC_TFAC * VacR + VAC_TOFS$ and we may replace the linear correction shown in the script with

```
VacR = VAC_TFAC * VacR + VAC_TOFS; // temp correction factor
VacR = 1.0 - VAC_KS * VacR; // = R_L(T)
VacS = ( VacS - VAC_VI ) / VacR + VAC_VI; // scale vac by temp fac
```

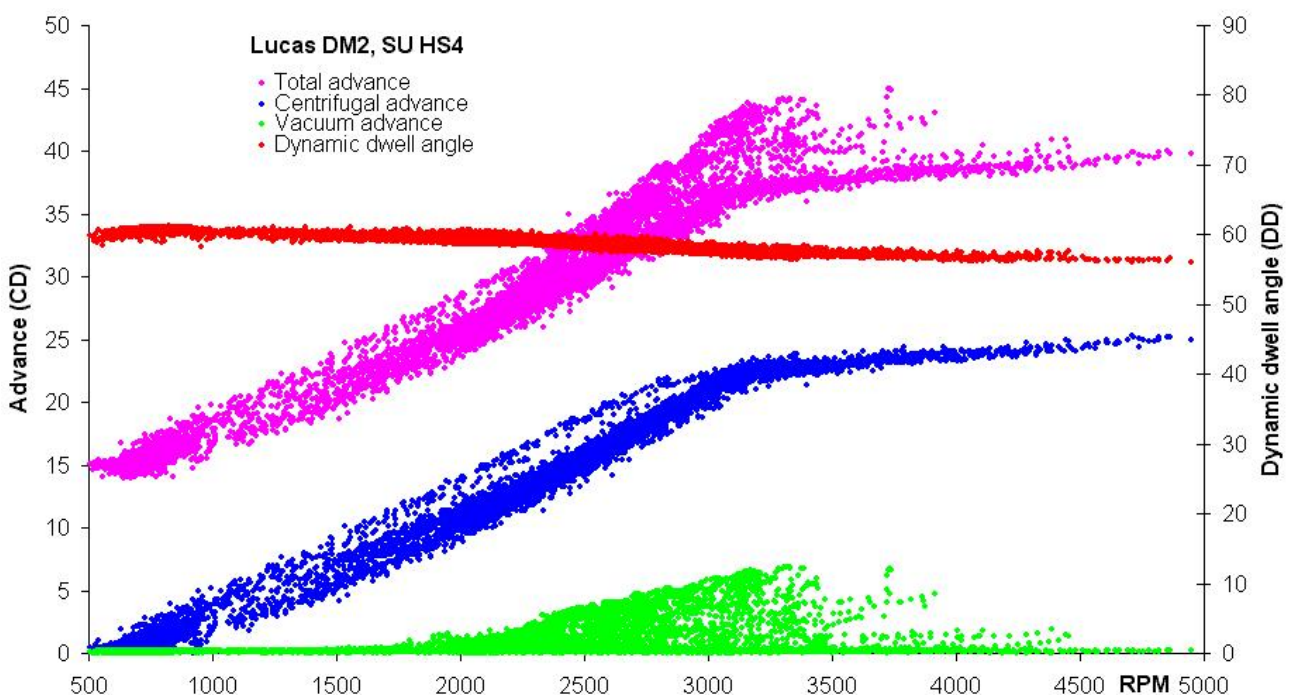
to encode the correction function $R_L(T)$ shown in the previous section, and adding a further label definition VAC_KS for K_S to the script header. A similar approach may be employed to implement the reference-sensor correction factor $R_C(T)$:

```
VacR = ( VacR - VAC_VI ) / ( VR_COLD - VAC_VI ); // temp corr fac
VacR = 1.0 - ( VAC_KM / VAC_KR ) * ( 1.0 - VacR ); // = R_C(T)
VacS = ( VacS - VAC_VI ) / VacR + VAC_VI; // scale vac by temp fac
```

where VR_COLD equals $R(20C)$ in the equation for $R_C(T)$ and labels VAC_KM and VAC_KR define the moving sensor and reference sensor thermal coefficients K_M and K_R respectively. These labels should be defined explicitly as floating-point decimal constants.

13.1.6. Data logger temperature correction calibration

Where a temp correction to the vac signal has been adopted for the data logger, temp calibration may be performed *in situ* after refitting the distributor to the vehicle. The vac sensor calibration given in section 9.4 must be performed at $\sim 20C$ prior to refit. The raw input voltages for the vac and temp inputs may be recorded in each log file entry by changing the definition of VAC_DIAG to `true` in the data logger program header. Values of K_S , K_M or K_R may be deduced by comparing logged values at cold engine start with those at running temp at equivalent known vacuum states (e.g. at idle) using the methods given previously in section 9.5. These constants may then be used in the definitions of the correction functions $R_L(T)$ or $R_C(T)$. Close examination of these sensor voltage pairings over a range of on-road conditions will also characterise the accuracy of the temp correction source used. An example of the degree of accuracy achievable using this scheme is shown below for a custom-modified DM2.



14. Modifications for 6, 8 or 12 cylinder MIDs

The circuits presented for the timing meter and data logger are readily modified to function with distributors possessing more than four HT output terminals. The primary issues raised by a greater number of serviced cylinders are a narrower distributor sector angle per ignition and a larger number of strobe magnets around the cent plate radius. Although four magnets could be used in an 8-cylinder distributor by timing on every second ignition, the lower RPM ranges typical in larger 8-cylinder engines are better characterised by a 1:1 timing scheme. Thus six magnets located 60DD apart are required for the 6-cylinder distributor and eight magnets located 45DD apart are required for the 8-cylinder distributor. Note that the majority of period V12 engines used paired 6-cylinder distributors – any timing scheme adopted in this case should time each distributor independently to identify ignition sequence timing bias or to localise faults to specific mechanisms. In principle, a monolithic 12-cylinder distributor could be timed adequately on every second ignition using a 6-cylinder timing scheme.

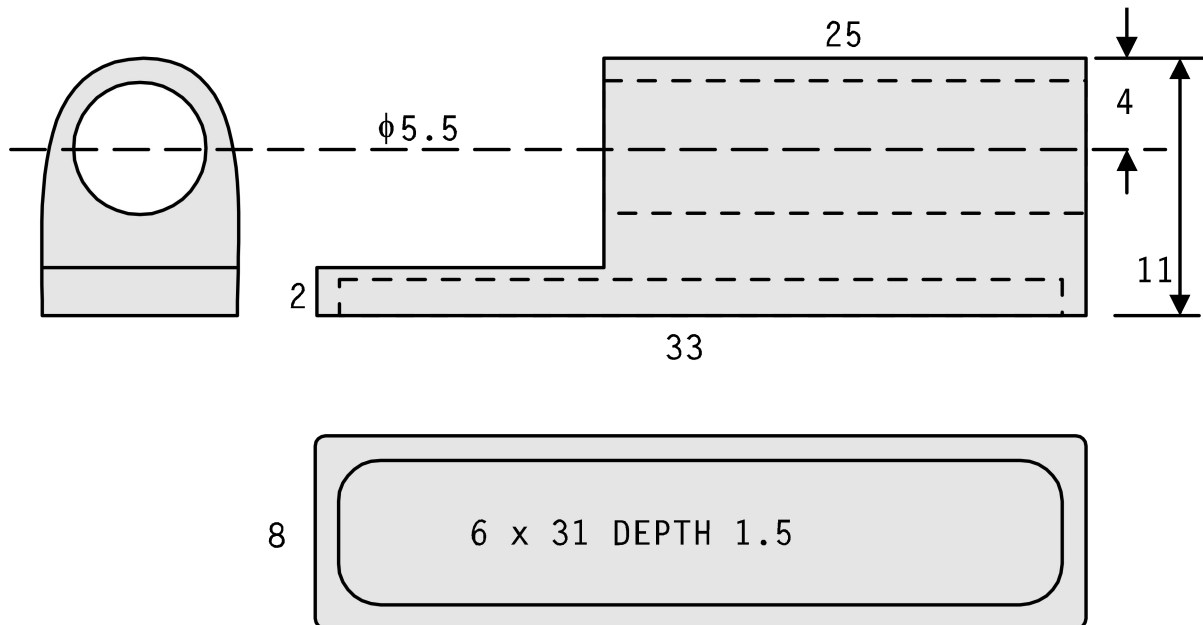
The location of the strobe sensor becomes more constrained by the narrower sector size in the 6 or 8 cylinder MID. The strobe signal ending an ignition timing interval must occur before the next ignition in sequence at maximum advance. This situation dictates a location much closer to TDC for the strobe sensor compared to the range allowed for the four-cylinder MID. For example, an eight cylinder distributor offering a total of 30DD of dynamic advance will commence a new ignition cycle only 15DD later at maximum advance and the strobe sensor must trigger before this angle is reached. Thus for a 10CD static advance offset the practical sensor position limit is ~15CD ATDC.

Configuration of the timing meter for 6 or 8 cylinder MIDs consists of setting the *SCALE* value (see section 8.9.1) to either 120.0CD or 90.0CD respectively, and selecting resistors R1 and R2 in the DWELL circuit (section 8.2) to produce a static closed-points DVM display value of either 60.0DD or 45.0DD respectively. Where a single timing meter such as the bench-test version is required to time different multiple-pole distributors, a multi-pole ganged rotary switch may be employed to select between sets of scaling resistors.

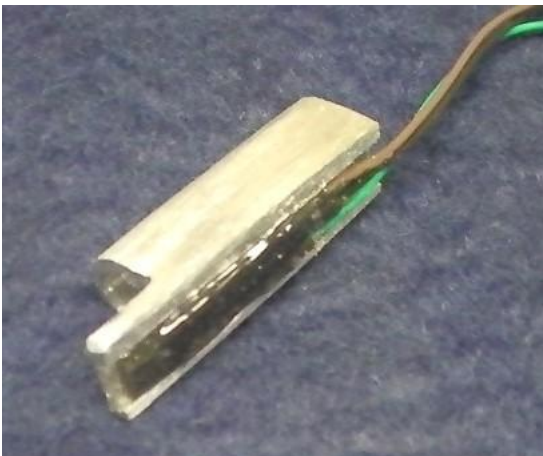
As the data logger uses the pre-compiled constants *DWEL_CAL* and *TIME_CAL* to set sector periods, these must be altered in the program script as stated above prior to the code being compiled and uploaded to the data logger. Where the data logger circuit has been implemented as a bench-test instrument or is required for use with multiple engine-cylinder configurations, an *n*-pole switch tied to *n* digital inputs input may be used to select between calibration values based on a *HIGH* logic level being observed on a selected input. Likewise, the timing sensor offset *TIME_OFS* and static advance constant *STAT_ADV* may be switch-selected or both may be replaced by a single scaled voltage from a potentiometer connected to an analog input.

15. Lucas DM2 / 25D vacuum sensor carrier

To make the carrier for the vacuum sensor described in section 8.5 an 8x11x33mm rectangular piece of aluminium is drilled $\phi 5.5$ mm through its length at 6mm from one side as shown in the diagram below. A 6x31mm channel is milled to a depth of 1.5mm along the flat further from the drilling before the 8x9mm section from the left of the shown figure is cut away. The 25mm edge around the drilling is rounded off to fit snugly in the recess occupied by the vac unit spindle.



Once the carrier has been shaped satisfactorily, it should be a push-on fit onto the vac unit spindle. Remove any corrosion on the latter using emery paper, but only enough to achieve an interference fit of the carrier on the spindle (otherwise some glue will be necessary). Test-fit the sensor carrier and vac unit body assembly to the distributor and ream off any casting seams that interfere with location of the vac unit in place. Either obtain or make a short, stiff spring of 6mm ID and about 12mm length to fit between the sensor carrier and distributor body on the vac unit spindle. This spring will prevent the vac unit from moving within the distributor under applied vacuum. After fixing the sensor to the carrier as described in section 8.5, fit the carrier to the vac unit spindle such that the sensor carrier is symmetrical to the vac unit casting and its wires are under the vac advance linkage. If the vac unit flange clamp detailed in section 12.2 is being used, fit the packing ring to the rear of the vac unit body, place the spring on the vac unit spindle and feed the sensor wires through the vac unit recess in the distributor followed by the vac unit itself, keeping the sensor wires free from entrapment in place under the vac advance linkage. Locate the indexing spring-clip in the static advance adjustment recess. Once the spindle appears at the opposite end of the vac unit recess,



fit the static advance adjuster nut with a crinkle-washer if end-play is evident between the nut and its recess in the casting. Wind the nut until the zero-degree (deep score line) marker on the vac unit body aligns with the edge of the vac unit recess. The sensor wires may now be connected to the 5V regulator in the distributor (if present) and timing meter cable, using heat-shrink tubing to insulate any exposed leads. In the DM2 / 25D distributors these wires may be routed under the points-plate assembly towards the terminal plate and held in place against the side of the distributor body with adhesive tape. Keep the leads short enough to remain clear of the cent advance mechanism irrespective of the fixing method.

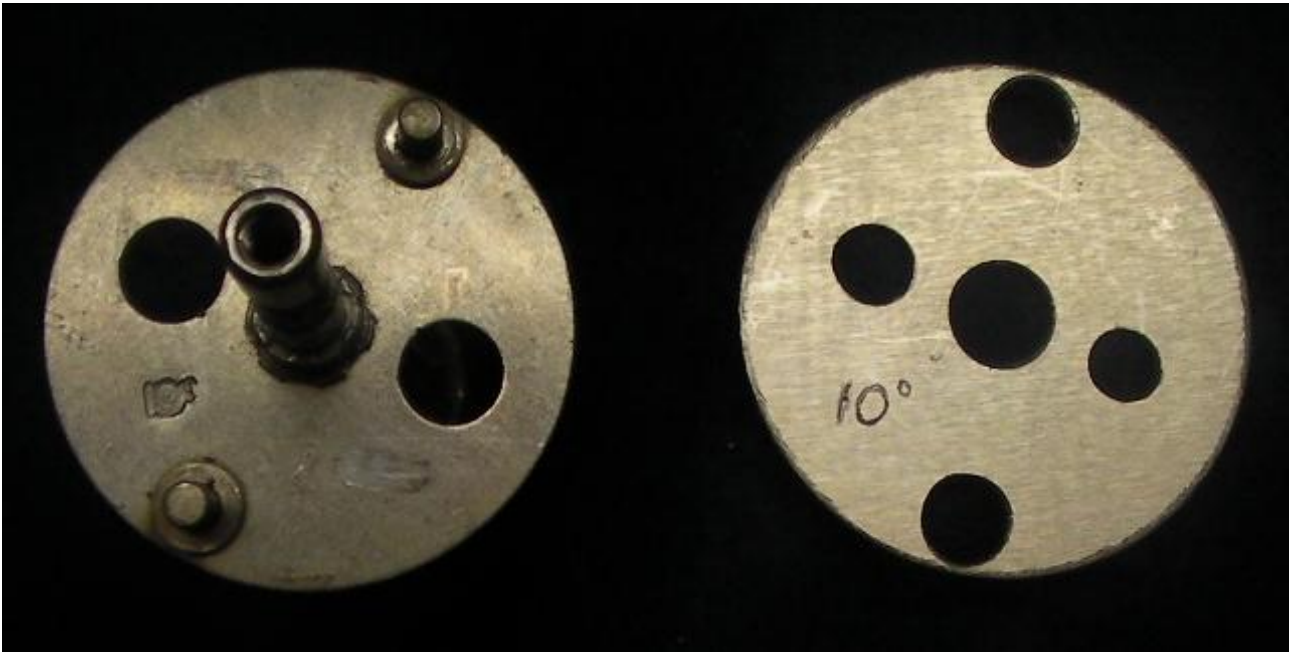
If the vac sensor calibration detailed in section 9.4 for the data logger is being performed, first check for rotational play of the vac unit within its recess in the distributor body. Such play will add +/-1DD of random error to the reported vac advance, but *not* the vac advance actually applied. If a precise characterisation of the vac unit is required, fix the vac unit in place within the distributor (e.g. by securing a shim between the two parts) before calibrating the vac sensor using the “degreeing” rig. Note that the static advance vernier adjustment nut will not operate in this case. A more elegant solution to this problem would involve eliminating rotational play without defeating the static advance adjustment by (for example) packing the space between the parts with Teflon sheet, or fitting some form of spring-loading against the rotational play of the vac unit.

If this sensor carrier is to be used with a reference thermistor for thermal compensation as described in section 13.1.2, the latter should be attached to the points plate with heat-transfer compound beside the magnet and connected to the sensor circuit with soft copper wiring.

16. Lucas DM2 centrifugal advance restrictor plate

The variants of the Lucas DM2 distributor were made with large centrifugal advance ranges to accommodate low-octane fuels in low-compression engines. These simple distributors are still useful as it is considerably easier to reduce a cent advance range than increase it in a MID. In addition, the modification can be made without any functional alteration to the distributor's original components and different amounts of maximum advance may be tested simply by swapping out the advance restrictor.

The DM2 centrifugal weights are pivoted at one end and counter-sprung against the rotor cam at the other. A peg under each weight protrudes through a large hole in the cent plate, limiting its outward travel range under centrifugal force. The cent plate will be stamped with a number in DD which relates the size of the peg holes to the max cent advance of the distributor. Fortunately, there is sufficient room between the cent weights and cent plate to place another flat metal plate between them. If this plate has been made with smaller holes for the cent weight pegs, the maximum cent advance will be restricted accordingly. The cent advance curve up to the limit set by the restrictor plate will be unchanged.



The image above shows at left the cent plate of an early DM2 with peg holes providing 19DD of max cent advance, as shown by the stamped figure. To the right is a 1.5mm-thick stainless steel restrictor plate made to locate precisely around the base bosses of the cent weight pivots, with smaller peg holes providing a maximum of 10DD cent advance. Note that the peg holes in the two plates are *not* concentric – the distance between the rotor axis and the nearest edge of each peg hole are the same. This distance must be preserved to retain the minimum cent advance, at which the two weights close against each other and not the peg holes. If its is desired to restrict the minimum cent advance, such that it begins at a higher RPM, then the peg holes may be located further apart so that the cent weight pegs locate on the restrictor plate at rest.

The image below shows the restrictor plate in position between the cent weights and cent plate. Note that the weights have not been raised on their pivots – the space occupied by the restrictor plate was always present in the original distributor. Also visible under the cent weight at the front of the image is the remains of its casting “tang” which was cut flat at production to float on the cent plate as a support, as evinced by the scuff marks on the cent plate corresponding to high cent advance operation. The tangs may be filed down to rest on the restrictor plate or clearance holes may be added to the latter to leave the tangs in contact with the cent plate. Likewise, casting seams on the cent weights should be filed off.



17. References

27701-AN Hall-effect IC application guide. Rev 4, Sep 2018. Allegro Microsystems Inc. MCO-0000300.

27702A – Linear Hall-Effect Sensors. Allegro Microsystems Inc. Dec 1998.

A1321-DS Rev. 3. A132X Datasheet. Allegro Microsystems Inc. 2004.

Arduino software, hardware and all documentation – <http://www.arduino.cc>

NE555 Datasheet. Rev 1.0.3. Fairchild Semiconductor, Nov 2002.

LM741 Datasheet. Texas Instruments, Oct 2015. SNOSC25D.

PN100 Datasheet. Rev C1. Fairchild Semiconductor, Oct 2008.

SBAS644B – DRV5056 Datasheet. Texas Instruments Inc. April 2018.

UGN3503 Datasheet. Allegro Microsystems Inc. 27501B.